NODE=S126

H

$J = 0$

was H^0

NODE=S126

In the following H refers to the signal that has been discovered in the Higgs searches. Whereas the observed signal is labeled as a spin 0 particle and is called a Higgs Boson, the detailed properties of H and its role in the context of electroweak symmetry breaking need to be further clarified. These issues are addressed by the measurements listed below.

Concerning mass limits and cross section limits that have been obtained in the searches for neutral and charged Higgs bosons, see the sections "Searches for Neutral Higgs Bosons" and "Searches for Charged Higgs Bosons ($H^{\pm}$ and $H^{\pm\pm}$)", respectively.

H MASS

NODE=S126M
NODE=S126M

VALUE (GeV)	*DOCUMENT ID*		*TECN*	*COMMENT*	
125.20±0.11 OUR AVERAGE	Error includes scale factor of 1.4. See the ideogram below.				NEW
[125.25 ± 0.17 GeV OUR 2023 AVERAGE Scale factor = 1.5]					
125.10±0.11	[1] AAD	23BP	ATLS	pp, 13 TeV, $\gamma\gamma$, $ZZ^* \rightarrow 4\ell$	
125.46±0.16	[2] SIRUNYAN	20L	CMS	pp, 13 TeV, $\gamma\gamma$, $ZZ^* \rightarrow 4\ell$	OCCUR=2
125.09±0.21±0.11	[3,4] AAD	15B	LHC	pp, 7, 8 TeV	
• • • We do not use the following data for averages, fits, limits, etc. • • •					
124.99±0.18±0.04	[5] AAD	23AU	ATLS	pp, 13 TeV, $ZZ^* \rightarrow 4\ell$	
124.94±0.17±0.03	[6] AAD	23AU	ATLS	pp, 7, 8, 13 TeV, $ZZ^* \rightarrow 4\ell$	OCCUR=2
125.11±0.11	[7] AAD	23BP	ATLS	pp, 7, 8, 13 TeV, $\gamma\gamma$, $ZZ^* \rightarrow 4\ell$	OCCUR=2
125.17±0.11±0.09	[8] AAD	23BU	ATLS	pp, 13 TeV, $\gamma\gamma$	
125.22±0.11±0.09	[9] AAD	23BU	ATLS	pp, 7, 8, 13 TeV, $\gamma\gamma$	OCCUR=2
125.78±0.26	[10] SIRUNYAN	20L	CMS	pp, 13 TeV, $\gamma\gamma$	
125.38±0.14	[11] SIRUNYAN	20L	CMS	pp, 7, 8, 13 TeV, $\gamma\gamma$, $ZZ^* \rightarrow 4\ell$	OCCUR=3
124.79±0.37	[12] AABOUD	18BM	ATLS	pp, 13 TeV, $ZZ^* \rightarrow 4\ell$	
124.93±0.40	[13] AABOUD	18BM	ATLS	pp, 13 TeV, $\gamma\gamma$	OCCUR=2
124.86±0.27	[3] AABOUD	18BM	ATLS	pp, 13 TeV, $\gamma\gamma$, $ZZ^* \rightarrow 4\ell$	OCCUR=3
124.97±0.24	[3,14] AABOUD	18BM	ATLS	pp, 7, 8, 13 TeV, $\gamma\gamma$, $ZZ^* \rightarrow 4\ell$	OCCUR=4
125.26±0.20±0.08	[15] SIRUNYAN	17AV	CMS	pp, 13 TeV, $ZZ^* \rightarrow 4\ell$	
125.07±0.25±0.14	[4] AAD	15B	LHC	pp, 7, 8 TeV, $\gamma\gamma$	OCCUR=2
125.15±0.37±0.15	[4] AAD	15B	LHC	pp, 7, 8 TeV, $ZZ^* \rightarrow 4\ell$	OCCUR=3
126.02±0.43±0.27	AAD	15B	ATLS	pp, 7, 8 TeV, $\gamma\gamma$	OCCUR=4
124.51±0.52±0.04	AAD	15B	ATLS	pp, 7, 8 TeV, $ZZ^* \rightarrow 4\ell$	OCCUR=5
125.59±0.42±0.17	AAD	15B	CMS	pp, 7, 8 TeV, $ZZ^* \rightarrow 4\ell$	OCCUR=6
$125.02^{+0.26}_{-0.27}{}^{+0.14}_{-0.15}$	[16] KHACHATRY...	15AM	CMS	pp, 7, 8 TeV	
125.36±0.37±0.18	[3,17] AAD	14W	ATLS	pp, 7, 8 TeV	
125.98±0.42±0.28	[17] AAD	14W	ATLS	pp, 7, 8 TeV, $\gamma\gamma$	OCCUR=2
124.51±0.52±0.06	[17] AAD	14W	ATLS	pp, 7, 8 TeV, $ZZ^* \rightarrow 4\ell$	OCCUR=3
125.6 ±0.4 ±0.2	[18] CHATRCHYAN	14AA	CMS	pp, 7, 8 TeV, $ZZ^* \rightarrow 4\ell$	
122 ±7	[19] CHATRCHYAN	14K	CMS	pp, 7, 8 TeV, $\tau\tau$	
124.70±0.31±0.15	[20] KHACHATRY...	14P	CMS	pp, 7, 8 TeV, $\gamma\gamma$	
$125.5 \pm 0.2\ {}^{+0.5}_{-0.6}$	[3,21] AAD	13AK	ATLS	pp, 7, 8 TeV	
126.8 ±0.2 ±0.7	[21] AAD	13AK	ATLS	pp, 7, 8 TeV, $\gamma\gamma$	OCCUR=2
$124.3\ {}^{+0.6}_{-0.5}\ {}^{+0.5}_{-0.3}$	[21] AAD	13AK	ATLS	pp, 7, 8 TeV, $ZZ^* \rightarrow 4\ell$	OCCUR=3
125.8 ±0.4 ±0.4	[3,22] CHATRCHYAN	13J	CMS	pp, 7, 8 TeV	
126.2 ±0.6 ±0.2	[22] CHATRCHYAN	13J	CMS	pp, 7, 8 TeV, $ZZ^* \rightarrow 4\ell$	OCCUR=2
126.0 ±0.4 ±0.4	[3,23] AAD	12AI	ATLS	pp, 7, 8 TeV	
125.3 ±0.4 ±0.5	[3,24] CHATRCHYAN	12N	CMS	pp, 7, 8 TeV	

[1] AAD 23BP combine 13 TeV results of $H \to \gamma\gamma$ (AAD 23BU) and $H \to ZZ^* \to 4\ell$ where $\ell = e, \mu$ (AAD 23AU) using 140 fb^{-1} of pp collision data. The result is 125.10 $\pm$ 0.09(stat)$\pm$0.07(syst) GeV. NODE=S126M;LINKAGE=P

[2] SIRUNYAN 20L result of $H \to \gamma\gamma$ is combined with that of $H \to ZZ^* \to 4\ell$ where $\ell = e, \mu$ (SIRUNYAN 17AV). NODE=S126M;LINKAGE=K

[3] Combined value from $\gamma\gamma$ and $ZZ^* \to 4\ell$ final states. NODE=S126M;LINKAGE=AA

[4] ATLAS and CMS data are fitted simultaneously. NODE=S126M;LINKAGE=LC

[5] AAD 23AU use 139 fb^{-1} of pp collisions at E_{cm} = 13 TeV with $H \to ZZ^* \to 4\ell$ where $\ell = e, \mu$. NODE=S126M;LINKAGE=N

[6] AAD 23AU combine 13 TeV results with 7 and 8 TeV results (AAD 14W). NODE=S126M;LINKAGE=O

[7] AAD 23BP combine 13 TeV results with 7 and 8 TeV results. The result is 125.11 $\pm$ 0.09(stat)$\pm$0.06(syst) GeV. NODE=S126M;LINKAGE=Q

[8] AAD 23BU use 140 fb^{-1} of pp collisions at E_{cm} = 13 TeV with $H \to \gamma\gamma$. NODE=S126M;LINKAGE=R

[9] AAD 23BU combine 13 TeV results with 7 and 8 TeV results (AAD 15B). NODE=S126M;LINKAGE=S

[10] SIRUNYAN 20L use 35.9 fb^{-1} of pp collisions at E_{cm} = 13 TeV with $H \to \gamma\gamma$. NODE=S126M;LINKAGE=J

[11] SIRUNYAN 20L combine 13 TeV results with 7 and 8 TeV results (KHACHATRYAN 15AM). NODE=S126M;LINKAGE=M

[12] AABOUD 18BM use 36.1 fb^{-1} of pp collisions at E_{cm} = 13 TeV with $H \to ZZ^* \to 4\ell$ where $\ell = e, \mu$. NODE=S126M;LINKAGE=G

[13] AABOUD 18BM use 36.1 fb^{-1} of pp collisions at E_{cm} = 13 TeV with $H \to \gamma\gamma$. NODE=S126M;LINKAGE=H

[14] AABOUD 18BM combine 13 TeV results with 7 and 8 TeV results. Other combined results are summarized in their Fig. 4. NODE=S126M;LINKAGE=I

[15] SIRUNYAN 17AV use 35.9 fb^{-1} of pp collisions at E_{cm} = 13 TeV with $H \to ZZ^* \to 4\ell$ where $\ell = e, \mu$. NODE=S126M;LINKAGE=F

[16] KHACHATRYAN 15AM use up to 5.1 fb^{-1} of pp collisions at E_{cm} = 7 TeV and up to 19.7 fb^{-1} at E_{cm} = 8 TeV. NODE=S126M;LINKAGE=E

[17] AAD 14W use 4.5 fb^{-1} of pp collisions at E_{cm} = 7 TeV and 20.3 fb^{-1} at 8 TeV. NODE=S126M;LINKAGE=A

[18] CHATRCHYAN 14AA use 5.1 fb^{-1} of pp collisions at E_{cm} = 7 TeV and 19.7 fb^{-1} at E_{cm} = 8 TeV. NODE=S126M;LINKAGE=B

[19] CHATRCHYAN 14K use 4.9 fb^{-1} of pp collisions at E_{cm} = 7 TeV and 19.7 fb^{-1} at E_{cm} = 8 TeV. NODE=S126M;LINKAGE=D

[20] KHACHATRYAN 14P use 5.1 fb^{-1} of pp collisions at E_{cm} = 7 TeV and 19.7 fb^{-1} at E_{cm} = 8 TeV. NODE=S126M;LINKAGE=C

[21] AAD 13AK use 4.7 fb^{-1} of pp collisions at E_{cm}=7 TeV and 20.7 fb^{-1} at E_{cm}=8 TeV. Superseded by AAD 14W. NODE=S126M;LINKAGE=LH

[22] CHATRCHYAN 13J use 5.1 fb^{-1} of pp collisions at E_{cm} = 7 TeV and 12.2 fb^{-1} at E_{cm} = 8 TeV. NODE=S126M;LINKAGE=CT

[23] AAD 12AI obtain results based on 4.6–4.8 fb^{-1} of pp collisions at E_{cm} = 7 TeV and 5.8–5.9 fb^{-1} at E_{cm} = 8 TeV. An excess of events over background with a local significance of 5.9 σ is observed at m_H = 126 GeV. See also AAD 12DA. NODE=S126M;LINKAGE=AI

[24] CHATRCHYAN 12N obtain results based on 4.9–5.1 fb^{-1} of pp collisions at E_{cm} = 7 TeV and 5.1–5.3 fb^{-1} at E_{cm} = 8 TeV. An excess of events over background with a local significance of 5.0 σ is observed at about m_H = 125 GeV. See also CHATRCHYAN 12BY and CHATRCHYAN 13Y. NODE=S126M;LINKAGE=CH

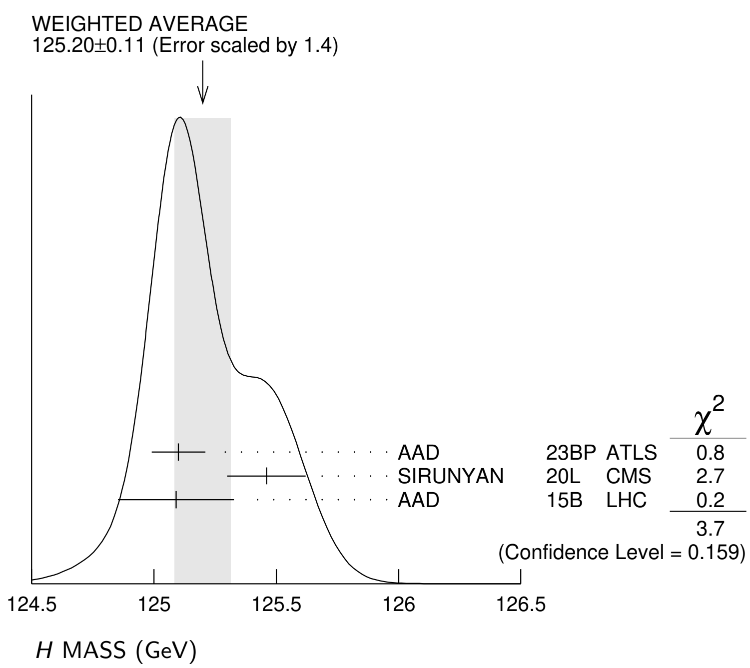

H SPIN AND *CP* PROPERTIES

NODE=S126CP
NODE=S126CP

The observation of the signal in the $\gamma\gamma$ final state rules out the possibility that the discovered particle has spin 1, as a consequence of the Landau-Yang theorem. This argument relies on the assumptions that the decaying particle is an on-shell resonance and that the decay products are indeed two photons rather than two pairs of boosted photons, which each could in principle be misidentified as a single photon.

Concerning distinguishing the spin 0 hypothesis from a spin 2 hypothesis, some care has to be taken in modelling the latter in order to ensure that the discriminating power is actually based on the spin properties rather than on unphysical behavior that may affect the model of the spin 2 state.

Under the assumption that the observed signal consists of a single state rather than an overlap of more than one resonance, it is sufficient to discriminate between distinct hypotheses in the spin analyses. On the other hand, the determination of the *CP* properties is in general much more difficult since in principle the observed state could consist of any admixture of *CP*-even and *CP*-odd components. As a first step, the compatibility of the data with distinct hypotheses of pure *CP*-even and pure *CP*-odd states with different spin assignments has been investigated. In order to treat the case of a possible mixing of different *CP* states, certain cross section ratios are considered. Those cross section ratios need to be distinguished from the amount of mixing between a *CP*-even and a *CP*-odd state, as the cross section ratios depend in addition also on the coupling strengths of the *CP*-even and *CP*-odd components to the involved particles. A small relative coupling implies a small sensitivity of the corresponding cross section ratio to effects of *CP* mixing.

NODE=S126CP

VALUE	DOCUMENT ID		TECN	COMMENT
• • • We do not use the following data for averages, fits, limits, etc. • • •				
	[1] AAD	23AK	ATLS	$H \to \tau\tau$, 13 TeV
	[2] AAD	23AN	ATLS	$H \to \gamma\gamma$, VBF, 13 TeV
	[3] TUMASYAN	23AJ	CMS	$H \to \tau\tau$, 13 TeV
	[4] TUMASYAN	23P	CMS	$t\bar{t}H$, $H \to WW^*$, $\tau\tau$, 13 TeV
	[5] AAD	22V	ATLS	WW^* ($\to e\nu\mu\nu$)+2j, 13 TeV
	[6] TUMASYAN	22Y	CMS	$H \to \tau\tau$, 13 TeV
	[7] AAD	20N	ATLS	$H \to \tau\tau$, VBF, 13 TeV
	[8] AAD	20Z	ATLS	$t\bar{t}H$, $H \to \gamma\gamma$, 13 TeV
	[9] SIRUNYAN	20AS	CMS	$t\bar{t}H$, $H \to \gamma\gamma$, 13 TeV
	[10] SIRUNYAN	19BL	CMS	pp, 7, 8, 13 TeV, $ZZ^*/ZZ \to 4\ell$
	[11] SIRUNYAN	19BZ	CMS	$pp \to H$+2jets (VBF, ggF, VH), $H \to \tau\tau$, 13 TeV
	[12] AABOUD	18AJ	ATLS	$H \to ZZ^* \to 4\ell$ ($\ell = e, \mu$), 13TeV
	[13] SIRUNYAN	17AM	CMS	$pp \to H + \geq 2j$, $H \to 4\ell$ ($\ell = e, \mu$)
	[14] AAD	16	ATLS	$H \to \gamma\gamma$
	[15] AAD	16BL	ATLS	$pp \to HjjX$ (VBF), $H \to \tau\tau$, 8 TeV
	[16] KHACHATRY...	16AB	CMS	$pp \to WH$, ZH, $H \to b\bar{b}$, 8 TeV
	[17] AAD	15AX	ATLS	$H \to WW^*$
	[18] AAD	15CI	ATLS	$H \to ZZ^*$, WW^*, $\gamma\gamma$
	[19] AALTONEN	15	TEVA	$p\bar{p} \to WH$, ZH, $H \to b\bar{b}$
	[20] AALTONEN	15B	CDF	$p\bar{p} \to WH$, ZH, $H \to b\bar{b}$
	[21] KHACHATRY...	15Y	CMS	$H \to 4\ell$, WW^*, $\gamma\gamma$
	[22] ABAZOV	14F	D0	$p\bar{p} \to WH$, ZH, $H \to b\bar{b}$
	[23] CHATRCHYAN	14AA	CMS	$H \to ZZ^*$
	[24] CHATRCHYAN	14G	CMS	$H \to WW^*$
	[25] KHACHATRY...	14P	CMS	$H \to \gamma\gamma$
	[26] AAD	13AJ	ATLS	$H \to \gamma\gamma$, $ZZ^* \to 4\ell$, $WW^* \to \ell\nu\ell\nu$
	[27] CHATRCHYAN	13J	CMS	$H \to ZZ^* \to 4\ell$

[1] AAD 23AK measure the *CP* structure of the τ Yukawa coupling using 139 fb^{-1} of data at E_{cm} = 13 TeV. The *CP*-mixing angle α for τ Yukawa coupling is measured to be $9 \pm 16^\circ$. The data disfavour the pure *CP*-odd ($\alpha = 90^\circ$) at 3.4 σ.

NODE=S126CP;LINKAGE=V

[2] AAD 23AN test *CP* invariance in H production via VBF using $H \to \gamma\gamma$ decay channel with 139 fb^{-1} at E_{cm} = 13 TeV. By using the Optimal Observable method, the data constrain parameters describing the strength of the *CP*-odd component in the coupling between Higgs and W/Z in effective field theory bases: $\tilde{d}$ in the HISZ basis and $c_{H\widetilde{W}}$ in the Warsaw basis. The result is -0.010 $\leq \tilde{d} \leq$ 0.040 and -0.15 $\leq c_{H\widetilde{W}} \leq$ 0.67 at 68% CL. See their Table I, which shows the result combined with $H \to \tau\tau$ (AAD 20N): -0.012 $\leq \tilde{d} \leq$ 0.030 at 68% CL.

NODE=S126CP;LINKAGE=X

[3] TUMASYAN 23AJ constraint anomalous couplings of the Higgs to vector bosons and fermions using $pp \to H \to \tau\tau$ at E_{cm} = 13 TeV with 138 fb^{-1} data. The CP-violating parameter in gluon-fusion production f_{a3}^{ggH} and the effective mixing angle α^{Hff} are given in their Table VII with $H \to \tau\tau$ and f_{a3}^{ggH} in their Table X with $H \to \tau\tau$ and $H \to 4\ell$. Using the VBF production analysis, the CP-violating parameter f_{a3} and the CP-conserving parameters f_{a2}, $f_{\Lambda 1}$ and $f_{\Lambda 1}^{Z\gamma}$ are given in their Table VIII with $H \to \tau\tau$ and Table IX with $H \to \tau\tau$ and $H \to 4\ell$. The CP-violating parameter f_{CP}^{Htt} is constrained to be $0.03^{+0.17}_{-0.03}$ using $H \to \tau\tau$, $H \to 4\ell$ and $H \to \gamma\gamma$. NODE=S126CP;LINKAGE=W

[4] TUMASYAN 23P constrain $\widetilde{\kappa}_t$ from $t\bar{t}H$ and tH decaying $H \to WW^*$ and $H \to \tau\tau$ (multilepton decay mode) with 138 fb^{-1} pp collision data at E_{cm} = 13 TeV. The $\widetilde{\kappa}_t$ is constrained to be $|\widetilde{\kappa}_t| \leq 1.4$ at 95% CL by fixing $\kappa_t = 1$ and other couplings (κ_V etc.) to the SM values, see their Table 6 (see their Fig. 9 for 2-dim contours). The fractional contribution of the CP-odd component $|f_{CP}^{Htt}|$ is constrained to (0.24, 0.81) at 68% CL with a best fit value of 0.59. The combination with other $t\bar{t}H$ decaying $H \to \gamma\gamma$ (SIRUNYAN 20AS) and $H \to 4\ell$ (SIRUNYAN 21AE) constraints to be $|\widetilde{\kappa}_t| \leq 1.07$ at 95% CL and $|f_{CP}^{Htt}|$ <0.55 at 68% CL with a best fit value of 0.28. NODE=S126CP;LINKAGE=Y

[5] AAD 22V measure the CP properties of the effective Higgs-gluon interaction using gluon fusion $H \to WW^* \to e\nu\mu\nu$ plus two jets with 36.1 fb^{-1} of data at E_{cm} = 13 TeV. The measured tangent of the CP-mixing angle tanα is 0.0 $\pm$ 0.4 $\pm$ 0.3 assuming the standard model HVV couplings. See their Fig. 6. NODE=S126CP;LINKAGE=U

[6] TUMASYAN 22Y measure the CP structure of the τ Yukawa coupling using 137 fb^{-1} of data at E_{cm} = 13 TeV. The CP-mixing angle α for τ Yukawa coupling is measured to be $-1 \pm 19^\circ$. The data disfavour the pure CP-odd ($\alpha = 90^\circ$) at 3.0 σ. NODE=S126CP;LINKAGE=T

[7] AAD 20N test CP invariance in H production via VBF using $H \to \tau\tau$ decay channel with 36.1 fb^{-1} at E_{cm} = 13 TeV. By using the Optimal Observable method, the data constrain a parameter $\widetilde{d}$, which is for the strength of CP violation in an effective field theory, to be $-0.090 \leq \widetilde{d} \leq 0.035$ at 68% CL (see their Fig. 6). NODE=S126CP;LINKAGE=Q

[8] AAD 20Z exclude a CP-mixing angle α, $|\alpha| > 43^\circ$ at 95% CL, where $\alpha = 0$ represents the Standard Model, in 139 fb^{-1} of data at E_{cm} = 13 TeV. The pure CP-odd structure of the top Yukawa coupling ($\alpha = 90^\circ$) is excluded at 3.9 σ. NODE=S126CP;LINKAGE=S

[9] SIRUNYAN 20AS exclude the pure CP-odd structure of the top Yukawa coupling at 3.2 σ using $t\bar{t}H$, $H \to \gamma\gamma$ in 137 fb^{-1} of data at E_{cm} = 13 TeV. The fractional contribution of the CP-odd component $f_{CP}^{t\bar{t}H}$ is measured to be 0.00 $\pm$ 0.33. NODE=S126CP;LINKAGE=R

[10] SIRUNYAN 19BL measure the anomalous HVV couplings from on-shell and off-shell production in the 4ℓ final state. Data of 80.2 fb^{-1} at 13 TeV, 19.7 fb^{-1} at 8 TeV, and 5.1 fb^{-1} at 7 TeV are used. See their Tables VI and VII for anomalous HVV couplings of CP-violating and CP-conserving parameters with on- and off-shells. NODE=S126CP;LINKAGE=P

[11] SIRUNYAN 19BZ constrain anomalous HVV couplings of the Higgs boson with data of 35.9 fb^{-1} at E_{cm} = 13 TeV using Higgs boson candidates with two jets produced in VBF, ggF, and VH that decay to $\tau\tau$. See their Table 2 and Fig. 10, which show 68% CL and 95% CL intervals. Combining those with the $H \to 4\ell$ (SIRUNYAN 19BL, on-shell scenario), results shown in their Tables 3, 4, and Fig. 11 are obtained. A CP-violating parameter is set to be $f_{a3}\cos(\phi_{a3}) = (0.00 \pm 0.27) \times 10^{-3}$ and CP-conserving parameters are $f_{a2}\cos(\phi_{a2}) = (0.08^{+1.04}_{-0.21}) \times 10^{-3}$, $f_{\Lambda 1}\cos(\phi_{\Lambda 1}) = (0.00^{+0.53}_{-0.09}) \times 10^{-3}$, and $f_{\Lambda 1}^{Z\gamma}\cos(\phi_{\Lambda 1}^{Z\gamma}) = (0.0^{+1.1}_{-1.3}) \times 10^{-3}$. NODE=S126CP;LINKAGE=O

[12] AABOUD 18AJ study the tensor structure of the Higgs boson couplings using an effective Lagrangian using 36.1 fb^{-1} of pp collision data at E_{cm} = 13 TeV. Constraints are set on the non-Standard-Model CP-even and CP-odd couplings to Z bosons and on the CP-odd coupling to gluons. See their Figs. 9 and 10, and Tables 10 and 11. NODE=S126CP;LINKAGE=N

[13] SIRUNYAN 17AM constrain anomalous couplings of the Higgs boson with 5.1 fb^{-1} of pp collisions at E_{cm} = 7 TeV, 19.7 fb^{-1} at E_{cm} = 8 TeV, and 38.6 fb^{-1} at E_{cm} = 13 TeV. See their Table 3 and Fig. 3, which show 68% CL and 95% CL intervals. A CP violation parameter f_{a3} is set to be $f_{a3}\cos(\phi_{a3})$ = [−0.38, 0.46] at 95% CL ($\phi_{a3} = 0$ or π). NODE=S126CP;LINKAGE=M

[14] AAD 16 study $H \to \gamma\gamma$ with an effective Lagrangian including CP even and odd terms in 20.3 fb^{-1} of pp collisions at E_{cm} = 8 TeV. The data is consistent with the expectations for the Higgs boson of the Standard Model. Limits on anomalous couplings are also given. NODE=S126CP;LINKAGE=J

[15] AAD 16BL study VBF $H \to \tau\tau$ with an effective Lagrangian including a CP odd term in 20.3 fb^{-1} of pp collisions at E_{cm} = 8 TeV. The measurement is consistent with the expectation of the Standard Model. The CP-mixing parameter $\widetilde{d}$ (a dimensionless coupling $\widetilde{d} = -(m_W^2/\Lambda^2) f_{\widetilde{W}W}$) is constrained to the interval of (−0.11, 0.05) at 68% CL under the assumption of $\widetilde{d} = \widetilde{d}_B$. NODE=S126CP;LINKAGE=L

[16] KHACHATRYAN 16AB search for anomalous pseudoscalar couplings of the Higgs boson to W and Z with 18.9 fb^{-1} of pp collisions at E_{cm} = 8 TeV. See their Table 5 and Figs 5 and 6 for limits on possible anomalous pseudoscalar coupling parameters. NODE=S126CP;LINKAGE=K

[17] AAD 15AX compare the $J^{CP} = 0^+$ Standard Model assignment with other J^{CP} hypotheses in 20.3 fb^{-1} of pp collisions at E_{cm} = 8 TeV, using the process $H \to WW^* \to e\nu\mu\nu$. 2^+ hypotheses are excluded at 84.5–99.4%CL, 0^- at 96.5%CL, 0^+ (field strength coupling) at 70.8%CL. See their Fig. 19 for limits on possible CP mixture parameters. NODE=S126CP;LINKAGE=F

[18] AAD 15CI compare the $J^{CP} = 0^+$ Standard Model assignment with other J^{CP} hypotheses in 4.5 fb^{-1} of pp collisions at E_{cm} = 7 TeV and 20.3 fb^{-1} at E_{cm} = 8 TeV, using the processes $H \to ZZ^* \to 4\ell$. $H \to \gamma\gamma$ and combine with AAD 15AX data. 0^+ (field strength coupling), 0^- and several 2^+ hypotheses are excluded at more than 99.9% CL. See their Tables 7–9 for limits on possible CP mixture parameters. NODE=S126CP;LINKAGE=G

[19] AALTONEN 15 combine AALTONEN 15B and ABAZOV 14F data. An upper limit of 0.36 of the Standard Model production rate at 95% CL is obtained both for a 0^- and a 2^+ state. Assuming the SM event rate, the $J^{CP} = 0^-$ (2^+) hypothesis is excluded at the 5.0σ (4.9σ) level. NODE=S126CP;LINKAGE=E

[20] AALTONEN 15B compare the $J^{CP} = 0^+$ Standard Model assignment with other J^{CP} hypotheses in 9.45 fb^{-1} of $p\overline{p}$ collisions at E_{cm} = 1.96 TeV, using the processes $ZH \to \ell\ell b\overline{b}$, $WH \to \ell\nu b\overline{b}$, and $ZH \to \nu\nu b\overline{b}$. Bounds on the production rates of 0^- and 2^+ (graviton-like) states are set, see their tables II and III. NODE=S126CP;LINKAGE=D

[21] KHACHATRYAN 15Y compare the $J^{CP} = 0^+$ Standard Model assignment with other J^{CP} hypotheses in up to 5.1 fb^{-1} of pp collisions at E_{cm} = 7 TeV and up to 19.7 fb^{-1} at E_{cm} = 8 TeV, using the processes $H \to 4\ell$, $H \to WW^*$, and $H \to \gamma\gamma$. 0^- is excluded at 99.98% CL, and several 2^+ hypotheses are excluded at more than 99% CL. Spin 1 models are excluded at more than 99.999% CL in ZZ^* and WW^* modes. Limits on anomalous couplings and several cross section fractions, treating the case of CP-mixed states, are also given. NODE=S126CP;LINKAGE=I

[22] ABAZOV 14F compare the $J^{CP} = 0^+$ Standard Model assignment with $J^{CP} = 0^-$ and 2^+ (graviton-like coupling) hypotheses in up to 9.7 fb^{-1} of $p\overline{p}$ collisions at E_{cm} = 1.96 TeV. They use kinematic correlations between the decay products of the vector boson and the Higgs boson in the final states $ZH \to \ell\ell b\overline{b}$, $WH \to \ell\nu b\overline{b}$, and $ZH \to \nu\nu b\overline{b}$. The 0^- (2^+) hypothesis is excluded at 97.6% CL (99.0% CL). In order to treat the case of a possible mixture of a 0^+ state with another J^{CP} state, the cross section fractions $f_X = \sigma_X/(\sigma_{0^+} + \sigma_X)$ are considered, where $X = 0^-$, 2^+. Values for f_{0^-} (f_{2^+}) above 0.80 (0.67) are excluded at 95% CL under the assumption that the total cross section is that of the SM Higgs boson. NODE=S126CP;LINKAGE=AB

[23] CHATRCHYAN 14AA compare the $J^{CP} = 0^+$ Standard Model assignment with various J^{CP} hypotheses in 5.1 fb^{-1} of pp collisions at E_{cm} = 7 TeV and 19.7 fb^{-1} at E_{cm} = 8 TeV. $J^{CP} = 0^-$ and $1^\pm$ hypotheses are excluded at 99% CL, and several $J = 2$ hypotheses are excluded at 95% CL. In order to treat the case of a possible mixture of a 0^+ state with another J^{CP} state, the cross section fraction $f_{a3} = |a_3|^2\, \sigma_3\, /\, (|a_1|^2\, \sigma_1 + |a_2|^2\, \sigma_2 + |a_3|^2\, \sigma_3)$ is considered, where the case $a_3 = 1$, $a_1 = a_2 = 0$ corresponds to a pure CP-odd state. Assuming $a_2 = 0$, a value for f_{a3} above 0.51 is excluded at 95% CL. NODE=S126CP;LINKAGE=A

[24] CHATRCHYAN 14G compare the $J^{CP} = 0^+$ Standard Model assignment with $J^{CP} = 0^-$ and 2^+ (graviton-like coupling) hypotheses in 4.9 fb^{-1} of pp collisions at E_{cm} = 7 TeV and 19.4 fb^{-1} at E_{cm} = 8 TeV. Varying the fraction of the production of the 2^+ state via gg and $q\overline{q}$, 2^+ hypotheses are disfavored at CL between 83.7 and 99.8%. The 0^- hypothesis is disfavored against 0^+ at the 65.3% CL. NODE=S126CP;LINKAGE=C

[25] KHACHATRYAN 14P compare the $J^{CP} = 0^+$ Standard Model assignment with a 2^+ (graviton-like coupling) hypothesis in 5.1 fb^{-1} of pp collisions at E_{cm} = 7 TeV and 19.7 fb^{-1} at E_{cm} = 8 TeV. Varying the fraction of the production of the 2^+ state via gg and $q\overline{q}$, 2^+ hypotheses are disfavored at CL between 71 and 94%. NODE=S126CP;LINKAGE=B

[26] AAD 13AJ compare the spin 0, CP-even hypothesis with specific alternative hypotheses of spin 0, CP-odd, spin 1, CP-even and CP-odd, and spin 2, CP-even models using the Higgs boson decays $H \to \gamma\gamma$, $H \to ZZ^* \to 4\ell$ and $H \to WW^* \to \ell\nu\ell\nu$ and combinations thereof. The data are compatible with the spin 0, CP-even hypothesis, while all other tested hypotheses are excluded at confidence levels above 97.8%. NODE=S126CP;LINKAGE=AA

[27] CHATRCHYAN 13J study angular distributions of the lepton pairs in the ZZ^* channel where both Z bosons decay to e or μ pairs. Under the assumption that the observed particle has spin 0, the data are found to be consistent with the pure CP-even hypothesis, while the pure CP-odd hypothesis is disfavored. NODE=S126CP;LINKAGE=CH

H DECAY WIDTH

NODE=S126W
NODE=S126W

The total decay width for a light Higgs boson with a mass in the observed range is not expected to be directly observable at the LHC. For the case of the Standard Model the prediction for the total width is about 4 MeV, which is three orders of magnitude smaller than the experimental mass resolution. There is no indication from the results observed so far that the natural width is broadened by new physics effects to such an extent that it could be directly observable. Furthermore, as all LHC Higgs channels rely on the identification of Higgs decay products, the total Higgs width cannot be measured indirectly without additional assumptions. The different dependence of on-peak and off-peak contributions on the total width in Higgs decays to ZZ^* and interference effects between signal and background in Higgs decays to $\gamma\gamma$ can provide additional information in this context. Constraints on the total width from the combination of on-peak and off-peak contributions in Higgs decays to ZZ^* rely on the assumption of equal on- and off-shell effective couplings. Without an experimental determination of the total width or further theoretical assumptions, only ratios of couplings can be determined at the LHC rather than absolute values of couplings.

NODE=S126W

VALUE (MeV)	CL%	DOCUMENT ID	TECN	COMMENT
$3.7^{+1.9}_{-1.4}$ OUR AVERAGE				
[$3.2^{+2.4}_{-1.7}$ MeV OUR 2023 AVERAGE]				
$4.5^{+3.3}_{-2.5}$		[1] AAD	23BR ATLS	pp, 13 TeV, $ZZ^*/ZZ \to 4\ell$, $ZZ \to 2\ell 2\nu$
$3.2^{+2.4}_{-1.7}$		[2] TUMASYAN	22AM CMS	pp, 13 TeV, $ZZ^*/ZZ \to 4\ell$, $ZZ \to 2\ell 2\nu$
• • • We do not use the following data for averages, fits, limits, etc. • • •				
$3.2^{+2.8}_{-2.2}$		[3] SIRUNYAN	19BL CMS	pp, 7, 8, 13 TeV, $ZZ^*/ZZ \to 4\ell$
$<$ 14.4	95	[4] AABOUD	18BP ATLS	pp, 13 TeV, $ZZ \to 4\ell$, $2\ell 2\nu$
$<$1100	95	[5] SIRUNYAN	17AV CMS	pp, 13 TeV, $ZZ^* \to 4\ell$
$<$ 26	95	[6] KHACHATRY...	16BA CMS	pp, 7, 8 TeV, $WW^{(*)}$
$<$ 13	95	[7] KHACHATRY...	16BA CMS	pp, 7, 8 TeV, $ZZ^{(*)}$, $WW^{(*)}$
$<$ 22.7	95	[8] AAD	15BE ATLS	pp, 8 TeV, $ZZ^{(*)}$, $WW^{(*)}$
$<$1700	95	[9] KHACHATRY...	15AM CMS	pp, 7, 8 TeV
$>$ 3.5×10^{-9}	95	[10] KHACHATRY...	15BA CMS	pp, 7, 8 TeV, flight distance
$<$ 46	95	[11] KHACHATRY...	15BA CMS	pp, 7, 8 TeV, $ZZ^{(*)} \to 4\ell$
$<$5000	95	[12] AAD	14W ATLS	pp, 7, 8 TeV, $\gamma\gamma$
$<$2600	95	[12] AAD	14W ATLS	pp, 7, 8 TeV, $ZZ^* \to 4\ell$
$<$3400	95	[13] CHATRCHYAN	14AA CMS	pp, 7, 8 TeV, $ZZ^* \to 4\ell$
$<$ 22	95	[14] KHACHATRY...	14D CMS	pp, 7, 8 TeV, $ZZ^{(*)}$
$<$2400	95	[15] KHACHATRY...	14P CMS	pp, 7, 8 TeV, $\gamma\gamma$

NEW

OCCUR=2

OCCUR=2

OCCUR=2

[1] AAD 23BR use 139 fb^{-1} at E_{cm} = 13 TeV. The off-shell Higgs boson production in the $ZZ \to 4\ell$ and $ZZ \to 2\ell 2\nu$ decay channels and the on-shell production in the $ZZ^* \to 4\ell$ ($\ell = e, \mu$, AAD 20AQ) decay channels are used to measure the total width. The off-shell Higgs signal strength is measured to be $1.1^{+0.7}_{-0.6}$ assuming the same on-shell and off-shell coupling modifiers are used individually for gluon-fusion and for gauge-boson modes. The scenario of no off-shell contribution is excluded at 3.3 σ. Combining with the on-shell signal strength measurement, the total width normalized to its SM expectation Γ_H/Γ_H^{SM} is measured to be $1.1^{+0.7}_{-0.6}$ assuming the same on-shell and off-shell coupling modifiers are used individually for gluon-fusion and for gauge-boson modes. The observed upper limit on the total width is 10.5 MeV at 95% CL. See their Fig. 7.

NODE=S126W;LINKAGE=N

[2] TUMASYAN 22AM use up to 140 fb^{-1} at E_{cm} = 13 TeV. The off-shell Higgs boson production in the $ZZ \to 4\ell$ and $ZZ \to 2\ell 2\nu$ decay channels and the on-shell production in the $ZZ^* \to 4\ell$ ($\ell = e, \mu$) decay channels are used to measure the total width. The off-shell Higgs signal strength is measured to be $0.62^{+0.68}_{-0.45}$ without the constraint on the ratio of the off-shell signal strengths for gluon-fusion and gauge-boson modes. The scenario of no off-shell contribution is excluded at 3.6 σ. The results are shown in their Table 1 with other constraint scenarios and the decay widths assuming the same coupling modifiers for on- and off-shell couplings (g_p and g_d in their notation). The measurement of anomalous HVV couplings is shown in their Extended Data Table 1 and Fig. 8.

NODE=S126W;LINKAGE=M

[3] SIRUNYAN 19BL measure the width and anomalous HVV couplings from on-shell and off-shell production in the 4ℓ final state. Data of 80.2 fb^{-1} at 13 TeV, 19.7 fb^{-1} at 8 TeV, and 5.1 fb^{-1} at 7 TeV are used. The total width for the SM-like couplings is measured to be also [0.08, 9.16] MeV with 95% CL, assuming SM-like couplings for on- and off-shells (see their Table VIII). Constraints on the total width for anomalous HVV interaction cases are found in their Table IX. See their Table X for the Higgs boson signal strength in the off-shell region.

NODE=S126W;LINKAGE=L

[4] AABOUD 18BP use 36.1 fb^{-1} at E_{cm} = 13 TeV. An observed upper limit on the off-shell Higgs signal strength of 3.8 is obtained at 95% CL using off-shell Higgs boson production in the $ZZ \to 4\ell$ and $ZZ \to 2\ell 2\nu$ decay channels ($\ell = e, \mu$). Combining with the on-shell signal strength measurements, the quoted upper limit on the Higgs boson total width is obtained, assuming the ratios of the relevant Higgs-boson couplings to the SM predictions are constant with energy from on-shell production to the high-mass range.

NODE=S126W;LINKAGE=K

[5] SIRUNYAN 17AV obtain an upper limit on the width from the $m_{4\ell}$ distribution in $ZZ^* \to 4\ell$ ($\ell = e,\ \mu$) decays. Data of 35.9 fb^{-1} pp collisions at E_{cm} = 13 TeV is used. The expected limit is 1.60 GeV. NODE=S126W;LINKAGE=J

[6] KHACHATRYAN 16BA derive constraints on the total width from comparing $WW^{(*)}$ production via on-shell and off-shell H using 4.9 fb^{-1} of pp collisions at E_{cm} = 7 TeV and 19.4 fb^{-1} at 8 TeV. NODE=S126W;LINKAGE=H

[7] KHACHATRYAN 16BA combine the $WW^{(*)}$ result with $ZZ^{(*)}$ results of KHACHATRYAN 15BA and KHACHATRYAN 14D. NODE=S126W;LINKAGE=I

[8] AAD 15BE derive constraints on the total width from comparing $ZZ^{(*)}$ and $WW^{(*)}$ production via on-shell and off-shell H using 20.3 fb^{-1} of pp collisions at E_{cm} = 8 TeV. The K factor for the background processes is assumed to be equal to that for the signal. NODE=S126W;LINKAGE=G

[9] KHACHATRYAN 15AM combine $\gamma\gamma$ and $ZZ^* \to 4\ell$ results. The expected limit is 2.3 GeV. NODE=S126W;LINKAGE=D

[10] KHACHATRYAN 15BA derive a lower limit on the total width from an upper limit on the decay flight distance $\tau < 1.9 \times 10^{-13}$ s. 5.1 fb^{-1} of pp collisions at E_{cm} = 7 TeV and 19.7 fb^{-1} at 8 TeV are used. NODE=S126W;LINKAGE=E

[11] KHACHATRYAN 15BA derive constraints on the total width from comparing $ZZ^{(*)}$ production via on-shell and off-shell H with an unconstrained anomalous coupling. 4ℓ final states in 5.1 fb^{-1} of pp collisions at E_{cm} = 7 TeV and 19.7 fb^{-1} at E_{cm} = 8 TeV are used. NODE=S126W;LINKAGE=F

[12] AAD 14W use 4.5 fb^{-1} of pp collisions at E_{cm} = 7 TeV and 20.3 fb^{-1} at 8 TeV. The expected limit is 6.2 GeV. NODE=S126W;LINKAGE=AA

[13] CHATRCHYAN 14AA use 5.1 fb^{-1} of pp collisions at E_{cm} = 7 TeV and 19.7 fb^{-1} at E_{cm} = 8 TeV. The expected limit is 2.8 GeV. NODE=S126W;LINKAGE=B

[14] KHACHATRYAN 14D derive constraints on the total width from comparing $ZZ^{(*)}$ production via on-shell and off-shell H. 4ℓ and $\ell\ell\nu\nu$ final states in 5.1 fb^{-1} of pp collisions at E_{cm} = 7 TeV and 19.7 fb^{-1} at E_{cm} = 8 TeV are used. NODE=S126W;LINKAGE=A

[15] KHACHATRYAN 14P use 5.1 fb^{-1} of pp collisions at E_{cm} = 7 TeV and 19.7 fb^{-1} at E_{cm} = 8 TeV. The expected limit is 3.1 GeV. NODE=S126W;LINKAGE=C

H DECAY MODES

NODE=S126220;NODE=S126

	Mode		Fraction (Γ_i/Γ)	Confidence level	
Γ_1	WW^*		(25.7 ± 2.5) %		DESIG=1
Γ_2	ZZ^*		(2.80 ± 0.30) %		DESIG=2
Γ_3	$\gamma\gamma$		$(2.50 \pm 0.20) \times 10^{-3}$		DESIG=3
Γ_4	$b\bar{b}$		(53 ± 8) %		DESIG=4
Γ_5	e^+e^-		$< 3.0 \times 10^{-4}$	95%	DESIG=10
Γ_6	$\mu^+\mu^-$		$(2.6 \pm 1.3) \times 10^{-4}$		DESIG=8
Γ_7	$\tau^+\tau^-$		$(6.0\ ^{+0.8}_{-0.7})$ %		DESIG=5
Γ_8	$Z\gamma$		$(3.4 \pm 1.1) \times 10^{-3}$		DESIG=6
Γ_9	$Z\rho(770)$		< 1.21 %	95%	DESIG=25
Γ_{10}	$Z\phi(1020)$		$< 3.6 \times 10^{-3}$	95%	DESIG=26
Γ_{11}	$Z\eta_c$				DESIG=27
Γ_{12}	ZJ/ψ		$< 1.9 \times 10^{-3}$	95%	DESIG=28
Γ_{13}	$Z\psi(2S)$		$< 6.6 \times 10^{-3}$	95%	DESIG=29
Γ_{14}	$J/\psi\gamma$		$< 2.0 \times 10^{-4}$	95%	DESIG=11
Γ_{15}	$J/\psi J/\psi$		$< 3.8 \times 10^{-4}$	95%	DESIG=22
Γ_{16}	$\psi(2S)\gamma$		$< 1.05 \times 10^{-3}$	95%	DESIG=20
Γ_{17}	$\psi(2S)J/\psi$		$< 2.1 \times 10^{-3}$	95%	DESIG=30
Γ_{18}	$\psi(2S)\psi(2S)$		$< 3.0 \times 10^{-3}$	95%	DESIG=31
Γ_{19}	$\Upsilon(1S)\gamma$		$< 2.5 \times 10^{-4}$	95%	DESIG=12
Γ_{20}	$\Upsilon(1S)\Upsilon(1S)$		$< 1.7 \times 10^{-3}$	95%	DESIG=32
Γ_{21}	$\Upsilon(2S)\gamma$		$< 4.2 \times 10^{-4}$	95%	DESIG=13
Γ_{22}	$\Upsilon(3S)\gamma$		$< 3.4 \times 10^{-4}$	95%	DESIG=14
Γ_{23}	$\Upsilon(\mathrm{nS})\Upsilon(\mathrm{mS})$		$< 3.5 \times 10^{-4}$	95%	DESIG=23
Γ_{24}	$\rho(770)\gamma$		$< 1.04 \times 10^{-3}$	95%	DESIG=19
Γ_{25}	$\omega(782)\gamma$		$< 5.5 \times 10^{-4}$	95%	DESIG=33
Γ_{26}	$K^*(892)\gamma$		$< 2.2 \times 10^{-4}$	95%	DESIG=34
Γ_{27}	$\phi(1020)\gamma$		$< 5 \times 10^{-4}$	95%	DESIG=15
Γ_{28}	$e\mu$	*LF*	$< 4.4 \times 10^{-5}$	95%	DESIG=17
Γ_{29}	$e\tau$	*LF*	$< 2.0 \times 10^{-3}$	95%	DESIG=18
Γ_{30}	$\mu\tau$	*LF*	$< 1.5 \times 10^{-3}$	95%	DESIG=9
Γ_{31}	invisible		< 10.7 %	95%	DESIG=7
Γ_{32}	γ invisible		< 2.9 %	95%	DESIG=24

H BRANCHING RATIOS

NODE=S126225

$\Gamma(WW^*)/\Gamma_{total}$ Γ_1/Γ

NODE=S126R20
NODE=S126R20

VALUE	DOCUMENT ID		TECN	COMMENT
$\mathbf{0.257^{+0.026}_{-0.024}}$	[1] ATLAS	22	ATLS	pp, 13 TeV

[1] ATLAS 22 report combined results (see their Extended Data Table 1) using up to 139 fb^{-1} of data at E_{cm} = 13 TeV, assuming m_H = 125.09 GeV. SM values for the production cross-sections are assumed. See their Fig. 2b.

NODE=S126R20;LINKAGE=A

$\Gamma(ZZ^*)/\Gamma_{total}$ Γ_2/Γ

NODE=S126R21
NODE=S126R21

VALUE	DOCUMENT ID		TECN	COMMENT
0.028±0.003	[1] ATLAS	22	ATLS	pp, 13 TeV

[1] ATLAS 22 report combined results (see their Extended Data Table 1) using up to 139 fb^{-1} of data at E_{cm} = 13 TeV, assuming m_H = 125.09 GeV. SM values for the production cross-sections are assumed. See their Fig. 2b.

NODE=S126R21;LINKAGE=A

$\Gamma(\gamma\gamma)/\Gamma_{total}$ Γ_3/Γ

NODE=S126R22
NODE=S126R22

VALUE	DOCUMENT ID		TECN	COMMENT
0.0025±0.0002	[1] ATLAS	22	ATLS	pp, 13 TeV

[1] ATLAS 22 report combined results (see their Extended Data Table 1) using up to 139 fb^{-1} of data at E_{cm} = 13 TeV, assuming m_H = 125.09 GeV. SM values for the production cross-sections are assumed. See their Fig. 2b.

NODE=S126R22;LINKAGE=A

$\Gamma(b\overline{b})/\Gamma_{total}$ Γ_4/Γ

NODE=S126R23
NODE=S126R23

VALUE	DOCUMENT ID		TECN	COMMENT
0.53±0.08	[1] ATLAS	22	ATLS	pp, 13 TeV

[1] ATLAS 22 report combined results (see their Extended Data Table 1) using up to 139 fb^{-1} of data at E_{cm} = 13 TeV, assuming m_H = 125.09 GeV. SM values for the production cross-sections are assumed. See their Fig. 2b.

NODE=S126R23;LINKAGE=A

$\Gamma(e^+e^-)/\Gamma_{total}$ Γ_5/Γ

NODE=S126R03
NODE=S126R03

VALUE	CL%	DOCUMENT ID		TECN	COMMENT
$\mathbf{<3.0 \times 10^{-4}}$ **(CL = 95%)** [$<3.6 \times 10^{-4}$ (CL = 95%) OUR 2023 BEST LIMIT]					
$\mathbf{<3.0 \times 10^{-4}}$	95	[1] TUMASYAN	23AU	CMS	pp, 13 TeV
• • • We do not use the following data for averages, fits, limits, etc. • • •					
$<3.6 \times 10^{-4}$	95	[2] AAD	20F	ATLS	pp, 13 TeV
$<1.9 \times 10^{-3}$	95	[3] KHACHATRY...	15H	CMS	pp, 7, 8 TeV

[1] TUMASYAN 23AU use 138 fb^{-1} of pp collisions at E_{cm} = 13 TeV.

NODE=S126R03;LINKAGE=C

[2] AAD 20F use 139 fb^{-1} of pp collisions at E_{cm} = 13 TeV. The best-fit value of the $H \rightarrow ee$ branching fraction is $(0.0 \pm 1.7 \pm 0.6) \times 10^{-4}$ for m_H = 125 GeV.

NODE=S126R03;LINKAGE=B

[3] KHACHATRYAN 15H use 5.0 fb^{-1} of pp collisions at E_{cm} = 7 TeV and 19.7 fb^{-1} at 8 TeV.

NODE=S126R03;LINKAGE=A

$\Gamma(\mu^+\mu^-)/\Gamma_{total}$ Γ_6/Γ

NODE=S126R24
NODE=S126R24

VALUE (units 10^{-4})	DOCUMENT ID		TECN	COMMENT
2.6±1.3	[1] ATLAS	22	ATLS	pp, 13 TeV

[1] ATLAS 22 report combined results (see their Extended Data Table 1) using up to 139 fb^{-1} of data at E_{cm} = 13 TeV, assuming m_H = 125.09 GeV. SM values for the production cross-sections are assumed. See their Fig. 2b.

NODE=S126R24;LINKAGE=A

$\Gamma(\tau^+\tau^-)/\Gamma_{total}$ Γ_7/Γ

NODE=S126R25
NODE=S126R25

VALUE	DOCUMENT ID		TECN	COMMENT
$\mathbf{0.060^{+0.008}_{-0.007}}$	[1] ATLAS	22	ATLS	pp, 13 TeV

[1] ATLAS 22 report combined results (see their Extended Data Table 1) using up to 139 fb^{-1} of data at E_{cm} = 13 TeV, assuming m_H = 125.09 GeV. SM values for the production cross-sections are assumed. See their Fig. 2b.

NODE=S126R25;LINKAGE=A

$\Gamma(Z\gamma)/\Gamma_{total}$ Γ_8/Γ

NODE=S126R26
NODE=S126R26

VALUE (units 10^{-3})	DOCUMENT ID		TECN	COMMENT
3.4±1.1 OUR AVERAGE [$(3.2 \pm 1.5) \times 10^{-3}$ OUR 2023 AVERAGE]				
3.4±1.1	[1] AAD	24D	LHC	pp, 13 TeV
• • • We do not use the following data for averages, fits, limits, etc. • • •				
3.2±1.5	[2] ATLAS	22	ATLS	pp, 13 TeV

NEW

[1] AAD 24D report combined results of ATLAS (AAD 20AG) and CMS (TUMASYAN 23F). SM values for the production cross-sections are assumed. NODE=S126R26;LINKAGE=B

[2] ATLAS 22 report combined results (see their Extended Data Table 1) using up to 139 fb^{-1} of data at E_{cm} = 13 TeV, assuming m_H = 125.09 GeV. SM values for the production cross-sections are assumed. See their Fig. 2b. NODE=S126R26;LINKAGE=A

$\Gamma(Z\rho(770))/\Gamma_{total}$ — Γ_9/Γ

NODE=S126R16
NODE=S126R16

VALUE	CL%	DOCUMENT ID	TECN	COMMENT
<1.21 × 10^{-2}	95	[1] SIRUNYAN 20BK	CMS	pp, 13 TeV

[1] SIRUNYAN 20BK search for $H \rightarrow Z\rho$, $Z \rightarrow e^+e^-/\mu^+\mu^-$, $\rho \rightarrow \pi^+\pi^-$ with 137 fb^{-1} of pp collision data at E_{cm} = 13 TeV. The quoted branching fraction is for the unpolarized decay. See their Table 3 for different polarizations. NODE=S126R16;LINKAGE=A

$\Gamma(Z\phi(1020))/\Gamma_{total}$ — Γ_{10}/Γ

NODE=S126R17
NODE=S126R17

VALUE	CL%	DOCUMENT ID	TECN	COMMENT
<3.6 × 10^{-3}	95	[1] SIRUNYAN 20BK	CMS	pp, 13 TeV

[1] SIRUNYAN 20BK search for $H \rightarrow Z\phi$, $Z \rightarrow e^+e^-/\mu^+\mu^-$, $\phi \rightarrow K^+K^-$ with 137 fb^{-1} of pp collision data at E_{cm} = 13 TeV. The quoted branching fraction is for the unpolarized decay. See their Table 4 for different polarizations. NODE=S126R17;LINKAGE=A

$\Gamma(Z\eta_c)/\Gamma_{total}$ — Γ_{11}/Γ

NODE=S126R18
NODE=S126R18

VALUE	DOCUMENT ID	TECN	COMMENT
• • • We do not use the following data for averages, fits, limits, etc. • • •			
	[1] AAD 20AE	ATLS	pp, 13 TeV

[1] AAD 20AE search for $H \rightarrow Z\eta_c$ with two-leptons ($e^+e^-/\mu^+\mu^-$) plus jet events using 139 fb^{-1} of pp collision data at E_{cm} = 13 TeV. The upper limit of $\sigma(pp \rightarrow H)\cdot B(H \rightarrow Z\eta_c)$ is 110 pb at 95% CL. NODE=S126R18;LINKAGE=A

$\Gamma(ZJ/\psi)/\Gamma_{total}$ — Γ_{12}/Γ

NODE=S126R19
NODE=S126R19

VALUE	CL%	DOCUMENT ID	TECN	COMMENT
<1.9 × 10^{-3}	95	[1] TUMASYAN 23C	CMS	pp, 13 TeV
• • • We do not use the following data for averages, fits, limits, etc. • • •				
		[2] AAD 20AE	ATLS	pp, 13 TeV

[1] TUMASYAN 23C search for $H \rightarrow ZJ/\psi$, $Z \rightarrow e^+e^-$ or $\mu^+\mu^-$, $J/\psi \rightarrow \mu^+\mu^-$ with 138 fb^{-1} of pp collision data at E_{cm} = 13 TeV. The quoted value is for the Higgs decays for longitudinally polarized mesons. See their Table 1 for other cases. NODE=S126R19;LINKAGE=B

[2] AAD 20AE search for $H \rightarrow ZJ/\psi$ with two-leptons ($e^+e^-/\mu^+\mu^-$) plus jet events using 139 fb^{-1} of pp collision data at E_{cm} = 13 TeV. The upper limit of $\sigma(pp \rightarrow H)\cdot B(H \rightarrow ZJ/\psi)$ is 100 pb at 95% CL. NODE=S126R19;LINKAGE=A

$\Gamma(Z\psi(2S))/\Gamma_{total}$ — Γ_{13}/Γ

NODE=S126R27
NODE=S126R27

VALUE	CL%	DOCUMENT ID	TECN	COMMENT
<6.6 × 10^{-3}	95	[1] TUMASYAN 23C	CMS	pp, 13 TeV

[1] TUMASYAN 23C search for $H \rightarrow Z\psi(2S)$, $Z \rightarrow e^+e^-$ or $\mu^+\mu^-$, $\psi(2S) \rightarrow \mu^+\mu^-$ with 138 fb^{-1} of pp collision data at E_{cm} = 13 TeV. The quoted value is for the Higgs decays for longitudinally polarized mesons. See their Table 1 for other cases. NODE=S126R27;LINKAGE=A

$\Gamma(J/\psi\gamma)/\Gamma_{total}$ — Γ_{14}/Γ

NODE=S126R04
NODE=S126R04

VALUE	CL%	DOCUMENT ID	TECN	COMMENT
<2.0 × 10^{-4} (CL = 95%) [<3.5 × 10^{-4} (CL = 95%) OUR 2023 BEST LIMIT]				
<2.0 × 10^{-4}	95	[1] AAD 23CD	ATLS	13 TeV, 138 fb^{-1}
• • • We do not use the following data for averages, fits, limits, etc. • • •				
<7.6 × 10^{-4}	95	[2] SIRUNYAN 19AJ	CMS	13 TeV, 35.9 fb^{-1}
<3.5 × 10^{-4}	95	[3] AABOUD 18BL	ATLS	13 TeV, 36.1 fb^{-1}
<1.5 × 10^{-3}	95	[4] KHACHATRY...16B	CMS	8 TeV
<1.5 × 10^{-3}	95	[5] AAD 15I	ATLS	8 TeV

[1] AAD 23CD search for $H \rightarrow J/\psi\gamma$, $J/\psi \rightarrow \mu^+\mu^-$ with 138 fb^{-1} of pp collision data at E_{cm} = 13 TeV. SM values for the production cross-sections are assumed. NODE=S126R04;LINKAGE=E

[2] SIRUNYAN 19AJ search for $H \rightarrow J/\psi\gamma$, $J/\psi \rightarrow \mu^+\mu^-$ with 35.9 fb^{-1} of pp collision data at E_{cm} = 13 TeV. The upper limit corresponds to 260 times the SM prediction and by combining the KHACHATRYAN 16B, it is 220 times the SM prediction. NODE=S126R04;LINKAGE=D

[3] AABOUD 18BL search for $H \rightarrow J/\psi\gamma$, $J/\psi \rightarrow \mu^+\mu^-$ with 36.1 fb^{-1} of pp collision data at E_{cm} = 13 TeV. NODE=S126R04;LINKAGE=C

[4] KHACHATRYAN 16B use 19.7 fb^{-1} of pp collision data at 8 TeV. NODE=S126R04;LINKAGE=B

[5] AAD 15I use 19.7 fb^{-1} of pp collision data at 8 TeV. NODE=S126R04;LINKAGE=A

$\Gamma(J/\psi J/\psi)/\Gamma_{total}$ Γ_{15}/Γ

NODE=S126R13
NODE=S126R13

VALUE	CL%	DOCUMENT ID	TECN	COMMENT
<3.8 × 10^−4 (CL = 95%) [<1.8 × 10^−3 (CL = 95%) OUR 2023 BEST LIMIT]				
<3.8 × 10^−4	95	[1] TUMASYAN	23C CMS	pp, 13 TeV
• • • We do not use the following data for averages, fits, limits, etc. • • •				
<1.8 × 10^−3	95	[2] SIRUNYAN	19BR CMS	pp at 13 TeV

[1] TUMASYAN 23C search for $H \to J/\psi J/\psi$, $J/\psi \to \mu^+\mu^-$ with 138 fb^{-1} of pp collision data at E_{cm} = 13 TeV. The quoted value is for the Higgs decays for longitudinally polarized mesons. See their Table 1 for other cases.
NODE=S126R13;LINKAGE=B

[2] SIRUNYAN 19BR search for $H \to J/\psi J/\psi$, $J/\psi \to \mu^+\mu^-$ with 37.5 fb^{-1} of pp collision data at E_{cm} = 13 TeV. J/ψs from the Higgs decay are assumed to be unpolarized. For fully longitudinal (transverse) polarized J/ψs, limits change by −22% (+10%).
NODE=S126R13;LINKAGE=A

$\Gamma(\psi(2S)\gamma)/\Gamma_{total}$ Γ_{16}/Γ

NODE=S126R12
NODE=S126R12

VALUE	CL%	DOCUMENT ID	TECN	COMMENT
<1.05 × 10^−3 (CL = 95%) [<2.0 × 10^−3 (CL = 95%) OUR 2023 BEST LIMIT]				
<1.05 × 10^−3	95	[1] AAD	23CD ATLS	13 TeV, 138 fb^{-1}
• • • We do not use the following data for averages, fits, limits, etc. • • •				
<2.0 × 10^−3	95	[2] AABOUD	18BL ATLS	13 TeV, 36.1 fb^{-1}

[1] AAD 23CD search for $H \to \psi(2S)\gamma$, $\psi(2S) \to \mu^+\mu^-$ with 138 fb^{-1} of pp collision data at E_{cm} = 13 TeV. SM values for the production cross-sections are assumed.
NODE=S126R12;LINKAGE=B

[2] AABOUD 18BL search for $H \to \psi(2S)\gamma$, $\psi(2S) \to \mu^+\mu^-$ with 36.1 fb^{-1} of pp collision data at E_{cm} = 13 TeV.
NODE=S126R12;LINKAGE=A

$\Gamma(\psi(2S)J/\psi)/\Gamma_{total}$ Γ_{17}/Γ

NODE=S126R28
NODE=S126R28

VALUE	CL%	DOCUMENT ID	TECN	COMMENT
<2.1 × 10^−3	95	[1] TUMASYAN	23C CMS	pp, 13 TeV

[1] TUMASYAN 23C search for $H \to \psi(2S)J/\psi$, $\psi(2S) \to \mu^+\mu^-$, $J/\psi \to \mu^+\mu^-$ with 138 fb^{-1} of pp collision data at E_{cm} = 13 TeV. The quoted value is for the Higgs decays for longitudinally polarized mesons. See their Table 1 for other cases.
NODE=S126R28;LINKAGE=A

$\Gamma(\psi(2S)\psi(2S))/\Gamma_{total}$ Γ_{18}/Γ

NODE=S126R29
NODE=S126R29

VALUE	CL%	DOCUMENT ID	TECN	COMMENT
<3.0 × 10^−3	95	[1] TUMASYAN	23C CMS	pp, 13 TeV

[1] TUMASYAN 23C search for $H \to \psi(2S)\psi(2S)$, $\psi(2S) \to \mu^+\mu^-$ with 138 fb^{-1} of pp collision data at E_{cm} = 13 TeV. The quoted value is for the Higgs decays for longitudinally polarized mesons. See their Table 1 for other cases.
NODE=S126R29;LINKAGE=A

$\Gamma(\Upsilon(1S)\gamma)/\Gamma_{total}$ Γ_{19}/Γ

NODE=S126R05
NODE=S126R05

VALUE	CL%	DOCUMENT ID	TECN	COMMENT
<2.5 × 10^−4 (CL = 95%) [<4.9 × 10^−4 (CL = 95%) OUR 2023 BEST LIMIT]				
<2.5 × 10^−4	95	[1] AAD	23CD ATLS	13 TeV, 138 fb^{-1}
• • • We do not use the following data for averages, fits, limits, etc. • • •				
<4.9 × 10^−4	95	[2] AABOUD	18BL ATLS	13 TeV, 36.1 fb^{-1}
<1.3 × 10^−3	95	[3] AAD	15I ATLS	8 TeV

[1] AAD 23CD search for $H \to \Upsilon(1S)\gamma$, $\Upsilon(1S) \to \mu^+\mu^-$ with 138 fb^{-1} of pp collision data at E_{cm} = 13 TeV. SM values for the production cross-sections are assumed.
NODE=S126R05;LINKAGE=C

[2] AABOUD 18BL search for $H \to \Upsilon(1S)\gamma$, $\Upsilon(1S) \to \mu^+\mu^-$ with 36.1 fb^{-1} of pp collision data at E_{cm} = 13 TeV.
NODE=S126R05;LINKAGE=B

[3] AAD 15I use 19.7 fb^{-1} of pp collision data at 8 TeV.
NODE=S126R05;LINKAGE=A

$\Gamma(\Upsilon(1S)\Upsilon(1S))/\Gamma_{total}$ Γ_{20}/Γ

NODE=S126R30
NODE=S126R30

VALUE	CL%	DOCUMENT ID	TECN	COMMENT
<1.7 × 10^−3	95	[1] TUMASYAN	23C CMS	pp, 13 TeV

[1] TUMASYAN 23C search for $H \to \Upsilon(1S)\Upsilon(1S)$, $\Upsilon(1S) \to \mu^+\mu^-$ with 138 fb^{-1} of pp collision data at E_{cm} = 13 TeV. The quoted value is for the Higgs decays for longitudinally polarized mesons. See their Table 1 for other cases.
NODE=S126R30;LINKAGE=A

$\Gamma(\Upsilon(2S)\gamma)/\Gamma_{total}$ Γ_{21}/Γ

NODE=S126R06
NODE=S126R06

VALUE	CL%	DOCUMENT ID	TECN	COMMENT
<4.2 × 10^−4 (CL = 95%) [<5.9 × 10^−4 (CL = 95%) OUR 2023 BEST LIMIT]				
<4.2 × 10^−4	95	[1] AAD	23CD ATLS	13 TeV, 138 fb^{-1}
• • • We do not use the following data for averages, fits, limits, etc. • • •				
<5.9 × 10^−4	95	[2] AABOUD	18BL ATLS	13 TeV, 36.1 fb^{-1}
<1.9 × 10^−3	95	[3] AAD	15I ATLS	8 TeV

[1] AAD 23CD search for $H \to \Upsilon(2S)\gamma$, $\Upsilon(2S) \to \mu^+\mu^-$ with 138 fb^{-1} of pp collision data at E_{cm} = 13 TeV. SM values for the production cross-sections are assumed. NODE=S126R06;LINKAGE=C

[2] AABOUD 18BL search for $H \to \Upsilon(2S)\gamma$, $\Upsilon(2S) \to \mu^+\mu^-$ with 36.1 fb^{-1} of pp collision data at E_{cm} = 13 TeV. NODE=S126R06;LINKAGE=B

[3] AAD 15I use 19.7 fb^{-1} of pp collision data at 8 TeV. NODE=S126R06;LINKAGE=A

$\Gamma(\Upsilon(3S)\gamma)/\Gamma_{total}$ Γ_{22}/Γ

NODE=S126R07
NODE=S126R07

VALUE	CL%	DOCUMENT ID	TECN	COMMENT
<3.4 × 10^{-4} (CL = 95%) [<5.7 × 10^{-4} (CL = 95%) OUR 2023 BEST LIMIT]				
<3.4 × 10^{-4}	95	[1] AAD	23CD ATLS	13 TeV, 138 fb^{-1}
• • • We do not use the following data for averages, fits, limits, etc. • • •				
<5.7 × 10^{-4}	95	[2] AABOUD	18BL ATLS	13 TeV, 36.1 fb^{-1}
<1.3 × 10^{-3}	95	[3] AAD	15I ATLS	8 TeV

[1] AAD 23CD search for $H \to \Upsilon(3S)\gamma$, $\Upsilon(3S) \to \mu^+\mu^-$ with 138 fb^{-1} of pp collision data at E_{cm} = 13 TeV. SM values for the production cross-sections are assumed. NODE=S126R07;LINKAGE=C

[2] AABOUD 18BL search for $H \to \Upsilon(3S)\gamma$, $\Upsilon(3S) \to \mu^+\mu^-$ with 36.1 fb^{-1} of pp collision data at E_{cm} = 13 TeV. NODE=S126R07;LINKAGE=B

[3] AAD 15I use 19.7 fb^{-1} of pp collision data at 8 TeV. NODE=S126R07;LINKAGE=A

$\Gamma(\Upsilon(\mathrm{nS})\,\Upsilon(\mathrm{mS}))/\Gamma_{total}$ Γ_{23}/Γ

NODE=S126R14
NODE=S126R14

VALUE	CL%	DOCUMENT ID	TECN	COMMENT
<3.5 × 10^{-4} (CL = 95%) [<1.4 × 10^{-3} (CL = 95%) OUR 2023 BEST LIMIT]				
<3.5 × 10^{-4}	95	[1] TUMASYAN	23C CMS	pp, 13 TeV
• • • We do not use the following data for averages, fits, limits, etc. • • •				
<1.4 × 10^{-3}	95	[2] SIRUNYAN	19BR CMS	pp, 13 TeV

[1] TUMASYAN 23C search for $H \to \Upsilon(\mathrm{nS})\,\Upsilon(\mathrm{mS})$ with $\Upsilon(\mathrm{nS})$, $\Upsilon(\mathrm{mS}) \to \mu^+\mu^-$ (n, m = 1, 2, 3) with 138 fb^{-1} of pp collision data at E_{cm} = 13 TeV. The quoted value is for the Higgs decays for longitudinally polarized mesons. See their Table 1 for other cases. NODE=S126R14;LINKAGE=B

[2] SIRUNYAN 19BR search for $H \to \Upsilon(\mathrm{nS})\,\Upsilon(\mathrm{mS})$ with $\Upsilon(\mathrm{nS}),\Upsilon(\mathrm{mS}) \to \mu^+\mu^-$ (n, m = 1, 2, 3) for 37.5 fb^{-1} of pp collision data at E_{cm} = 13 TeV. Υs from the Higgs decay are assumed to be unpolarized. For fully longitudinal (transverse) polarized Υs, limits change by −22% (+10%). The three Υ states selected in a mass range of 8.5–11 GeV are not distinguished. NODE=S126R14;LINKAGE=A

$\Gamma(\rho(770)\gamma)/\Gamma_{total}$ Γ_{24}/Γ

NODE=S126R11
NODE=S126R11

VALUE	CL%	DOCUMENT ID	TECN	COMMENT
<10.4 × 10^{-4} (CL = 95%) [<8.8 × 10^{-4} (CL = 95%) OUR 2023 BEST LIMIT]				
<10.4 × 10^{-4}	95	[1] AABOUD	18AU ATLS	pp, 13 TeV

[1] AABOUD 18AU use 35.6 fb^{-1} of pp collision data at 13 TeV. See their erratum AABOUD 23A. NODE=S126R11;LINKAGE=A

$\Gamma(\omega(782)\gamma)/\Gamma_{total}$ Γ_{25}/Γ

NODE=S126R31
NODE=S126R31

VALUE	CL%	DOCUMENT ID	TECN	COMMENT
<5.5 × 10^{-4}	95	[1] AAD	23BS ATLS	pp, 13 TeV

[1] AAD 23BS use 89.5 fb^{-1} of pp collision data at 13 TeV. NODE=S126R31;LINKAGE=A

$\Gamma(K^*(892)\gamma)/\Gamma_{total}$ Γ_{26}/Γ

NODE=S126R32
NODE=S126R32

VALUE	CL%	DOCUMENT ID	TECN	COMMENT
<2.2 × 10^{-4}	95	[1] AAD	23BS ATLS	pp, 13 TeV

[1] AAD 23BS use 134 fb^{-1} of pp collision data at 13 TeV. NODE=S126R32;LINKAGE=A

$\Gamma(\phi(1020)\gamma)/\Gamma_{total}$ Γ_{27}/Γ

NODE=S126R00
NODE=S126R00

VALUE	CL%	DOCUMENT ID	TECN	COMMENT
<5 × 10^{-4} (CL = 95%) [<4.8 × 10^{-4} (CL = 95%) OUR 2023 BEST LIMIT]				
<5 × 10^{-4}	95	[1] AABOUD	18AU ATLS	pp, 13 TeV
• • • We do not use the following data for averages, fits, limits, etc. • • •				
<1.4 × 10^{-3}	95	[2] AABOUD	16K ATLS	pp, 13 TeV

[1] AABOUD 18AU use 35.6 fb^{-1} of pp collision data at 13 TeV. See their erratum AABOUD 23A. NODE=S126R00;LINKAGE=B

[2] AABOUD 16K use 2.7 fb^{-1} of pp collision data at 13 TeV. NODE=S126R00;LINKAGE=A

$\Gamma(e\mu)/\Gamma_{total}$ Γ_{28}/Γ

NODE=S126R09
NODE=S126R09

VALUE	CL%	DOCUMENT ID	TECN	COMMENT
$<4.4 \times 10^{-5}$ (CL = 95%) [$<6.1 \times 10^{-5}$ (CL = 95%) OUR 2023 BEST LIMIT]				
$<4.4 \times 10^{-5}$	95	[1] HAYRAPETY...23C	CMS	pp, 13 TeV
• • • We do not use the following data for averages, fits, limits, etc. • • •				
$<6.1 \times 10^{-5}$	95	[2] AAD 20F	ATLS	pp, 13 TeV
$<3.5 \times 10^{-4}$	95	[3] KHACHATRY...16CD	CMS	pp, 8 TeV

[1] HAYRAPETYAN 23C use 138 fb^{-1} of pp collisions at E_{cm} = 13 TeV. The limit constrains the $Y_{e\mu}$ Yukawa coupling to $\sqrt{|Y_{e\mu}|^2+|Y_{\mu e}|^2} < 1.9 \times 10^{-4}$ at 95% CL (see their Fig. 6). NODE=S126R09;LINKAGE=C

[2] AAD 20F use 139 fb^{-1} of pp collisions at E_{cm} = 13 TeV. The best-fit value of the $H \rightarrow e\mu$ branching fraction is $(0.4 \pm 2.9 \pm 0.3) \times 10^{-5}$ for m_H = 125 GeV. NODE=S126R09;LINKAGE=B

[3] KHACHATRYAN 16CD search for $H \rightarrow e\mu$ in 19.7 fb^{-1} of pp collisions at E_{cm} = 8 TeV. The limit constrains the $Y_{e\mu}$ Yukawa coupling to $\sqrt{|Y_{e\mu}|^2+|Y_{\mu e}|^2} < 5.4 \times 10^{-4}$ at 95% CL (see their Fig. 6). NODE=S126R09;LINKAGE=A

$\Gamma(e\tau)/\Gamma_{total}$ Γ_{29}/Γ

NODE=S126R10
NODE=S126R10

VALUE	CL%	DOCUMENT ID	TECN	COMMENT
$< 2.0 \times 10^{-3}$ (CL = 95%) [$<2.2 \times 10^{-3}$ (CL = 95%) OUR 2023 BEST LIMIT]				
$< 2.0 \times 10^{-3}$	95	[1] AAD 23Q	ATLS	pp, 13 TeV
• • • We do not use the following data for averages, fits, limits, etc. • • •				
$< 2.3 \times 10^{-3}$	95	[2] AAD 23Q	ATLS	pp, 13 TeV (OCCUR=2)
$< 2.2 \times 10^{-3}$	95	[3] SIRUNYAN 21Z	CMS	pp, 13 TeV
$< 4.7 \times 10^{-3}$	95	[4] AAD 20A	ATLS	pp, 13 TeV
$< 6.1 \times 10^{-3}$	95	[5] SIRUNYAN 18BH	CMS	pp, 13 TeV
$<10.4 \times 10^{-3}$	95	[6] AAD 17	ATLS	pp, 8 TeV
$< 6.9 \times 10^{-3}$	95	[7] KHACHATRY...16CD	CMS	pp, 8 TeV

[1] AAD 23Q search for $H \rightarrow e\tau$ in 138 fb^{-1} of pp collisions at E_{cm} = 13 TeV. The result is obtained from a simultaneous fit of possible $H \rightarrow e\tau$ and $H \rightarrow \mu\tau$ signals (see their Figs. 13 and 14). The limit constrains the $Y_{e\tau}$ Yukawa coupling to $\sqrt{|Y_{e\tau}|^2+|Y_{\tau e}|^2} < 1.3 \times 10^{-3}$ at 95% CL (see their Fig. 15). NODE=S126R10;LINKAGE=F

[2] AAD 23Q search for $H \rightarrow e\tau$ in 138 fb^{-1} of pp collisions at E_{cm} = 13 TeV. The limit constrains the $Y_{e\tau}$ Yukawa coupling to $\sqrt{|Y_{e\tau}|^2+|Y_{\tau e}|^2} < 1.4 \times 10^{-3}$ at 95% CL (see their Fig. 12). NODE=S126R10;LINKAGE=G

[3] SIRUNYAN 21Z search for $H \rightarrow e\tau$ in 137 fb^{-1} of pp collisions at E_{cm} = 13 TeV. The limit constrains the $Y_{e\tau}$ Yukawa coupling to $\sqrt{|Y_{e\tau}|^2+|Y_{\tau e}|^2} < 1.35 \times 10^{-3}$ at 95% CL (see their Fig. 8). NODE=S126R10;LINKAGE=E

[4] AAD 20A search for $H \rightarrow e\tau$ in 36.1 fb^{-1} of pp collisions at E_{cm} = 13 TeV. The limit constrains the $Y_{e\tau}$ Yukawa coupling to $\sqrt{|Y_{e\tau}|^2+|Y_{\tau e}|^2} < 2.0 \times 10^{-3}$ at 95% CL (see their Fig. 5). NODE=S126R10;LINKAGE=D

[5] SIRUNYAN 18BH search for $H \rightarrow e\tau$ in 35.9 fb^{-1} of pp collisions at E_{cm} = 13 TeV. The limit constrains the $Y_{e\tau}$ Yukawa coupling to $\sqrt{|Y_{e\tau}|^2+|Y_{\tau e}|^2} < 2.26 \times 10^{-3}$ at 95% CL (see their Fig. 10). NODE=S126R10;LINKAGE=C

[6] AAD 17 search for $H \rightarrow e\tau$ in 20.3 fb^{-1} of pp collisions at E_{cm} = 8 TeV. NODE=S126R10;LINKAGE=B

[7] KHACHATRYAN 16CD search for $H \rightarrow e\tau$ in 19.7 fb^{-1} of pp collisions at E_{cm} = 8 TeV. The limit constrains the $Y_{e\tau}$ Yukawa coupling to $\sqrt{|Y_{e\tau}|^2+|Y_{\tau e}|^2} < 2.4 \times 10^{-3}$ at 95% CL (see their Fig. 6). NODE=S126R10;LINKAGE=A

$\Gamma(\mu\tau)/\Gamma_{total}$ Γ_{30}/Γ

NODE=S126R02
NODE=S126R02

VALUE	CL%	DOCUMENT ID	TECN	COMMENT
$< 1.5 \times 10^{-3}$	95	[1] SIRUNYAN 21Z	CMS	pp, 13 TeV
• • • We do not use the following data for averages, fits, limits, etc. • • •				
$< 1.8 \times 10^{-3}$	95	[2] AAD 23Q	ATLS	pp, 13 TeV
$< 1.7 \times 10^{-3}$	95	[3] AAD 23Q	ATLS	pp, 13 TeV (OCCUR=2)
$< 2.8 \times 10^{-3}$	95	[4] AAD 20A	ATLS	pp, 13 TeV
$<26 \times 10^{-2}$	95	[5] AAIJ 18AM	LHCB	pp, 8 TeV
$< 2.5 \times 10^{-3}$	95	[6] SIRUNYAN 18BH	CMS	pp, 13 TeV
$< 1.43 \times 10^{-2}$	95	[7] AAD 17	ATLS	pp, 8 TeV
$< 1.51 \times 10^{-2}$	95	[8] KHACHATRY...15Q	CMS	pp, 8 TeV

[1] SIRUNYAN 21Z search for $H \to \mu\tau$ in 137 fb^{-1} of pp collisions at E_{cm} = 13 TeV. The limit constrains the $Y_{\mu\tau}$ Yukawa coupling to $\sqrt{|Y_{\mu\tau}|^2+|Y_{\tau\mu}|^2} < 1.11\times10^{-3}$ at 95% CL (see their Fig. 8). NODE=S126R02;LINKAGE=F

[2] AAD 23Q search for $H \to \mu\tau$ in 138 fb^{-1} of pp collisions at E_{cm} = 13 TeV. The result is obtained from a simultaneous fit of possible $H \to e\tau$ and $H \to \mu\tau$ signals (see their Figs. 13 and 14). The limit constrains the $Y_{\mu\tau}$ Yukawa coupling to $\sqrt{|Y_{\mu\tau}|^2+|Y_{\tau\mu}|^2} < 1.2\times10^{-3}$ at 95% CL (see their Fig. 15). NODE=S126R02;LINKAGE=G

[3] AAD 23Q search for $H \to \mu\tau$ in 138 fb^{-1} of pp collisions at E_{cm} = 13 TeV. The limit constrains the $Y_{\mu\tau}$ Yukawa coupling to $\sqrt{|Y_{\mu\tau}|^2+|Y_{\tau\mu}|^2} < 1.2\times10^{-3}$ at 95% CL (see their Fig. 12). NODE=S126R02;LINKAGE=H

[4] AAD 20A search for $H \to \mu\tau$ in 36.1 fb^{-1} of pp collisions at E_{cm} = 13 TeV. The limit constrains the $Y_{\mu\tau}$ Yukawa coupling to $\sqrt{|Y_{\mu\tau}|^2+|Y_{\tau\mu}|^2} < 1.5\times10^{-3}$ at 95% CL (see their Fig. 5). NODE=S126R02;LINKAGE=E

[5] AAIJ 18AM search for $H \to \mu\tau$ in 2.0 fb^{-1} of pp collisions at E_{cm} = 8 TeV. The limit constrains the $Y_{\mu\tau}$ Yukawa coupling to $\sqrt{|Y_{\mu\tau}|^2+|Y_{\tau\mu}|^2} < 1.7\times10^{-2}$ at 95% CL assuming SM production cross sections. NODE=S126R02;LINKAGE=D

[6] SIRUNYAN 18BH search for $H \to \mu\tau$ in 35.9 fb^{-1} of pp collisions at E_{cm} = 13 TeV. The limit constrains the $Y_{\mu\tau}$ Yukawa coupling to $\sqrt{|Y_{\mu\tau}|^2+|Y_{\tau\mu}|^2} < 1.43\times10^{-3}$ at 95% CL (see their Fig. 10). NODE=S126R02;LINKAGE=C

[7] AAD 17 search for $H \to \mu\tau$ in 20.3 fb^{-1} of pp collisions at E_{cm} = 8 TeV. NODE=S126R02;LINKAGE=B

[8] KHACHATRYAN 15Q search for $H \to \mu\tau$ with τ decaying electronically or hadronically in 19.7 fb^{-1} of pp collisions at E_{cm} = 8 TeV. The fit gives B($H \to \mu\tau$) = $(0.84^{+0.39}_{-0.37})$% with a significance of 2.4 σ. NODE=S126R02;LINKAGE=A

Γ(invisible)/Γ_{total} Γ_{31}/Γ

NODE=S126R01

Invisible final states. NODE=S126R01

NODE=S126R01

VALUE	CL%	DOCUMENT ID	TECN	COMMENT	
<0.107 (CL = 95%)	[<0.13 (CL = 95%) OUR 2023 BEST LIMIT]				
<0.107	95	[1] AAD 23A	ATLS	pp, 7, 8, 13 TeV	OCCUR=2
• • • We do not use the following data for averages, fits, limits, etc. • • •					
<0.113	95	[2] AAD 23A	ATLS	pp, 13 TeV	
<0.38	95	[3] AAD 23AF	ATLS	$pp \to t\overline{t}H$, 13 TeV	
<0.54	95	[4] TUMASYAN 23BA	CMS	$pp \to t\overline{t}H$, $V(\to q\overline{q})$ H, 13 TeV	
<0.15	95	[5] TUMASYAN 23BA	CMS	pp, 7, 8, 13 TeV	OCCUR=2
<0.19	95	[6] AAD 22D	ATLS	$pp \to ZH$, 13 TeV	
<0.145	95	[7] AAD 22P	ATLS	$pp \to qqH$, 13 TeV	
<0.37	95	[8] AAD 22S	ATLS	$pp \to qqH\gamma$, 13 TeV	
<0.13	95	[9] ATLAS 22	ATLS	pp, 13 TeV	
<0.16	95	[10] CMS 22	CMS	pp, 13 TeV	
<0.18	95	[11] TUMASYAN 22G	CMS	$pp \to qqH$, 8, 13 TeV	
<0.18	95	[12] TUMASYAN 22G	CMS	$pp \to qqH$, 13 TeV	OCCUR=2
<0.34	95	[13] AAD 21F	ATLS	pp, 13 TeV	
<0.29	95	[14] SIRUNYAN 21A	CMS	$pp \to ZH$, 13 TeV	
<0.278	95	[15] TUMASYAN 21D	CMS	pp, 13 TeV, jet or $V(\to q\overline{q})$	
<0.37	95	[16] AABOUD 19AI	ATLS	$pp \to qqH$, 13 TeV	
<0.38	95	[17] AABOUD 19AL	ATLS	pp, 13 TeV	
<0.26	95	[18] AABOUD 19AL	ATLS	pp, 7, 8, 13 TeV	OCCUR=2
<0.22	95	[19] SIRUNYAN 19AT	CMS	pp, 13 TeV	
<0.33	95	[20] SIRUNYAN 19BO	CMS	$pp \to qqH$, 13 TeV	
<0.26	95	[21] SIRUNYAN 19BO	CMS	pp, 13 TeV	OCCUR=2
<0.19	95	[22] SIRUNYAN 19BO	CMS	pp, 7, 8, 13 TeV	OCCUR=3
<0.67	95	[23] AABOUD 18	ATLS	$pp \to ZH$, 13 TeV	
<0.83	95	[24] AABOUD 18CA	ATLS	$pp \to WH/ZH$, $W/Z \to jj$, 13 TeV	
<0.40	95	[25] SIRUNYAN 18BV	CMS	$pp \to ZH$, 13 TeV	
<0.53	95	[26] SIRUNYAN 18S	CMS	pp, 13 TeV, jet or $V(\to q\overline{q})$	
<0.46	95	[27] AABOUD 17BD	ATLS	$pp \to Hj$, qqH, 13 TeV	
<0.24	95	[28] KHACHATRY... 17F	CMS	pp, 7, 8, 13 TeV	
<0.28	95	[29] AAD 16AF	ATLS	$pp \to qqH$, 8 TeV	
<0.34	95	[30] AAD 16AN	LHC	pp, 7, 8 TeV	
<0.78	95	[31] AAD 15BD	ATLS	$pp \to WH/ZH$, 8 TeV	
<0.25	95	[32] AAD 15CX	ATLS	pp, 7, 8 TeV	
<0.75	95	[33] AAD 14O	ATLS	$pp \to ZH$, 7, 8 TeV	
<0.58	95	[34] CHATRCHYAN 14B	CMS	$pp \to ZH$, qqH	
<0.81	95	[35] CHATRCHYAN 14B	CMS	$pp \to ZH$, 7, 8 TeV	OCCUR=2
<0.65	95	[36] CHATRCHYAN 14B	CMS	$pp \to qqH$, 8 TeV	OCCUR=3

[1] AAD 23A report the combined results of 7, 8 (AAD 15CX) and 13 TeV assuming the Standard Model cross section (m_H = 125 GeV). See their Table 1 and Fig. 3. NODE=S126R01;LINKAGE=GA

[2] AAD 23A report the combined results using 139 fb^{-1} of data at E_{cm} = 13 TeV, where H decaying to invisible final states in VBF (AAD 22P), ZH, $Z \to ee$, $\mu\mu$ (AAD 22D), $pp \to t\bar{t}H$ (AAD 23AF), VBF+γ (AAD 22S) and gluon-fusion production with an energetic jet (AAD 21F) assuming the Standard Model cross section (m_H = 125 GeV). See their Table 1 and Fig. 3. NODE=S126R01;LINKAGE=FA

[3] AAD 23AF search for $pp \to t\bar{t}H$ with H decaying to invisible final states using 139 fb^{-1} of data. The quoted limit on the branching ratio is given for m_H = 125 GeV and assumes the Standard Model cross section. See their Table 3 for different decay topologies. NODE=S126R01;LINKAGE=EA

[4] TUMASYAN 23BA search for H decaying to invisible final states produced in association with a $t\bar{t}$ or a V, which decay to a fully hadronic final state. 138 fb^{-1} of data is used. The quoted limit on the branching ratio is given for m_H = 125 GeV and assumes the Standard Model cross section. See their Fig. 6 for the results of individual topologies. NODE=S126R01;LINKAGE=HA

[5] TUMASYAN 23BA report the combined results of 7, 8, and 13 TeV assuming the Standard Model cross section (m_H = 125 GeV). They combine results from TUMASYAN 22G, SIRUNYAN 21A, SIRUNYAN 21B, TUMASYAN 21D, SIRUNYAN 20AH, KHACHATRYAN 17F, CHATRCHYAN 14B as shown in their Table 8. See their Fig. 7 and Table 9 for the results of individual topologies. NODE=S126R01;LINKAGE=IA

[6] AAD 22D search for H decaying to invisible final states associated with a Z decaying $ee/\mu\mu$ using 139 fb^{-1} at 13 TeV. The limit is obtained for m_H = 125 GeV and assuming the SM ZH production cross section. The branching ratio is obtained to be (0.3 $\pm$ 9.0)%. NODE=S126R01;LINKAGE=X

[7] AAD 22P search for $pp \to qqHX$ (VBF) with H decaying to invisible final states using 139 fb^{-1} of data. The quoted limit on the branching ratio is given for m_H = 125 GeV and assumes the Standard Model cross section. NODE=S126R01;LINKAGE=Y

[8] AAD 22S observe electroweak $Z(\to \nu\nu)\gamma$+2jets production process with 139 fb^{-1} of data. This result is applicable to search for $pp \to qqH\gamma X$ (VBF+γ) with H decaying to invisible final states. The quoted limit on the branching ratio is given for m_H = 125 GeV and assumes the Standard Model cross section. NODE=S126R01;LINKAGE=BA

[9] ATLAS 22 report the combined results using 139 fb^{-1} of data at E_{cm} = 13 TeV, where H decaying to invisible final states in VBF (AAD 22P), and ZH, $Z \to ee$, $\mu\mu$ (AAD 22D), assuming $\kappa_V \leq 1$ and $B_{undetected} \geq 0$. NODE=S126R01;LINKAGE=DA

[10] CMS 22 report the combined results using (a part of) 138 fb^{-1} of data at E_{cm} = 13 TeV, where H decaying to invisible final states in VBF (SIRUNYAN 19BO), associated with an energetic jet or a $V(\to q\bar{q})$ (TUMASYAN 21D), and ZH, $Z \to ee$, $\mu\mu$ (SIRUNYAN 21A) and assuming $\kappa_V \leq 1$ and $B_{undetected} \geq 0$. NODE=S126R01;LINKAGE=CA

[11] TUMASYAN 22G combine 13 TeV 101 fb^{-1} results with 8 TeV (KHACHATRYAN 17F) and other 13 TeV (KHACHATRYAN 17F for 2015 and SIRUNYAN 19BO for 2016) for H decaying to invisible final states with VBF topology. The quoted limit on the branching ratio is given for m_H = 125.38 GeV and assumes the Standard Model production rates. The branching ratio is obtained to be $0.086^{+0.054}_{-0.052}$. See their Figs. 11 and 12. NODE=S126R01;LINKAGE=Z

[12] TUMASYAN 22G search for $pp \to qqHX$ (VBF) with H decaying to invisible final states using 101 fb^{-1} of data (2017 and 2018). The quoted limit on the branching ratio is given for m_H = 125.38 GeV and assumes the Standard Model cross section. See their Figs. 11 and 12. NODE=S126R01;LINKAGE=AA

[13] AAD 21F search for an invisibly decaying Higgs boson with an energetic jet (p_T > 150 GeV) and missing transverse momentum (> 200 GeV) in 139 fb^{-1} at E_{cm} = 13 TeV. The quoted limit on the branching ratio is given for m_H = 125 GeV. NODE=S126R01;LINKAGE=V

[14] SIRUNYAN 21A search for H decaying to invisible final states associated with a Z decaying $ee/\mu\mu$ using 137 fb^{-1} at 13 TeV. The limit is obtained for m_H = 125 GeV and assuming the SM ZH production cross section. NODE=S126R01;LINKAGE=U

[15] TUMASYAN 21D search for H decaying to invisible final states associated with an energetic jet or a V, $V \to q\bar{q}$ using 101 fb^{-1} at 13 TeV and the result is combined with SIRUNYAN 18S. NODE=S126R01;LINKAGE=W

[16] AABOUD 19AI search for $pp \to qqHX$ (VBF) with H decaying to invisible final states using 36.1 fb^{-1} of data. The quoted limit on the branching ratio is given for m_H = 125 GeV and assumes the Standard Model rates for VBF and gluon-fusion production. NODE=S126R01;LINKAGE=K

[17] AABOUD 19AL combine results of H decaying to invisible final states with VBF(AABOUD 19AI), ZH, and WH productions (AABOUD 18, AABOUD 18CA), which use 36.1 fb^{-1} of data at 13 TeV. The quoted limit is given for m_H = 125 GeV and assumes the Standard Model rates for gluon fusion, VBF, ZH, and WH productions. NODE=S126R01;LINKAGE=M

[18] AABOUD 19AL combine results of 7, 8 (AAD 15CX), and 13 TeV for H decaying to invisible final states. NODE=S126R01;LINKAGE=N

[19] SIRUNYAN 19AT perform a combined fit with visible decay using 35.9 fb^{-1} of data at 13 TeV. NODE=S126R01;LINKAGE=O

[20] SIRUNYAN 19BO search for $pp \to qqHX$ (VBF) with H decaying to invisible final states using 35.9 fb^{-1} of data. The quoted limit on the branching ratio is given for m_H = 125.09 GeV and assumes the Standard Model production rates. NODE=S126R01;LINKAGE=P

[21] SIRUNYAN 19BO combine the VBF channel with results of other 13 TeV analyses: SIRUNYAN 18BV and SIRUNYAN 18S. The quoted limit on the branching ratio is given for m_H = 125.09 GeV and assumes the Standard Model production rates. NODE=S126R01;LINKAGE=S

[22] SIRUNYAN 19BO combine 13 TeV 35.9 fb^{-1} results with 7, 8, 13 TeV (KHACHATRYAN 17F) for H decaying to invisible final states. The quoted limit on the branching ratio is given for m_H = 125.09 GeV and assumes the Standard Model production rates. The branching ratio is obtained to be 0.05 ± 0.03 (stat) ±0.07(syst). NODE=S126R01;LINKAGE=T

[23] AABOUD 18 search for $pp \to HZX$, $Z \to ee$, $\mu\mu$ with H decaying to invisible final states in 36.1 fb^{-1} at E_{cm} = 13 TeV. The quoted limit on the branching ratio is given for m_H = 125 GeV and assumes the Standard Model rate for HZ production. NODE=S126R01;LINKAGE=H

[24] AABOUD 18CA search for H decaying to invisible final states using WH, and ZH productions, where W and Z hadronically decay. The data of 36.1 fb^{-1} at E_{cm} = 13 TeV is used. The quoted limit assumes SM production cross sections with combining the contributions from WH, ZH, ggF and VBF production modes. NODE=S126R01;LINKAGE=J

[25] SIRUNYAN 18BV search for H decaying to invisible final states associated with a Z, $Z \to \ell\ell$ using 35.9 fb^{-1} at 13 TeV.The limit is obtained for m_H = 125 GeV and assuming the SM ZH production cross section. NODE=S126R01;LINKAGE=R

[26] SIRUNYAN 18S search for H decaying to invisible final states associated with an energetic jet or a V, $V \to q\overline{q}$ using 35.9 fb^{-1} at 13 TeV. NODE=S126R01;LINKAGE=Q

[27] AABOUD 17BD search for H decaying to invisible final states with $\geq$ 1 jet and VBF events using 3.2 fb^{-1} of pp collisions at E_{cm} = 13 TeV. A cross-section ratio R^{miss} is used in the measurement. The quoted limit is given for m_H = 125 GeV. NODE=S126R01;LINKAGE=I

[28] KHACHATRYAN 17F search for H decaying to invisible final states with gluon fusion, VBF, ZH, and WH productions using 2.3 fb^{-1} of pp collisions at E_{cm} = 13 TeV, 19.7 fb^{-1} at 8 TeV, and 5.1 fb^{-1} at 7 TeV. The quoted limit is given for m_H = 125 GeV and assumes the Standard Model rates for gluon fusion, VBF, ZH, and WH productions. NODE=S126R01;LINKAGE=G

[29] AAD 16AF search for $pp \to qqHX$ (VBF) with H decaying to invisible final states in 20.3 fb^{-1} at E_{cm} = 8 TeV. The quoted limit on the branching ratio is given for m_H = 125 GeV and assumes the Standard Model rates for VBF and gluon-fusion production. NODE=S126R01;LINKAGE=E

[30] AAD 16AN perform fits to the ATLAS and CMS data at E_{cm} = 7 and 8 TeV. The branching fraction of decays into BSM particles that are invisible or into undetected decay modes is measured for m_0 = 125.09 GeV. NODE=S126R01;LINKAGE=F

[31] AAD 15BD search for $pp \to HWX$ and $pp \to HZX$ with W or Z decaying hadronically and H decaying to invisible final states using data at E_{cm} = 8 TeV. The quoted limit is given for m_H = 125 GeV, assumes the Standard Model rates for the production processes and is based on a combination of the contributions from HW, HZ and the gluon-fusion process. NODE=S126R01;LINKAGE=D

[32] AAD 15CX search for H decaying to invisible final states with VBF, ZH, and WH productions using 20.3 fb^{-1} at 8 TeV, and 4.7 fb^{-1} at 7 TeV. The quoted limit is given for m_H = 125.36 GeV and assumes the Standard Model rates for gluon fusion, VBF, ZH, and WH productions. The upper limit is improved to 0.23 by adding the measured visible decay rates. NODE=S126R01;LINKAGE=L

[33] AAD 14O search for $pp \to HZX$, $Z \to \ell\ell$, with H decaying to invisible final states in 4.5 fb^{-1} at E_{cm} = 7 TeV and 20.3 fb^{-1} at E_{cm} = 8 TeV. The quoted limit on the branching ratio is given for m_H = 125.5 GeV and assumes the Standard Model rate for HZ production. NODE=S126R01;LINKAGE=A

[34] CHATRCHYAN 14B search for $pp \to HZX$, $Z \to \ell\ell$ and $Z \to b\overline{b}$, and also $pp \to qqHX$ with H decaying to invisible final states using data at E_{cm} = 7 and 8 TeV. The quoted limit on the branching ratio is obtained from a combination of the limits from HZ and qqH. It is given for m_H = 125 GeV and assumes the Standard Model rates for the two production processes. NODE=S126R01;LINKAGE=B

[35] CHATRCHYAN 14B search for $pp \to HZX$ with H decaying to invisible final states and $Z \to \ell\ell$ in 4.9 fb^{-1} at E_{cm} = 7 TeV and 19.7 fb^{-1} at E_{cm} = 8 TeV, and also with $Z \to b\overline{b}$ in 18.9 fb^{-1} at E_{cm} = 8 TeV. The quoted limit on the branching ratio is given for m_H = 125 GeV and assumes the Standard Model rate for HZ production. NODE=S126R01;LINKAGE=CH

[36] CHATRCHYAN 14B search for $pp \to qqHX$ (vector boson fusion) with H decaying to invisible final states in 19.5 fb^{-1} at E_{cm} = 8 TeV. The quoted limit on the branching ratio is given for m_H = 125 GeV and assumes the Standard Model rate for qqH production. NODE=S126R01;LINKAGE=C

$\Gamma(\gamma\,\text{invisible})/\Gamma_{total}$ Γ_{32}/Γ

NODE=S126R15
NODE=S126R15

VALUE	CL%	DOCUMENT ID		TECN	COMMENT
<0.029	95	[1,2] SIRUNYAN	21L	CMS	VBF, HZ, $H \to \gamma$ + invisible, 13 TeV
• • • We do not use the following data for averages, fits, limits, etc. • • •					
<0.035	95	[1] SIRUNYAN	21L	CMS	VBF, $H \to \gamma$+ invisible, 13 TeV
<0.046	95	[3] SIRUNYAN	19CG	CMS	$pp \to HZ$, $H \to \gamma$+ invisible, $Z \to \ell\ell$, 13 TeV

OCCUR=2

[1] SIRUNYAN 21L search for H decaying to an invisible final state plus a γ in the VBF production using 130 fb^{-1} data at E_{cm} = 13 TeV. The invisible state is called a dark photon. The quoted limit on the branching ratio is given for m_H = 125 GeV assuming the Standard Model rates. NODE=S126R15;LINKAGE=B

[2] The result of the VBF production is combined with the $pp \to HZ$ result (SIRUNYAN 19CG). NODE=S126R15;LINKAGE=C

[3] SIRUNYAN 19CG search for $pp \to HZ$, $Z \to ee$, $\mu\mu$ with H decaying to invisible final states plus a γ in 137 fb^{-1} at E_{cm} = 13 TeV. The quoted limit on the branching ratio is given for m_H = 125 GeV assuming the Standard Model rate for HZ production and is obtained in the context of a theoretical model, where the undetected (invisible) particle is massless. NODE=S126R15;LINKAGE=A

H SIGNAL STRENGTHS IN DIFFERENT CHANNELS

NODE=S126230

The H signal strength in a particular final state xx is given by the cross section times branching ratio in this channel normalized to the Standard Model (SM) value, $\sigma \cdot$ B($H \to xx$) / ($\sigma \cdot$ B($H \to xx$))$_{SM}$, for the specified mass value of H. For the SM predictions, see DITTMAIER 11, DITTMAIER 12, and HEINEMEYER 13A. Results for fiducial and differential cross sections are also listed below. NODE=S126230

Combined Final States

NODE=S126SA
NODE=S126SA

VALUE	DOCUMENT ID		TECN	COMMENT	
1.03 ±0.04 OUR AVERAGE					
1.05 ±0.06	[1] ATLAS	22	ATLS	pp, 13 TeV	
1.002±0.057	[2] CMS	22	CMS	pp, 13 TeV	
1.09 ±0.07 ±0.04 $^{+0.08}_{-0.07}$	[3,4] AAD	16AN	LHC	pp, 7, 8 TeV	
1.44 $^{+0.59}_{-0.56}$	[5] AALTONEN	13M	TEVA	$p\overline{p} \to HX$, 1.96 TeV	
• • • We do not use the following data for averages, fits, limits, etc. • • •					
1.11 $^{+0.09}_{-0.08}$	[6] AAD	20	ATLS	pp, 13 TeV	
1.17 ±0.10	[7] SIRUNYAN	19AT	CMS	pp, 13 TeV	
	[8] SIRUNYAN	19BA	CMS	pp, 13 TeV, diiferential cross sections	
1.20 ±0.10 ±0.06 $^{+0.09}_{-0.08}$	[4] AAD	16AN	ATLS	pp, 7, 8 TeV	OCCUR=2
0.97 ±0.09 ±0.05 $^{+0.08}_{-0.07}$	[4] AAD	16AN	CMS	pp, 7, 8 TeV	OCCUR=3
1.18 ±0.10 ±0.07 $^{+0.08}_{-0.07}$	[9] AAD	16K	ATLS	pp, 7, 8 TeV	
0.75 $^{+0.28}_{-0.26}$ $^{+0.13}_{-0.11}$ $^{+0.08}_{-0.05}$	[9] AAD	16K	ATLS	pp, 7 TeV	OCCUR=2
1.28 ±0.11 $^{+0.08}_{-0.07}$ $^{+0.10}_{-0.08}$	[9] AAD	16K	ATLS	pp, 8 TeV	OCCUR=3
	[10] AAD	15P	ATLS	pp, 8 TeV, cross section	
1.00 ±0.09 ±0.07 $^{+0.08}_{-0.07}$	[11] KHACHATRY...	15AM	CMS	pp, 7, 8 TeV	
1.33 $^{+0.14}_{-0.10}$ ±0.15	[12] AAD	13AK	ATLS	pp, 7 and 8 TeV	
1.54 $^{+0.77}_{-0.73}$	[13] AALTONEN	13L	CDF	$p\overline{p} \to HX$, 1.96 TeV	
1.40 $^{+0.92}_{-0.88}$	[14] ABAZOV	13L	D0	$p\overline{p} \to HX$, 1.96 TeV	
1.4 ±0.3	[15] AAD	12AI	ATLS	$pp \to HX$, 7, 8 TeV	
1.2 ±0.4	[15] AAD	12AI	ATLS	$pp \to HX$, 7 TeV	OCCUR=2
1.5 ±0.4	[15] AAD	12AI	ATLS	$pp \to HX$, 8 TeV	OCCUR=3
0.87 ±0.23	[16] CHATRCHYAN	12N	CMS	$pp \to HX$, 7, 8 TeV	

[1] ATLAS 22 report combined results (see their Extended Data Table 1) using up to 139 fb^{-1} of data at E_{cm} = 13 TeV, assuming m_H = 125.09 GeV. The Higgs production cross-sections, branching fractions and several ratios are found in their Figs. 2 and 3. NODE=S126SA;LINKAGE=J

[2] CMS 22 report combined results (see their Extended Data Table 2) using 138 fb^{-1} of data at E_{cm} = 13 TeV, assuming m_H = 125.38 GeV. Signal strengths for production modes and decay channels are found in their Fig. 2. NODE=S126SA;LINKAGE=I

[3] AAD 16AN perform fits to the ATLAS and CMS data at E_{cm} = 7 and 8 TeV. The signal strengths for individual production processes are $1.03^{+0.16}_{-0.14}$ for gluon fusion, $1.18^{+0.25}_{-0.23}$ for vector boson fusion, $0.89^{+0.40}_{-0.38}$ for WH production, $0.79^{+0.38}_{-0.36}$ for ZH production, and $2.3^{+0.7}_{-0.6}$ for $t\overline{t}H$ production. NODE=S126SA;LINKAGE=F

[4] AAD 16AN: The uncertainties represent statistics, experimental systematics, and added in quadrature theory systematics on the background and on the signal. The quoted signal strengths are given for m_H = 125.09 GeV. In the fit, relative branching ratios and relative production cross sections are fixed to those in the Standard Model. NODE=S126SA;LINKAGE=G

[5] AALTONEN 13M combine all Tevatron data from the CDF and D0 Collaborations with up to 10.0 fb^{-1} and 9.7 fb^{-1}, respectively, of $p\overline{p}$ collisions at E_{cm} = 1.96 TeV. The quoted signal strength is given for m_H = 125 GeV. NODE=S126SA;LINKAGE=AT

[6] AAD 20 combine results of up to 79.8 fb^{-1} of data at E_{cm} = 13 TeV, assuming m_H = 125.09 GeV: $\gamma\gamma$, ZZ^*, WW^*, $\tau\tau$, $b\overline{b}$, $\mu\mu$, invisible, and off-shell analyses (see their Table I). The signal strengths for individual production processes are 1.04 ± 0.09 for gluon NODE=S126SA;LINKAGE=H

fusion, $1.21^{+0.24}_{-0.22}$ for vector boson fusion, $1.30^{+0.40}_{-0.38}$ for WH production, $1.05^{+0.31}_{-0.29}$ for ZH production, and $1.21^{+0.26}_{-0.24}$ for $t\bar{t}H$+tH production (see their Fig. 2 and Table IV). Several results with the simplified template cross section and κ-frameworks are presented: see their Figs. 9–11, Figs 20, 21 and Table VIII for stage-1 simplified template cross sections, their Figs. 12–17 and Tables X–XII for the κ-framework.

[7] SIRUNYAN 19AT combine results of 35.9 fb^{-1} of data at E_{cm} = 13 TeV, assuming m_H = 125.09 GeV. The signal strengths for individual production processes are $1.22^{+0.14}_{-0.12}$ for gluon fusion, $0.73^{+0.30}_{-0.27}$ for vector boson fusion, $2.18^{+0.58}_{-0.55}$ for WH production, $0.87^{+0.44}_{-0.42}$ for ZH production, and $1.18^{+0.30}_{-0.27}$ for $t\bar{t}H$ production. Several results with the simplified template cross section and κ-frameworks are presented: see their Fig. 8 and Table 5 for stage-0 simplified template cross sections, their Figs. 9–18 and Tables 7–11 for the κ-framework. NODE=S126SA;LINKAGE=D

[8] SIRUNYAN 19BA measure differential cross sections for the Higgs boson transverse momentum, the number of jets, the rapidity of the Higgs boson and the transverse momentum of the leading jet using 35.9 fb^{-1} of data at E_{cm} = 13 TeV with $H \to \gamma\gamma$, $H \to ZZ^*$, and $H \to b\bar{b}$. The total cross section for Higgs boson production is measured to be 61.1 ± 6.0 ± 3.7 pb using $H \to \gamma\gamma$ and $H \to ZZ^*$ channels. Several coupling measurements in the κ-framework are performed. NODE=S126SA;LINKAGE=E

[9] AAD 16K use up to 4.7 fb^{-1} of pp collisions at E_{cm} = 7 TeV and up to 20.3 fb^{-1} at E_{cm} = 8 TeV. The third uncertainty in the measurement is theory systematics. The signal strengths for individual production modes are $1.23 \pm 0.14^{+0.09}_{-0.08}{}^{+0.16}_{-0.12}$ for gluon fusion, $1.23^{+0.28}_{-0.27}{}^{+0.13}_{-0.12}{}^{+0.11}_{-0.09}$ for vector boson fusion, $0.80^{+0.31}_{-0.30} \pm 0.17^{+0.10}_{-0.05}$ for W/ZH production, and $1.81^{+0.52}_{-0.50}{}^{+0.58}_{-0.55}{}^{+0.31}_{-0.12}$ for $t\bar{t}H$ production. The quoted signal strengths are given for m_H = 125.36 GeV. NODE=S126SA;LINKAGE=B

[10] AAD 15P measure total and differential cross sections of the process $pp \to HX$ at E_{cm} = 8 TeV with 20.3 fb^{-1}. $\gamma\gamma$ and 4ℓ final states are used. $\sigma(pp \to HX)$ = 33.0 ± 5.3 ± 1.6 pb is given. See their Figs. 2 and 3 for data on differential cross sections. NODE=S126SA;LINKAGE=C

[11] KHACHATRYAN 15AM use up to 5.1 fb^{-1} of pp collisions at E_{cm} = 7 TeV and up to 19.7 fb^{-1} at E_{cm} = 8 TeV. The third uncertainty in the measurement is theory systematics. Fits to each production mode give the value of $0.85^{+0.19}_{-0.16}$ for gluon fusion, $1.16^{+0.37}_{-0.34}$ for vector boson fusion, $0.92^{+0.38}_{-0.36}$ for WH, ZH production, and $2.90^{+1.08}_{-0.94}$ for $t\bar{t}H$ production. NODE=S126SA;LINKAGE=A

[12] AAD 13AK use 4.7 fb^{-1} of pp collisions at E_{cm} = 7 TeV and 20.7 fb^{-1} at E_{cm} = 8 TeV. The combined signal strength is based on the $\gamma\gamma$, $ZZ^* \to 4\ell$, and $WW^* \to \ell\nu\ell\nu$ channels. The quoted signal strength is given for m_H = 125.5 GeV. Reported statistical error value modified following private communication with the experiment. NODE=S126SA;LINKAGE=LH

[13] AALTONEN 13L combine all CDF results with 9.45–10.0 fb^{-1} of $p\bar{p}$ collisions at E_{cm} = 1.96 TeV. The quoted signal strength is given for m_H = 125 GeV. NODE=S126SA;LINKAGE=LL

[14] ABAZOV 13L combine all D0 results with up to 9.7 fb^{-1} of $p\bar{p}$ collisions at E_{cm} = 1.96 TeV. The quoted signal strength is given for m_H = 125 GeV. NODE=S126SA;LINKAGE=AB

[15] AAD 12AI obtain results based on 4.6–4.8 fb^{-1} of pp collisions at E_{cm} = 7 TeV and 5.8–5.9 fb^{-1} at E_{cm} = 8 TeV. An excess of events over background with a local significance of 5.9 σ is observed at m_H = 126 GeV. The quoted signal strengths are given for m_H = 126 GeV. See also AAD 12DA. NODE=S126SA;LINKAGE=AA

[16] CHATRCHYAN 12N obtain results based on 4.9–5.1 fb^{-1} of pp collisions at E_{cm} = 7 TeV and 5.1–5.3 fb^{-1} at E_{cm} = 8 TeV. An excess of events over background with a local significance of 5.0 σ is observed at about m_H = 125 GeV. The combined signal strength is based on the $\gamma\gamma$, ZZ^*, WW^*, $\tau^+\tau^-$, and $b\bar{b}$ channels. The quoted signal strength is given for m_H = 125.5 GeV. See also CHATRCHYAN 13Y. NODE=S126SA;LINKAGE=CA

WW^* Final State

NODE=S126SWW
NODE=S126SWW

VALUE	DOCUMENT ID		TECN	COMMENT	
1.00±0.08 OUR AVERAGE					
0.97±0.09	[1] CMS	22	CMS	pp, 13 TeV	
$1.09^{+0.18}_{-0.16}$	[2,3] AAD	16AN	LHC	pp, 7, 8 TeV	
$0.94^{+0.85}_{-0.83}$	[4] AALTONEN	13M	TEVA	$p\bar{p} \to HX$, 1.96 TeV	
• • • We do not use the following data for averages, fits, limits, etc. • • •					
	[5] AAD	23AP	ATLS	pp, 13 TeV, cross sections	
	[6] AAD	23BV	ATLS	pp, 13 TeV, cross sections	
$0.95^{+0.10}_{-0.09}$	[7,8] TUMASYAN	23W	CMS	pp, 13 TeV	
$0.92^{+0.11}_{-0.10}$	[7,9,10] TUMASYAN	23W	CMS	pp, 13 TeV	OCCUR=2
$0.71^{+0.28}_{-0.25}$	[7,9,11] TUMASYAN	23W	CMS	pp, 13 TeV	OCCUR=3
2.2 ±0.6	[7,9,12] TUMASYAN	23W	CMS	pp, 13 TeV	OCCUR=4

2.0 ± 0.7	[7,9,13] TUMASYAN	23W	CMS	pp, 13 TeV	OCCUR=5
	[7,14] TUMASYAN	23W	CMS	pp, 13 TeV	OCCUR=6
$0.5 \pm 0.4\ ^{+0.7}_{-0.6}$	[15] AAD	22V	ATLS	pp, WW^* ($\rightarrow e\nu\mu\nu$) $+2j$, 13 TeV	
	[16] AAD	22V	ATLS	pp, WW^* ($\rightarrow e\nu\mu\nu$) $+2j$, 13 TeV	OCCUR=2
	[17] AABOUD	19F	ATLS	pp, 13 TeV, cross sections	
$2.5\ ^{+0.9}_{-0.8}$	[18] AAD	19A	ATLS	$pp \rightarrow HW/HZ$, $H \rightarrow WW^*$, 13 TeV	
$1.28^{+0.17}_{-0.16}$	[19] SIRUNYAN	19AT	CMS	pp, 13 TeV	
$1.28^{+0.18}_{-0.17}$	[20] SIRUNYAN	19AX	CMS	pp, 13 TeV	
$1.22^{+0.23}_{-0.21}$	[3] AAD	16AN	ATLS	pp, 7, 8 TeV	OCCUR=2
$0.90^{+0.23}_{-0.21}$	[3] AAD	16AN	CMS	pp, 7, 8 TeV	OCCUR=3
	[21] AAD	16AO	ATLS	pp, 8 TeV, cross sections	
$1.18 \pm 0.16\ ^{+0.17}_{-0.14}$	[22] AAD	16K	ATLS	pp, 7, 8 TeV	
$1.09\ ^{+0.16}_{-0.15}\ ^{+0.17}_{-0.14}$	[23] AAD	15AA	ATLS	pp, 7, 8 TeV	
$3.0\ ^{+1.3}_{-1.1}\ ^{+1.0}_{-0.7}$	[24] AAD	15AQ	ATLS	$pp \rightarrow HW/ZX$, 7, 8 TeV	
$1.16\ ^{+0.16}_{-0.15}\ ^{+0.18}_{-0.15}$	[25] AAD	15AQ	ATLS	pp, 7, 8 TeV	OCCUR=2
$0.72 \pm 0.12 \pm 0.10\ ^{+0.12}_{-0.10}$	[26] CHATRCHYAN	14G	CMS	pp, 7, 8 TeV	
$0.99^{+0.31}_{-0.28}$	[27] AAD	13AK	ATLS	pp, 7 and 8 TeV	
$0.00^{+1.78}_{-0.00}$	[28] AALTONEN	13L	CDF	$p\overline{p} \rightarrow HX$, 1.96 TeV	
$1.90^{+1.63}_{-1.52}$	[29] ABAZOV	13L	D0	$p\overline{p} \rightarrow HX$, 1.96 TeV	
1.3 ± 0.5	[30] AAD	12AI	ATLS	$pp \rightarrow HX$, 7, 8 TeV	
0.5 ± 0.6	[30] AAD	12AI	ATLS	$pp \rightarrow HX$, 7 TeV	OCCUR=2
1.9 ± 0.7	[30] AAD	12AI	ATLS	$pp \rightarrow HX$, 8 TeV	OCCUR=3
$0.60^{+0.42}_{-0.37}$	[31] CHATRCHYAN	12N	CMS	$pp \rightarrow HX$, 7, 8 TeV	

[1] CMS 22 report combined results (see their Extended Data Table 2) using up to 138 fb^{-1} of data at E_{cm} = 13 TeV, assuming m_H = 125.38 GeV. See their Fig. 2 right. NODE=S126SWW;LINKAGE=O

[2] AAD 16AN perform fits to the ATLAS and CMS data at E_{cm} = 7 and 8 TeV. The signal strengths for individual production processes are 0.84 ± 0.17 for gluon fusion, 1.2 ± 0.4 for vector boson fusion, $1.6^{+1.2}_{-1.0}$ for WH production, $5.9^{+2.6}_{-2.2}$ for ZH production, and $5.0^{+1.8}_{-1.7}$ for $t\overline{t}H$ production. NODE=S126SWW;LINKAGE=I

[3] AAD 16AN: In the fit, relative production cross sections are fixed to those in the Standard Model. The quoted signal strength is given for m_H = 125.09 GeV. NODE=S126SWW;LINKAGE=J

[4] AALTONEN 13M combine all Tevatron data from the CDF and D0 Collaborations with up to 10.0 fb^{-1} and 9.7 fb^{-1}, respectively, of $p\overline{p}$ collisions at E_{cm} = 1.96 TeV. The quoted signal strength is given for m_H = 125 GeV. NODE=S126SWW;LINKAGE=AT

[5] AAD 23AP measure cross-sections times the $H \rightarrow WW^*$ branching fraction in the $H \rightarrow WW^* \rightarrow e\nu\mu\nu$ channel using 139 fb^{-1} of pp collisions at E_{cm} = 13 TeV: $\sigma_{ggF} \times$B($H \rightarrow WW^*$) = 12.0 ± 1.4 pb, $\sigma_{VBF} \times$B($H \rightarrow WW^*$) = $0.75^{+0.19}_{-0.16}$ pb, and $\sigma_{ggF+VBF} \times$B($H \rightarrow WW^*$) = 12.3 ± 1.3 pb. The results are given for m_H = 125.09 GeV. Measured cross sections and ratios to the SM predictions in the reduced stage-1.2 (see their Fig. 5) simplified template cross section framework are shown in their Table VII and Fig. 15. NODE=S126SWW;LINKAGE=P

[6] AAD 23BV measure fiducial total and differential cross sections of VBF process at E_{cm} = 13 TeV with 139 fb^{-1} using $H \rightarrow WW^* \rightarrow e\nu\mu\nu$. The measured total fiducial cross section is 1.68 ± 0.33(stat)± 0.23(syst) fb in their fiducial region (Table II and Section V). See their Fig. 9 for the comparison with theory predictions. The fiducial differential cross sections are shown in their Figs. 11, 12, and 13. Wilson coefficients in the Warsaw basis at 95% confidence interval are measured; see their Table V and Fig. 16. NODE=S126SWW;LINKAGE=Z

[7] TUMASYAN 23W measure Higgs production rates with $H \rightarrow WW^*$ at E_{cm} = 13 TeV with 138 fb^{-1} data. The quoted results are given for m_H = 125.38 GeV. NODE=S126SWW;LINKAGE=Q

[8] The quoted global signal strength is obtained assuming the relative ratios of different Higgs production modes fixed to the SM values. NODE=S126SWW;LINKAGE=R

[9] The 4 signal strengths for gluon-fusion (ggF), VBF, WH and ZH modes are fit assuming $t\overline{t}H$ and $b\overline{b}H$ fixed to the SM values. NODE=S126SWW;LINKAGE=T

[10] The quoted result is for ggF production mode. NODE=S126SWW;LINKAGE=V

[11] The quoted result is for VBF production mode. NODE=S126SWW;LINKAGE=U

[12] The quoted result is for WH production mode. NODE=S126SWW;LINKAGE=W

[13] The quoted result is for ZH production mode. NODE=S126SWW;LINKAGE=X

[14] Measured cross sections and ratios to the SM predictions in the reduced stage-1.2 (see their Fig. 17) simplified template cross section framework (6 ggF, 4 VBF, and 4 VH) are shown in their Table 18 and Fig. 26. NODE=S126SWW;LINKAGE=Y

[15] AAD 22V measure the signal strength for ggF+2jets with 36.1 fb^{-1} data at 13 TeV. NODE=S126SWW;LINKAGE=M

[16] AAD 22V probe the Higgs couplings to longitudinally and transversely polarized W and Z using VBF ($H \to WW^* \to e\nu\mu\nu$ plus two jets) with 36.1 fb^{-1} of data at E_{cm} = 13 TeV. The ratios of the polarization-dependent couplings $g_{HV_L V_L}$ and $g_{HV_T V_T}$ to the Higgs-V coupling predicted by the SM, $a_L = g_{HV_L V_L}/g^{SM}_{HVV}$ and $a_T = g_{HV_T V_T}/g^{SM}_{HVV}$ are measured to be $0.91^{+0.10+0.09}_{-0.18-0.17}$ and $1.2 \pm 0.4^{+0.2}_{-0.3}$, respectively, assuming the standard Hgg coupling. These measurements are translated into pseudo-observables of κ_{VV} and ϵ_{VV}: $\kappa_{VV} = 0.91^{+0.10+0.09}_{-0.18-0.17}$ and $\epsilon_{VV} = 0.13^{+0.28+0.08}_{-0.20-0.10}$, where $\kappa_{VV} = 1$ and $\epsilon_{VV} = 0$ for the SM. See their Tables 9 and 10. NODE=S126SWW;LINKAGE=N

[17] AABOUD 19F measure cross-sections times the $H \to WW^*$ branching fraction in the $H \to WW^* \to e\nu\mu\nu$ channel using 36.1 fb^{-1} of pp collisions at E_{cm} = 13 TeV: $\sigma_{ggF} \times$B($H \to WW^*$) = $11.4^{+1.2+1.8}_{-1.1-1.7}$ pb and $\sigma_{VBF} \times$B($H \to WW^*$) = $0.50^{+0.24}_{-0.22} \pm 0.17$ pb. NODE=S126SWW;LINKAGE=F

[18] AAD 19A use 36.1 fb^{-1} data at 13 TeV. The cross section times branching fraction values are measured to be $0.67^{+0.31+0.18}_{-0.27-0.14}$ pb for WH, $H \to WW^*$ and $0.54^{+0.31+0.15}_{-0.24-0.07}$ pb for ZH, $H \to WW^*$. NODE=S126SWW;LINKAGE=L

[19] SIRUNYAN 19AT perform a combine fit to 35.9 fb^{-1} of data at E_{cm} = 13 TeV. NODE=S126SWW;LINKAGE=G

[20] SIRUNYAN 19AX measure the signal strengths, cross sections and so on using gluon fusion, VBF and VH production processes with 35.9 fb^{-1} of data. The quoted signal strength is given for m_H = 125.09 GeV. Signal strengths for each production process is found in their Fig. 9. Measured cross sections and ratios to the SM predictions in the stage-0 simplified template cross section framework are shown in their Fig. 10. $\kappa_F = 1.52^{+0.48}_{-0.41}$ and $\kappa_V = 1.10 \pm 0.08$ are obtained (see their Fig. 11 (right)). NODE=S126SWW;LINKAGE=K

[21] AAD 16AO measure fiducial total and differential cross sections of gluon fusion process at E_{cm} = 8 TeV with 20.3 fb^{-1} using $H \to WW^* \to e\nu\mu\nu$. The measured fiducial total cross section is 36.0 ± 9.7 fb in their fiducial region (Table 7). See their Fig. 6 for fiducial differential cross sections. The results are given for m_H = 125 GeV. NODE=S126SWW;LINKAGE=H

[22] AAD 16K use up to 4.7 fb^{-1} of pp collisions at E_{cm} = 7 TeV and up to 20.3 fb^{-1} at E_{cm} = 8 TeV. The quoted signal strength is given for m_H = 125.36 GeV. NODE=S126SWW;LINKAGE=E

[23] AAD 15AA use 4.5 fb^{-1} of pp collisions at E_{cm} = 7 TeV and 20.3 fb^{-1} at E_{cm} = 8 TeV. The signal strength for the gluon fusion and vector boson fusion mode is $1.02 \pm 0.19^{+0.22}_{-0.18}$ and $1.27^{+0.44+0.30}_{-0.40-0.21}$, respectively. The quoted signal strengths are given for m_H = 125.36 GeV. NODE=S126SWW;LINKAGE=B

[24] AAD 15AQ use 4.5 fb^{-1} of pp collisions at E_{cm} = 7 TeV and 20.3 fb^{-1} at E_{cm} = 8 TeV. The quoted signal strength is given for m_H = 125.36 GeV. NODE=S126SWW;LINKAGE=C

[25] AAD 15AQ combine their result on W/ZH production with the results of AAD 15AA (gluon fusion and vector boson fusion, slightly updated). The quoted signal strength is given for m_H = 125.36 GeV. NODE=S126SWW;LINKAGE=D

[26] CHATRCHYAN 14G use 4.9 fb^{-1} of pp collisions at E_{cm} = 7 TeV and 19.4 fb^{-1} at E_{cm} = 8 TeV. The last uncertainty in the measurement is theory systematics. The quoted signal strength is given for m_H = 125.6 GeV. NODE=S126SWW;LINKAGE=A

[27] AAD 13AK use 4.7 fb^{-1} of pp collisions at E_{cm} = 7 TeV and 20.7 fb^{-1} at E_{cm} = 8 TeV. The quoted signal strength is given for m_H = 125.5 GeV. Superseded by AAD 15AA. NODE=S126SWW;LINKAGE=LH

[28] AALTONEN 13L combine all CDF results with 9.45–10.0 fb^{-1} of $p\overline{p}$ collisions at E_{cm} = 1.96 TeV. The quoted signal strength is given for m_H = 125 GeV. NODE=S126SWW;LINKAGE=LL

[29] ABAZOV 13L combine all D0 results with up to 9.7 fb^{-1} of $p\overline{p}$ collisions at E_{cm} = 1.96 TeV. The quoted signal strength is given for m_H = 125 GeV. NODE=S126SWW;LINKAGE=AB

[30] AAD 12AI obtain results based on 4.7 fb^{-1} of pp collisions at E_{cm} = 7 TeV and 5.8 fb^{-1} at E_{cm} = 8 TeV. The quoted signal strengths are given for m_H = 126 GeV. See also AAD 12DA. NODE=S126SWW;LINKAGE=AA

[31] CHATRCHYAN 12N obtain results based on 4.9 fb^{-1} of pp collisions at E_{cm} = 7 TeV and 5.1 fb^{-1} at E_{cm} = 8 TeV. The quoted signal strength is given for m_H = 125.5 GeV. See also CHATRCHYAN 13Y. NODE=S126SWW;LINKAGE=CA

ZZ^* Final State

NODE=S126SZZ
NODE=S126SZZ

VALUE	CL%	DOCUMENT ID	TECN	COMMENT	
1.02±0.08 OUR AVERAGE					
$0.97^{+0.12}_{-0.11}$		[1] CMS 22	CMS	pp, 13 TeV	
1.01 ± 0.11		[2,3] AAD 20AQ	ATLS	pp, 13 TeV	OCCUR=3
$1.29^{+0.26}_{-0.23}$		[4,5] AAD 16AN	LHC	pp, 7, 8 TeV	

• • • We do not use the following data for averages, fits, limits, etc. • • •

		[6] HAYRAPETY...23		CMS	pp, 13 TeV cross sections	
		[7] SIRUNYAN	21AE	CMS	pp, 13 TeV, couplings	
$0.94 \pm 0.07 ^{+0.09}_{-0.08}$		[8] SIRUNYAN	21S	CMS	pp, 13 TeV	
		[2,9] AAD	20AQ	ATLS	pp, 13 TeV	OCCUR=2
		[10] AAD	20BA	ATLS	pp, 13 TeV cross sections	
<6.5	95	[11] AABOUD	19N	ATLS	pp, 13 TeV, off-shell	
$1.06 ^{+0.19}_{-0.17}$		[12] SIRUNYAN	19AT	CMS	pp, 13 TeV	
$1.28 ^{+0.21}_{-0.19}$		[13] AABOUD	18AJ	ATLS	pp, 13 TeV	
<3.8	95	[14] AABOUD	18BP	ATLS	pp, 13 TeV, off-shell	
$1.05 ^{+0.15}_{-0.14} {}^{+0.11}_{-0.09}$		[15] SIRUNYAN	17AV	CMS	pp, 13 TeV	
$1.52 ^{+0.40}_{-0.34}$		[5] AAD	16AN	ATLS	pp, 7, 8 TeV	OCCUR=2
$1.04 ^{+0.32}_{-0.26}$		[5] AAD	16AN	CMS	pp, 7, 8 TeV	OCCUR=3
$1.46 ^{+0.35}_{-0.31} {}^{+0.19}_{-0.13}$		[16] AAD	16K	ATLS	pp, 7, 8 TeV	
		[17] KHACHATRY...16AR		CMS	pp, 7, 8 TeV cross sections	
$1.44 ^{+0.34}_{-0.31} {}^{+0.21}_{-0.11}$		[18] AAD	15F	ATLS	$pp \to HX$, 7, 8 TeV	
		[19] AAD	14AR	ATLS	pp, 8 TeV, cross sections	
$0.93 ^{+0.26}_{-0.23} {}^{+0.13}_{-0.09}$		[20] CHATRCHYAN	14AA	CMS	pp, 7, 8 TeV	
$1.43 ^{+0.40}_{-0.35}$		[21] AAD	13AK	ATLS	pp, 7 and 8 TeV	
$0.80 ^{+0.35}_{-0.28}$		[22] CHATRCHYAN	13J	CMS	$pp \to HX$, 7, 8 TeV	
1.2 ± 0.6		[23] AAD	12AI	ATLS	$pp \to HX$, 7, 8 TeV	
1.4 ± 1.1		[23] AAD	12AI	ATLS	$pp \to HX$, 7 TeV	OCCUR=2
1.1 ± 0.8		[23] AAD	12AI	ATLS	$pp \to HX$, 8 TeV	OCCUR=3
$0.73 ^{+0.45}_{-0.33}$		[24] CHATRCHYAN	12N	CMS	$pp \to HX$, 7, 8 TeV	

[1] CMS 22 report combined results (see their Extended Data Table 2) using up to 138 fb^{-1} of data at E_{cm} = 13 TeV, assuming m_H = 125.38 GeV. See their Fig. 2 right. NODE=S126SZZ;LINKAGE=S

[2] AAD 20AQ perform analyses using $H \to ZZ^* \to 4\ell$ ($\ell = e, \mu$) with data of 139 fb^{-1} at E_{cm} = 13 TeV. Results are given for m_H = 125 GeV. NODE=S126SZZ;LINKAGE=P

[3] AAD 20AQ measured the inclusive cross section times branching ratio for $H \to ZZ^*$ decay ($|y(H)| < 2.5$) to be 1.34 ± 0.12 pb (with 1.33 ± 0.08 pb expected in the SM). NODE=S126SZZ;LINKAGE=Q

[4] AAD 16AN perform fits to the ATLAS and CMS data at E_{cm} = 7 and 8 TeV. The signal strengths for individual production processes are $1.13^{+0.34}_{-0.31}$ for gluon fusion and $0.1^{+1.1}_{-0.6}$ for vector boson fusion. NODE=S126SZZ;LINKAGE=G

[5] AAD 16AN: In the fit, relative production cross sections are fixed to those in the Standard Model. The quoted signal strength is given for m_H = 125.09 GeV. NODE=S126SZZ;LINKAGE=H

[6] HAYRAPETYAN 23 measure the cross sections for $pp \to H \to ZZ^* \to 4\ell$ ($\ell = e, \mu$) using 138 fb^{-1} at E_{cm} = 13 TeV. They give σ = 2.73 ± 0.22(stat) ±0.15(syst) fb in their fiducial region (see their Section5 and Table 2), where 2.86 ± 0.15 fb is expected in the Standard Model for m_H = 125.38 GeV. 26 differential and 6 double-differential cross sections are given; see their Figs. 6-23 and 24-25. NODE=S126SZZ;LINKAGE=T

[7] SIRUNYAN 21AE obtains constraints on anomalous couplings to vector bosons (W, Z, and gluon) and top quark using $H \to ZZ^* \to 4\ell$ ($\ell = e, \mu$) with data of 137 fb^{-1} at E_{cm} = 13 TeV. Their Table 5 and Figs 14–17 show (effective) couplings to gluon and top with combining gluon fusion, $t\bar{t}H$ and tH production channels and the result of $t\bar{t}H$, $H \to \gamma\gamma$ (SIRUNYAN 20AS). Their Tables 6–9 and Figs 18–22 show couplings to W and Z for different assumptions and bases (Higgs and Warsaw). NODE=S126SZZ;LINKAGE=N

[8] SIRUNYAN 21S measure cross sections with the $H \to ZZ^* \to 4\ell$ ($\ell = e, \mu$) channel using 137 fb^{-1} data at E_{cm} = 13 TeV. Results are given for m_H = 125.38 GeV. The signal strengths for individual production processes in their Table 4. Cross sections are given in their Table 6 and Fig. 14, which are based on the simplified template cross section framework (reduced stage-1.2). NODE=S126SZZ;LINKAGE=R

[9] AAD 20AQ present several results for the channel $H \to ZZ^* \to 4\ell$ ($\ell = e, \mu$) with the simplified template cross section with κ-frameworks and the effective field theory (EFT) approach; see their Table 8 and Fig. 10 for simplified template cross sections. κ_V = 1.02 ± 0.06 and κ_F = 0.88 ± 0.16 are obtained, see their Fig. 12 for the κ-framework. See their Tables 9 and 10 and Figs. 16–18 for the EFT-framework. NODE=S126SZZ;LINKAGE=O

[10] AAD 20BA measure the cross section for $pp \to H \to ZZ^* \to 4\ell$ ($\ell = e, \mu$) using 139 fb^{-1} at E_{cm} = 13 TeV. They give $\sigma \cdot B$ = 3.28 ± 0.30 ± 0.11 fb in their fiducial region, where 3.41 ± 0.18 fb is expected in the Standard Model for m_H = 125 GeV. NODE=S126SZZ;LINKAGE=M

Various differential cross sections are also given; see their Figs. 19-39. Constraints on Yukawa couplings for bottom and charm quarks are given in their Table 9 and Fig. 41.

[11] AABOUD 19N measure the spectrum of the four-lepton invariant mass $m_{4\ell}$ ($\ell = e$ or μ) using 36.1 fb^{-1} of data at E_{cm} = 13 TeV. The quoted signal strength upper limit is obtained from 180 GeV $< m_{4\ell} <$ 1200 GeV. NODE=S126SZZ;LINKAGE=K

[12] SIRUNYAN 19AT perform a combine fit to 35.9 fb^{-1} of data at E_{cm} = 13 TeV. NODE=S126SZZ;LINKAGE=J

[13] AABOUD 18AJ perform analyses using $H \rightarrow ZZ^* \rightarrow 4\ell$ ($\ell = e, \mu$) with data of 36.1 fb^{-1} at E_{cm} = 13 TeV. Results are given for m_H = 125.09 GeV. The inclusive cross section times branching ratio for $H \rightarrow ZZ^*$ decay ($|\eta(H)| < 2.5$) is measured to be $1.73^{+0.26}_{-0.24}$ pb (with $1.34^{+0.09}_{-0.09}$ pb expected in the SM). NODE=S126SZZ;LINKAGE=F

[14] AABOUD 18BP measure an off-shell Higgs boson production using $ZZ \rightarrow 4\ell$ and $ZZ \rightarrow 2\ell 2\nu$ ($\ell = e, \mu$) decay channels with 36.1 fb^{-1} of data at E_{cm} = 13 TeV. The quoted signal strength upper limit is obtained from a combination of these two channels, where 220 GeV $< m_{4\ell} <$ 2000 GeV for $ZZ \rightarrow 4\ell$ and 250 GeV $< m_T^{ZZ} <$ 2000 GeV for $ZZ \rightarrow 2\ell 2\nu$ (m_T^{ZZ} is defined in their Section 5). See their Table 2 for each measurement. NODE=S126SZZ;LINKAGE=L

[15] SIRUNYAN 17AV use 35.9 fb^{-1} of pp collisions at E_{cm} = 13 TeV. The quoted signal strength, obtained from the analysis of $H \rightarrow ZZ^* \rightarrow 4\ell$ ($\ell = e, \mu$) decays, is given for m_H = 125.09 GeV. The signal strengths for different production modes are given in their Table 3. The fiducial and differential cross sections are shown in their Fig. 10. NODE=S126SZZ;LINKAGE=E

[16] AAD 16K use up to 4.7 fb^{-1} of pp collisions at E_{cm} = 7 TeV and up to 20.3 fb^{-1} at E_{cm} = 8 TeV. The quoted signal strength is given for m_H = 125.36 GeV. NODE=S126SZZ;LINKAGE=D

[17] KHACHATRYAN 16AR use data of 5.1 fb^{-1} at E_{cm} = 7 TeV and 19.7 fb^{-1} at 8 TeV. The fiducial cross sections for the production of 4 leptons via $H \rightarrow 4\ell$ decays are measured to be $0.56^{+0.67}_{-0.44}{}^{+0.21}_{-0.06}$ fb at 7 TeV and $1.11^{+0.41}_{-0.35}{}^{+0.14}_{-0.10}$ fb at 8 TeV in their fiducial region (Table 2). The differential cross sections at E_{cm} = 8 TeV are also shown in Figs. 4 and 5. The results are given for m_H = 125 GeV. NODE=S126SZZ;LINKAGE=I

[18] AAD 15F use 4.5 fb^{-1} of pp collisions at E_{cm} = 7 TeV and 20.3 fb^{-1} at E_{cm} = 8 TeV. The quoted signal strength is given for m_H = 125.36 GeV. The signal strength for the gluon fusion production mode is $1.66^{+0.45}_{-0.41}{}^{+0.25}_{-0.15}$, while the signal strength for the vector boson fusion production mode is $0.26^{+1.60}_{-0.91}{}^{+0.36}_{-0.23}$. NODE=S126SZZ;LINKAGE=B

[19] AAD 14AR measure the cross section for $pp \rightarrow H \rightarrow ZZ^* \rightarrow 4\ell$ ($\ell = e, \mu$) using 20.3fb^{-1} at E_{cm} = 8 TeV. They give $\sigma \cdot B = 2.11^{+0.53}_{-0.47} \pm 0.08$ fbin their fiducial region, where 1.30 $\pm$ 0.13 fb is expected in the Standard Model for m_H= 125.4 GeV. Various differential cross sections are also given; see their Fig. 2. NODE=S126SZZ;LINKAGE=C

[20] CHATRCHYAN 14AA use 5.1 fb^{-1} of pp collisions at E_{cm} = 7 TeV and 19.7 fb^{-1} at E_{cm} = 8 TeV. The quoted signal strength is given for m_H = 125.6 GeV. The signal strength for the gluon fusion and $t\bar{t}H$ production mode is $0.80^{+0.46}_{-0.36}$, while the signal strength for the vector boson fusion and WH, ZH production mode is $1.7^{+2.2}_{-2.1}$. NODE=S126SZZ;LINKAGE=A

[21] AAD 13AK use 4.7 fb^{-1} of pp collisions at E_{cm} = 7 TeV and 20.7 fb^{-1} at E_{cm} = 8 TeV. The quoted signal strength is given for m_H = 125.5 GeV. NODE=S126SZZ;LINKAGE=LH

[22] CHATRCHYAN 13J obtain results based on $ZZ \rightarrow 4\ell$ final states in 5.1 fb^{-1} of pp collisions at E_{cm} = 7 TeV and 12.2 fb^{-1} at E_{cm} = 8 TeV. The quoted signal strength is given for m_H = 125.8 GeV. Superseded by CHATRCHYAN 14AA. NODE=S126SZZ;LINKAGE=CA

[23] AAD 12AI obtain results based on 4.7–4.8 fb^{-1} of pp collisions at E_{cm} = 7 TeV and 5.8 fb^{-1} at E_{cm} = 8 TeV. The quoted signal strengths are given for m_H = 126 GeV. See also AAD 12DA. NODE=S126SZZ;LINKAGE=AA

[24] CHATRCHYAN 12N obtain results based on 4.9–5.1 fb^{-1} of pp collisions at E_{cm} = 7 TeV and 5.1–5.3 fb^{-1} at E_{cm} = 8 TeV. An excess of events over background with a local significance of 5.0 σ is observed at about m_H = 125 GeV. The quoted signal strengths are given for m_H = 125.5 GeV. See also CHATRCHYAN 12BY and CHATRCHYAN 13Y. NODE=S126SZZ;LINKAGE=CH

$\gamma\gamma$ Final State

NODE=S126SGG
NODE=S126SGG
NEW

VALUE	DOCUMENT ID		TECN	COMMENT
1.10±0.06 OUR AVERAGE				
[1.10 ± 0.07 OUR 2023 AVERAGE]				
$1.04^{+0.10}_{-0.09}$	[1] AAD	23Y	ATLS	pp, 13 TeV
1.13±0.09	[2] CMS	22	CMS	pp, 13 TeV
$1.14^{+0.19}_{-0.18}$	[3,4] AAD	16AN	LHC	pp, 7, 8 TeV
$5.97^{+3.39}_{-3.12}$	[5] AALTONEN	13M	TEVA	$p\bar{p} \rightarrow HX$, 1.96 TeV

• • • We do not use the following data for averages, fits, limits, etc. • • •

	[6] TUMASYAN	23Q	CMS	pp, 13 TeV, cross sections	
	[7] AAD	22N	ATLS	pp, 13 TeV, diff. x-sections	
1.12 ± 0.09	[8] SIRUNYAN	21O	CMS	pp, 13 TeV	
$1.20^{+0.18}_{-0.14}$	[9] SIRUNYAN	19AT	CMS	pp, 13 TeV	
	[10] SIRUNYAN	19L	CMS	pp, 13 TeV, diff. x-section	
$0.99^{+0.15}_{-0.14}$	[11] AABOUD	18BO	ATLS	pp, 13 TeV	
$1.18^{+0.17}_{-0.14}$	[12] SIRUNYAN	18DS	CMS	pp, $H \to \gamma\gamma$, 13 TeV, floated m_H	
$1.14^{+0.27}_{-0.25}$	[4] AAD	16AN	ATLS	pp, 7, 8 TeV	OCCUR=2
$1.11^{+0.25}_{-0.23}$	[4] AAD	16AN	CMS	pp, 7, 8 TeV	OCCUR=3
	[13] KHACHATRY...	16G	CMS	pp, 8 TeV, diff. x-section	
$1.17 \pm 0.23^{+0.10}_{-0.08}{}^{+0.12}_{-0.08}$	[14] AAD	14BC	ATLS	$pp \to HX$, 7, 8 TeV	
	[15] AAD	14BJ	ATLS	pp, 8 TeV, diff. x-section	
$1.14 \pm 0.21^{+0.09}_{-0.05}{}^{+0.13}_{-0.09}$	[16] KHACHATRY...	14P	CMS	pp, 7, 8 TeV	
$1.55^{+0.33}_{-0.28}$	[17] AAD	13AK	ATLS	pp, 7 and 8 TeV	
$7.81^{+4.61}_{-4.42}$	[18] AALTONEN	13L	CDF	$p\overline{p} \to HX$, 1.96 TeV	
$4.20^{+4.60}_{-4.20}$	[19] ABAZOV	13L	D0	$p\overline{p} \to HX$, 1.96 TeV	
1.8 ± 0.5	[20] AAD	12AI	ATLS	$pp \to HX$, 7, 8 TeV	
2.2 ± 0.7	[20] AAD	12AI	ATLS	$pp \to HX$, 7 TeV	OCCUR=2
1.5 ± 0.6	[20] AAD	12AI	ATLS	$pp \to HX$, 8 TeV	OCCUR=3
$1.54^{+0.46}_{-0.42}$	[21] CHATRCHYAN	12N	CMS	$pp \to HX$, 7, 8 TeV	

[1] AAD 23Y use 139 fb^{-1} of pp collisions at E_{cm} = 13 TeV. The quoted results are given for m_H = 125.09 GeV and Γ_H = 4.07 MeV. Measured $\sigma{\cdot}B$ and ratios to the SM predictions for the different production modes are shown in their Table 9 and Fig. 9. Measured cross sections and ratios to the SM predictions in the reduced stage-1.2 (see their Fig. 11) simplified template cross section framework are shown in their Table 10 and Fig. 12. Wilson coefficients in the Warsaw basis (see their Table 11) at 95% CL are measured; see their Table 16 and Fig. 17. NODE=S126SGG;LINKAGE=P

[2] CMS 22 report combined results (see their Extended Data Table 2) using up to 138 fb^{-1} of data at E_{cm} = 13 TeV, assuming m_H = 125.38 GeV. See their Fig. 2 right. NODE=S126SGG;LINKAGE=N

[3] AAD 16AN perform fits to the ATLAS and CMS data at E_{cm} = 7 and 8 TeV. The signal strengths for individual production processes are $1.10^{+0.23}_{-0.22}$ for gluon fusion, 1.3 ± 0.5 for vector boson fusion, $0.5^{+1.3}_{-1.2}$ for WH production, $0.5^{+3.0}_{-2.5}$ for ZH production, and $2.2^{+1.6}_{-1.3}$ for $t\overline{t}H$ production. NODE=S126SGG;LINKAGE=H

[4] AAD 16AN: In the fit, relative production cross sections are fixed to those in the Standard Model. The quoted signal strength is given for m_H = 125.09 GeV. NODE=S126SGG;LINKAGE=I

[5] AALTONEN 13M combine all Tevatron data from the CDF and D0 Collaborations with up to 10.0 fb^{-1} and 9.7 fb^{-1}, respectively, of $p\overline{p}$ collisions at E_{cm} = 1.96 TeV. The quoted signal strength is given for m_H = 125 GeV. NODE=S126SGG;LINKAGE=AT

[6] TUMASYAN 23Q measure fiducial and differential cross sections at E_{cm} = 13 TeV with 137 fb^{-1} data. The quoted results are given for m_H = 125.38 GeV. The inclusive fiducial $\sigma{\cdot}B$ is $73.4^{+5.4}_{-5.3}$(stat)$^{+2.4}_{-2.2}$(syst) fb with their defined fiducial region (see their Section 7 and Table 2), where 75.4 ± 4.1 fb is expected in the Standard Model. See their Fig. 8 including other fiducial $\sigma{\cdot}B$ defined in their Table 3. Differential $\sigma{\cdot}B$ are shown in their Figs. 10–15. Double-differential $\sigma{\cdot}B$ are in their Figs. 16 and 17. NODE=S126SGG;LINKAGE=O

[7] AAD 22N measure fiducial and differential cross sections of $pp \to H \to \gamma\gamma$ at E_{cm} = 13 TeV with 139 fb^{-1} data. The quoted results are given for m_H = 125.09 GeV. The inclusive fiducial $\sigma \cdot B$ is $67 \pm 5 \pm 4$ fb with their defined fiducial region. Other fiducial $\sigma{\cdot}B$ are in their Table 3. Differential $\sigma{\cdot}B$ are shown in their Figs. 8–13, 15, 25–32, 35, 36. Double-differential $\sigma{\cdot}B$ are in their Figs. 14, 33, 34. Modifications of the b- and c-quark Yukawa couplings to H, κ_b and κ_c at 95% CL are in their Table 6 and Fig. 18. Wilson coefficients at 95% CL are in their Table 7 and Fig. 21. NODE=S126SGG;LINKAGE=M

[8] SIRUNYAN 21O measures cross sections and couplings with the $H \to \gamma\gamma$ channel using 137 fb^{-1} data at E_{cm} = 13 TeV. Results are given for m_H = 125.38 GeV. The signal strengths for individual production processes are given in their Fig. 16. Cross sections are given in their Tables 12 and 13 and Figs. 18 and 20, which are based on the simplified template cross section framework (reduced stage-1.2). Results in the κ-framework are given in their Fig. 22. NODE=S126SGG;LINKAGE=L

[9] SIRUNYAN 19AT perform a combine fit to 35.9 fb^{-1} of data at E_{cm} = 13 TeV. NODE=S126SGG;LINKAGE=K

[10] SIRUNYAN 19L measure fiducial and differential cross sections of the process $pp \to H \to \gamma\gamma$ at E_{cm} = 13 TeV with 35.9 fb^{-1}. See their Figs. 4–11. NODE=S126SGG;LINKAGE=J

[11] AABOUD 18BO use 36.1 fb^{-1} of pp collisions at E_{cm} = 13 TeV. The signal strengths for the individual production modes are: $0.81^{+0.19}_{-0.18}$ for gluon fusion, $2.0^{+0.6}_{-0.5}$ for vector boson fusion, $0.7^{+0.9}_{-0.8}$ for VH production ($V = W, Z$), and 0.5 ± 0.6 for $t\bar{t}H$ and tH production. Other measurements of cross sections and couplings are summarized in their Section 10. The quoted values are given for m_H = 125.09 GeV. NODE=S126SGG;LINKAGE=F

[12] SIRUNYAN 18DS use 35.9 fb^{-1} of $pp \to H$ collisions with $H \to \gamma\gamma$ at E_{cm} = 13 TeV. The Higgs mass is floated in the measurement of a signal strength. The result is $1.18^{+0.12}_{-0.11}$(stat.)$^{+0.09}_{-0.07}$(syst.)$^{+0.07}_{-0.06}$(theory), which is largely insensitive to the Higgs mass around 125 GeV. NODE=S126SGG;LINKAGE=G

[13] KHACHATRYAN 16G measure fiducial and differential cross sections of the process $pp \to HX$, $H \to \gamma\gamma$ at E_{cm} = 8 TeV with 19.7 fb^{-1}. See their Figs. 4–6 and Table 1 for data. NODE=S126SGG;LINKAGE=E

[14] AAD 14BC use 4.5 fb^{-1} of pp collisions at E_{cm} = 7 TeV and 20.3 fb^{-1} at E_{cm} = 8 TeV. The last uncertainty in the measurement is theory systematics. The quoted signal strength is given for m_H = 125.4 GeV. The signal strengths for the individual production modes are: 1.32 ± 0.38 for gluon fusion, 0.8 ± 0.7 for vector boson fusion, 1.0 ± 1.6 for WH production, $0.1^{+3.7}_{-0.1}$ for ZH production, and $1.6^{+2.7}_{-1.8}$ for $t\bar{t}H$ production. NODE=S126SGG;LINKAGE=B

[15] AAD 14BJ measure fiducial and differential cross sections of the process $pp \to HX$, $H \to \gamma\gamma$ at E_{cm} = 8 TeV with 20.3 fb^{-1}. See their Table 3 and Figs. 3–12 for data. NODE=S126SGG;LINKAGE=D

[16] KHACHATRYAN 14P use 5.1 fb^{-1} of pp collisions at E_{cm} = 7 TeV and 19.7 fb^{-1} at E_{cm} = 8 TeV. The last uncertainty in the measurement is theory systematics. The quoted signal strength is given for m_H = 124.7 GeV. The signal strength for the gluon fusion and $t\bar{t}H$ production mode is $1.13^{+0.37}_{-0.31}$, while the signal strength for the vector boson fusion and WH, ZH production mode is $1.16^{+0.63}_{-0.58}$. NODE=S126SGG;LINKAGE=A

[17] AAD 13AK use 4.7 fb^{-1} of pp collisions at E_{cm} = 7 TeV and 20.7 fb^{-1} at E_{cm} = 8 TeV. The quoted signal strength is given for m_H = 125.5 GeV. NODE=S126SGG;LINKAGE=LH

[18] AALTONEN 13L combine all CDF results with 9.45–10.0 fb^{-1} of $p\bar{p}$ collisions at E_{cm} = 1.96 TeV. The quoted signal strength is given for m_H = 125 GeV. NODE=S126SGG;LINKAGE=LL

[19] ABAZOV 13L combine all D0 results with up to 9.7 fb^{-1} of $p\bar{p}$ collisions at E_{cm} = 1.96 TeV. The quoted signal strength is given for m_H = 125 GeV. NODE=S126SGG;LINKAGE=AB

[20] AAD 12AI obtain results based on 4.8 fb^{-1} of pp collisions at E_{cm} = 7 TeV and 5.9 fb^{-1} at E_{cm} = 8 TeV. The quoted signal strengths are given for m_H = 126 GeV. See also AAD 12DA. NODE=S126SGG;LINKAGE=AA

[21] CHATRCHYAN 12N obtain results based on 5.1 fb^{-1} of pp collisions at E_{cm}=7 TeV and 5.3 fb^{-1} at E_{cm}=8 TeV. The quoted signal strength is given for m_H=125.5 GeV. See also CHATRCHYAN 13Y. NODE=S126SGG;LINKAGE=CA

$c\bar{c}$ Final State

NODE=S126SCC
NODE=S126SCC

VALUE	CL%	DOCUMENT ID	TECN	COMMENT	
< 14 (CL = 95%) [<110 (CL = 95%) OUR 2020 BEST LIMIT]					
< 14	95	[1] TUMASYAN	23AH CMS	$pp \to WH/ZH$, 13 TeV	
• • • We do not use the following data for averages, fits, limits, etc. • • •					
$9.4^{+20.3}_{-19.9}$		[2] TUMASYAN	23AD CMS	$pp \to WH/ZH$ (boosted), 13 TeV	
< 47	95	[2] TUMASYAN	23AD CMS	$pp \to WH/ZH$ (boosted), 13 TeV	OCCUR=3
−9 ±10 ±11		[3,4] AAD	22W ATLS	$pp \to WH/ZH$, 13 TeV	
−9 ±10 ±12		[3,5] AAD	22W ATLS	$pp \to WH/ZH$, 13 TeV	OCCUR=2
< 26	95	[3] AAD	22W ATLS	$pp \to WH/ZH$, 13 TeV	OCCUR=3
37 ±17 $^{+11}_{-9}$		[6] SIRUNYAN	20AE CMS	pp, 13 TeV	OCCUR=2
< 110	95	[7] AABOUD	18M ATLS	pp, 13 TeV	

[1] TUMASYAN 23AH search for VH, $H \to c\bar{c}$ ($V = W, Z$) using 138 fb^{-1} of pp collision data at E_{cm} = 13 TeV. The upper limit on $\sigma(pp \to VH)\cdot B(H \to c\bar{c})$ is 0.94 pb at 95% CL. See their Fig. 4. The quoted values are given for m_H = 125.38 GeV. NODE=S126SCC;LINKAGE=H

[2] TUMASYAN 23AD search for Higgs produced with transverse momenta greater than 450 GeV and decaying to $c\bar{c}$ using 138 fb^{-1} of pp collision data at E_{cm} = 13 TeV. NODE=S126SCC;LINKAGE=G

[3] AAD 22W search for VH, $H \to c\bar{c}$ ($V = W, Z$) using 139 fb^{-1} of pp collision data at E_{cm} = 13 TeV. The results are given for m_H = 125 GeV. NODE=S126SCC;LINKAGE=D

[4] The analysis of VH, $H \to c\bar{c}$ is combined with VH, $H \to b\bar{b}$ (AAD 21AB). The ratio $|\kappa_c/\kappa_b|$ is constrained to be less than 4.5 at 95% CL. See their Fig. 7. NODE=S126SCC;LINKAGE=E

[5] The constraint on the charm Yukawa coupling modifier κ_c is measured to be $|\kappa_c|$ <8.5 at 95% CL. See their Fig. 4. NODE=S126SCC;LINKAGE=F

[6] SIRUNYAN 20AE use 35.9 fb^{-1} at of pp collisions at E_{cm} = 13 TeV. The measured best fit value of $\sigma(pp \to VH)\cdot B(H \to c\bar{c})$ is $2.40^{+1.12}_{-1.11}{}^{+0.65}_{-0.61}$ pb (equivalent to < 4.5 pb at 95% CL upper limit, i.e. 70 times the standard model), where V is $W \to \ell\nu$, $Z \to \ell\ell$, or $Z \to \nu\nu$ ($\ell = e, \mu$). The quoted values are given for m_H = 125 GeV. NODE=S126SCC;LINKAGE=C

[7] AABOUD 18M use 36.1 fb^{-1} at of pp collisions at E_{cm} = 13 TeV. The upper limit on $\sigma(pp \to ZH)\cdot B(H \to c\bar{c})$ is 2.7 pb at 95% CL. This corresponds to 110 times the standard model. The quoted values are given for m_H = 125 GeV. NODE=S126SCC;LINKAGE=A

$b\overline{b}$ Final State

NODE=S126SBB
NODE=S126SBB

VALUE	DOCUMENT ID	TECN	COMMENT	
0.99±0.12 OUR AVERAGE				
$1.05^{+0.22}_{-0.21}$	[1] CMS 22	CMS	pp, 13 TeV	
$1.02^{+0.12}_{-0.11}{}^{+0.14}_{-0.13}$	[2] AAD 21AB	ATLS	$pp \to HW/HZ$, $H \to b\overline{b}$, 13 TeV, 139 fb^{-1}	
$0.95\pm0.32^{+0.20}_{-0.17}$	[3] AAD 21AJ	ATLS	VBF, $H \to b\overline{b}$, pp, 13 TeV, 126 fb^{-1}	
$0.70^{+0.29}_{-0.27}$	[4,5] AAD 16AN	LHC	pp, 7, 8 TeV	
$1.59^{+0.69}_{-0.72}$	[6] AALTONEN 13M	TEVA	$p\overline{p} \to HX$, 1.96 TeV	
• • • We do not use the following data for averages, fits, limits, etc. • • •				
0.8 ± 3.2	[7] AAD 22X	ATLS	boosted $H \to b\overline{b}$, pp, 13 TeV	
$0.95\pm0.18^{+0.19}_{-0.18}$	[2] AAD 21AB	ATLS	$pp \to HW$, $H \to b\overline{b}$, 13 TeV, 139 fb^{-1}	OCCUR=2
$1.08\pm0.17^{+0.18}_{-0.15}$	[2] AAD 21AB	ATLS	$pp \to HZ$, $H \to b\overline{b}$, 13 TeV, 139 fb^{-1}	OCCUR=3
$0.72^{+0.29}_{-0.28}{}^{+0.26}_{-0.22}$	[8] AAD 21H	ATLS	$pp \to HW/HZ$, $H \to b\overline{b}$, boosted W/Z, 13 TeV, 139 fb^{-1}	
1.3 ± 1.0	[9] AAD 21M	ATLS	VBF+γ, $H \to b\overline{b}$, pp, 13 TeV, 132 fb^{-1}	
$3.7 \pm1.2 {}^{+0.11}_{-0.9}$	[10] SIRUNYAN 20BL	CMS	boosted $H \to b\overline{b}$, pp, 13 TeV	
	[11] AABOUD 19U	ATLS	$pp \to VH$, $H \to b\overline{b}$, 13 TeV, cross sections	
1.12 ± 0.29	[12] SIRUNYAN 19AT	CMS	pp, 13 TeV	
$1.16^{+0.27}_{-0.25}$	[13] AABOUD 18BN	ATLS	$pp \to HW/HZ$, $H \to b\overline{b}$, 13 TeV, 79.8 fb^{-1}	
$0.98^{+0.22}_{-0.21}$	[14] AABOUD 18BN	ATLS	$pp \to HW/HZ$, $H \to b\overline{b}$, 7, 8, 13 TeV	OCCUR=2
1.01 ± 0.20	[15] AABOUD 18BN	ATLS	$pp \to HX$, ggF, VBF, VH, $t\overline{t}H$ 7, 8, 13 TeV	OCCUR=3
$2.5 {}^{+1.4}_{-1.3}$	[16,17] AABOUD 18BQ	ATLS	$pp \to HX$, VBF, ggF, VH, $t\overline{t}H$, 13 TeV	
$3.0 {}^{+1.7}_{-1.6}$	[16,18] AABOUD 18BQ	ATLS	$pp \to HX$, VBF, 13 TeV	OCCUR=2
	[19] AALTONEN 18C	CDF	$p\overline{p} \to HX$, 1.96 TeV	
$1.19^{+0.40}_{-0.38}$	[20] SIRUNYAN 18AE	CMS	$pp \to HW/HZ$, $H \to b\overline{b}$, 13 TeV	
$1.06^{+0.31}_{-0.29}$	[21] SIRUNYAN 18AE	CMS	$pp \to HW/HZ$, $H \to b\overline{b}$, 7, 8, 13 TeV	OCCUR=2
1.06 ± 0.26	[22] SIRUNYAN 18DB	CMS	$pp \to HW/HZ$, $H \to b\overline{b}$, 13 TeV, 77.2 fb^{-1}	
1.01 ± 0.22	[23] SIRUNYAN 18DB	CMS	$pp \to HW/HZ$, $H \to b\overline{b}$, 7, 8, 13 TeV	OCCUR=2
1.04 ± 0.20	[24] SIRUNYAN 18DB	CMS	$pp \to HX$, ggF, VBF, VH, $t\overline{t}H$ 7, 8, 13 TeV	OCCUR=3
$2.3 {}^{+1.8}_{-1.6}$	[25] SIRUNYAN 18E	CMS	$pp \to HX$, boosted, 13 TeV	
$1.20^{+0.24}_{-0.23}{}^{+0.34}_{-0.28}$	[26] AABOUD 17BA	ATLS	$pp \to HW/ZX$, $H \to b\overline{b}$, 13 TeV, 36.1 fb^{-1}	
$0.90\pm0.18^{+0.21}_{-0.19}$	[27] AABOUD 17BA	ATLS	$pp \to HW/ZX$, $H \to b\overline{b}$, 7, 8, 13 TeV	OCCUR=2
$-0.8 \pm1.3 {}^{+1.8}_{-1.9}$	[28] AABOUD 16X	ATLS	$pp \to HX$, VBF, 8 TeV	
0.62 ± 0.37	[5] AAD 16AN	ATLS	pp, 7, 8 TeV	OCCUR=2
$0.81^{+0.45}_{-0.43}$	[5] AAD 16AN	CMS	pp, 7, 8 TeV	OCCUR=3
$0.63^{+0.31}_{-0.30}{}^{+0.24}_{-0.23}$	[29] AAD 16K	ATLS	pp, 7, 8 TeV	
$0.52\pm0.32\pm0.24$	[30] AAD 15G	ATLS	$pp \to HW/ZX$, 7, 8 TeV	
$2.8 {}^{+1.6}_{-1.4}$	[31] KHACHATRY... 15Z	CMS	$pp \to HX$, VBF, 8 TeV	
$1.03^{+0.44}_{-0.42}$	[32] KHACHATRY... 15Z	CMS	pp, 8 TeV, combined	OCCUR=2
1.0 ± 0.5	[33] CHATRCHYAN 14AI	CMS	$pp \to HW/ZX$, 7, 8 TeV	
$1.72^{+0.92}_{-0.87}$	[34] AALTONEN 13L	CDF	$p\overline{p} \to HX$, 1.96 TeV	

$1.23^{+1.24}_{-1.17}$	[35] ABAZOV	13L	D0	$p\overline{p} \rightarrow HX$, 1.96 TeV
0.5 ± 2.2	[36] AAD	12AI	ATLS	$pp \rightarrow HW/ZX$, 7 TeV
	[37] AALTONEN	12T	TEVA	$p\overline{p} \rightarrow HW/ZX$, 1.96 TeV
$0.48^{+0.81}_{-0.70}$	[38] CHATRCHYAN	12N	CMS	$pp \rightarrow HW/ZX$, 7, 8 TeV

[1] CMS 22 report combined results (see their Extended Data Table 2) using up to 138 fb^{-1} of data at E_{cm} = 13 TeV, assuming m_H = 125.38 GeV. See their Fig. 2 right. NODE=S126SBB;LINKAGE=HA

[2] AAD 21AB search for VH, $H \rightarrow b\overline{b}$ ($V = W$, Z) using 139 fb^{-1} of pp collision data at E_{cm} = 13 TeV. The results are given for m_H = 125 GeV. Cross sections are given in their Table 13 and Fig. 7, which are based on the simplified template cross section framework (reduced stage-1.2). Wilson coefficients of the Warsaw-basis operators are given in their Fig. 9. NODE=S126SBB;LINKAGE=BA

[3] AAD 21AJ present measurements of $H \rightarrow b\overline{b}$ in the VBF production mode. The inclusive VBF cross sections with and without the branching ratio of $H \rightarrow b\overline{b}$ are $2.07 \pm 0.70^{+0.46}_{-0.37}$ fb and $3.56 \pm 1.21^{+0.80}_{-0.64}$ fb, respectively. The latter is obtained assuming the SM value of B($H \rightarrow b\overline{b}$) = 0.5809 and m_H = 125 GeV. NODE=S126SBB;LINKAGE=DA

[4] AAD 16AN perform fits to the ATLAS and CMS data at E_{cm} = 7 and 8 TeV. The signal strengths for individual production processes are 1.0 ± 0.5 for WH production, 0.4 ± 0.4 for ZH production, and 1.1 ± 1.0 for $t\overline{t}H$ production. NODE=S126SBB;LINKAGE=H

[5] AAD 16AN: In the fit, relative production cross sections are fixed to those in the Standard Model. The quoted signal strength is given for m_H = 125.09 GeV. NODE=S126SBB;LINKAGE=I

[6] AALTONEN 13M combine all Tevatron data from the CDF and D0 Collaborations with up to 10.0 fb^{-1} and 9.7 fb^{-1}, respectively, of $p\overline{p}$ collisions at E_{cm} = 1.96 TeV. The quoted signal strength is given for m_H = 125 GeV. NODE=S126SBB;LINKAGE=AT

[7] AAD 22X measure cross sections using a boosted $H \rightarrow b\overline{b}$ with large-radius jets. The data is 136 fb^{-1} of pp collisions at E_{cm} = 13 TeV. All the results are given for m_H = 125 GeV. The inclusive signal strength is given using data with a H candidate jet p_T >250 GeV. The fiducial H production cross section ($p_T(H)$>450 GeV and $|y(H)|$ <2) is <115 fb (95% CL) and the upper limits for other four different p_T regions are shown in their Fig 12. The measured fiducial H production cross section ($p_T(H)$>1 TeV) is 2.3 ± 3.9(stat)± 1.3(syst)± 0.5(theory) fb. NODE=S126SBB;LINKAGE=GA

[8] AAD 21H present measurements of $H \rightarrow b\overline{b}$ with a boosted vector boson (p_T > 250 GeV) using 139 fb^{-1} of pp collision data at E_{cm} = 13 TeV. Cross sections are given in their Table 6 and Fig. 4, which are based on the simplified template cross section framework (reduced stage-1.2). Wilson coefficients of the Warsaw-basis operators are given in their Fig. 5. NODE=S126SBB;LINKAGE=EA

[9] AAD 21M search for VBF+γ, $H \rightarrow b\overline{b}$ using 132 fb^{-1} of pp collision data at E_{cm} = 13 TeV. NODE=S126SBB;LINKAGE=FA

[10] SIRUNYAN 20BL search for boosted $H \rightarrow b\overline{b}$ (a H candidate jet p_T >450 GeV) using 137 fb^{-1} of pp collision data at E_{cm} = 13 TeV. The quoted signal strength corresponds to a significance of 2.5 standard deviations and is given for m_H = 125 GeV. A differential fiducial cross section as a function of Higgs boson p_T for ggF is shown in their Fig. 7, assuming the other production modes occur at the expected SM rates. The reported value is $3.7 \pm 1.2^{+0.8}_{-0.7}{}^{+0.8}_{-0.5}$ where the last uncertainty comes from theoretical modeling. We have combined the systematic uncertainties in quadrature. NODE=S126SBB;LINKAGE=Z

[11] AABOUD 19U measure cross sections of $pp \rightarrow VH$, $H \rightarrow b\overline{b}$ production as a function of the gauge boson transverse momentum using data of 79.8 fb^{-1}. The kinematic fiducial volumes used is based on the simplified template cross section framework (reduced stage-1). See their Table 3 and Fig. 3. NODE=S126SBB;LINKAGE=Y

[12] SIRUNYAN 19AT perform a combine fit to 35.9 fb^{-1} of data at E_{cm} = 13 TeV. NODE=S126SBB;LINKAGE=X

[13] AABOUD 18BN search for VH, $H \rightarrow b\overline{b}$ ($V = W$, Z) using 79.8 fb^{-1} of pp collision data at E_{cm} = 13 TeV. The quoted signal strength corresponds to a significance of 4.9 standard deviations and is given for m_H = 125 GeV. NODE=S126SBB;LINKAGE=N

[14] AABOUD 18BN combine results of 79.8 fb^{-1} at E_{cm} = 13 TeV with results of VH at E_{cm} = 7 and 8 TeV. NODE=S126SBB;LINKAGE=O

[15] AABOUD 18BN combine results of VH at E_{cm} = 7, 8 and 13 TeV with results of VBF (+gluon fusion) and $t\overline{t}H$ at E_{cm} = 7, 8, and 13 TeV to perform a search for the $H \rightarrow b\overline{b}$ decay. The quoted signal strength assumes a SM production strength and corresponds to a significance of 5.4 standard deviations. NODE=S126SBB;LINKAGE=P

[16] AABOUD 18BQ search for $H \rightarrow b\overline{b}$ produced through vector-boson fusion (VBF) and VBF+γ with 30.6 fb^{-1} pp collision data at E_{cm} = 13 TeV. The quoted signal strength is given for m_H = 125 GeV. NODE=S126SBB;LINKAGE=Q

[17] The signal strength is measured including all production modes (VBF, ggF, VH, $t\overline{t}H$). NODE=S126SBB;LINKAGE=U

[18] The signal strength is measured for VBF-only and others (ggF, VH, $t\overline{t}H$) are constrained to Standard Model expectations with uncertainties described in their Section VIII B. NODE=S126SBB;LINKAGE=V

[19] AALTONEN 18C use 5.4 fb^{-1} of $p\overline{p}$ collisions at E_{cm} = 1.96 TeV. The upper limit at 95% CL on $p\overline{p} \rightarrow H \rightarrow b\overline{b}$ is 33 times the SM predicion, which corresponds to a cross section of 40.6 pb. NODE=S126SBB;LINKAGE=W

[20] SIRUNYAN 18AE use 35.9 fb^{-1} of pp collision data at E_{cm} = 13 TeV. The quoted signal strength corresponds to 3.3 standard deviations and is given for m_H = 125.09 GeV. NODE=S126SBB;LINKAGE=L

[21] SIRUNYAN 18AE combine the result of 35.9 fb^{-1} at E_{cm} = 13 TeV with the results obtained from data of up to 5.1 fb^{-1} at E_{cm} = 7 TeV and up to 18.9 fb^{-1} at E_{cm} = 8 TeV (CHATRCHYAN 14AI and KHACHATRYAN 15Z). The quoted signal strength corresponds to 3.8 standard deviations and is given for m_H = 125.09 GeV. NODE=S126SBB;LINKAGE=M

[22] SIRUNYAN 18DB search for VH, $H \to b\overline{b}$ ($V = W$, Z) using 77.2 fb^{-1} of pp collision data at E_{cm} = 13 TeV. The quoted signal strength corresponds to a significance of 4.4 standard deviations and is given for m_H = 125.09 GeV. NODE=S126SBB;LINKAGE=R

[23] SIRUNYAN 18DB combine the result of 77.2 fb^{-1} at E_{cm} = 13 TeV with the results obtained from data of up to 5.1 fb^{-1} at E_{cm} = 7 TeV and up to 18.9 fb^{-1} at E_{cm} = 8 TeV. The quoted signal strength corresponds to a significance of 4.8 standard deviations and is given for m_H = 125.09 GeV. NODE=S126SBB;LINKAGE=S

[24] SIRUNYAN 18DB combine results of 77.2 fb^{-1} at E_{cm} = 13 TeV with results of gluon fusion (ggF), VBF and $t\overline{t}H$ at E_{cm} = 7 TeV, 8 TeV and 13 TeV to perform a search for the $H \to b\overline{b}$ decay. The quoted signal strength assumes a SM production strength and corresponds to a significance of 5.6 standard deviations and is given for m_H = 125.09 GeV. NODE=S126SBB;LINKAGE=T

[25] SIRUNYAN 18E use 35.9 fb^{-1} at E_{cm} = 13 TeV. The quoted signal strength is given for m_H = 125 GeV. They measure $\sigma \cdot B$ for gluon fusion production of $H \to b\overline{b}$ with p_T >450 GeV, $|\eta|$ <2.5 to be 74 $\pm$ 48^{+17}_{-10} fb. NODE=S126SBB;LINKAGE=K

[26] AABOUD 17BA use 36.1 fb^{-1} at E_{cm} = 13 TeV. The quoted signal strength is given for m_H = 125 GeV. They give σ(W H)$\cdot B(H \to b\overline{b}) = 1.08^{+0.54}_{-0.47}$ pb and σ(Z H)$\cdot B(H \to b\overline{b}) = 0.57^{+0.26}_{-0.23}$ pb. NODE=S126SBB;LINKAGE=F

[27] AABOUD 17BA combine 7, 8 and 13 TeV analyses. The quoted signal strength is given for m_H = 125 GeV. NODE=S126SBB;LINKAGE=G

[28] AABOUD 16X search for vector-boson fusion production of H decaying to $b\overline{b}$ in 20.2 fb^{-1} of pp collisions at E_{cm} = 8 TeV. The quoted signal strength is given for m_H = 125 GeV. NODE=S126SBB;LINKAGE=J

[29] AAD 16K use up to 4.7 fb^{-1} of pp collisions at E_{cm} = 7 TeV and up to 20.3 fb^{-1} at E_{cm} = 8 TeV. The quoted signal strength is given for m_H = 125.36 GeV. NODE=S126SBB;LINKAGE=E

[30] AAD 15G use 4.7 fb^{-1} of pp collisions at E_{cm} = 7 TeV and 20.3 fb^{-1} at E_{cm} = 8 TeV. The quoted signal strength is given for m_H = 125.36 GeV. NODE=S126SBB;LINKAGE=B

[31] KHACHATRYAN 15Z search for vector-boson fusion production of H decaying to $b\overline{b}$ in up to 19.8 fb^{-1} of pp collisions at E_{cm} = 8 TeV. The quoted signal strength is given for m_H = 125 GeV. NODE=S126SBB;LINKAGE=C

[32] KHACHATRYAN 15Z combined vector boson fusion, WH, ZH production, and $t\overline{t}H$ production results. The quoted signal strength is given for m_H = 125 GeV. NODE=S126SBB;LINKAGE=D

[33] CHATRCHYAN 14AI use up to 5.1 fb^{-1} of pp collisions at E_{cm} = 7 TeV and up to 18.9 fb^{-1} at E_{cm} = 8 TeV. The quoted signal strength is given for m_H = 125 GeV. See also CHATRCHYAN 14AJ. NODE=S126SBB;LINKAGE=A

[34] AALTONEN 13L combine all CDF results with 9.45–10.0 fb^{-1} of $p\overline{p}$ collisions at E_{cm} = 1.96 TeV. The quoted signal strength is given for m_H = 125 GeV. NODE=S126SBB;LINKAGE=LL

[35] ABAZOV 13L combine all D0 results with up to 9.7 fb^{-1} of $p\overline{p}$ collisions at E_{cm} = 1.96 TeV. The quoted signal strength is given for m_H = 125 GeV. NODE=S126SBB;LINKAGE=AB

[36] AAD 12AI obtain results based on 4.6–4.8 fb^{-1} of pp collisions at E_{cm} = 7 TeV. The quoted signal strengths are given in their Fig. 10 for m_H = 126 GeV. See also Fig. 13 of AAD 12DA. NODE=S126SBB;LINKAGE=AA

[37] AALTONEN 12T combine AALTONEN 12Q, AALTONEN 12R, AALTONEN 12S, ABAZOV 12O, ABAZOV 12P, and ABAZOV 12K. An excess of events over background is observed which is most significant in the region m_H = 120–135 GeV, with a local significance of up to 3.3 σ. The local significance at m_H = 125 GeV is 2.8 σ, which corresponds to $(\sigma(HW) + \sigma(HZ)) \cdot$ B$(H \to b\overline{b}) = (0.23^{+0.09}_{-0.08})$ pb, compared to the Standard Model expectation at m_H = 125 GeV of 0.12 $\pm$ 0.01 pb. Superseded by AALTONEN 13M. NODE=S126SBB;LINKAGE=AL

[38] CHATRCHYAN 12N obtain results based on 5.0 fb^{-1} of pp collisions at E_{cm}=7 TeV and 5.1 fb^{-1} at E_{cm}=8 TeV. The quoted signal strength is given for m_H=125.5 GeV. See also CHATRCHYAN 13Y. NODE=S126SBB;LINKAGE=CA

$\mu^+\mu^-$ Final State

NODE=S126SMU
NODE=S126SMU

VALUE	CL%	DOCUMENT ID		TECN	COMMENT
1.21±0.35 OUR AVERAGE					
$1.21^{+0.45}_{-0.42}$		[1] CMS	22	CMS	pp, 13 TeV
1.2 ±0.6		[2] AAD	21	ATLS	pp, 13 TeV
• • • We do not use the following data for averages, fits, limits, etc. • • •					
$1.19^{+0.40}_{-0.39}{}^{+0.15}_{-0.14}$		[3] SIRUNYAN	21C	CMS	pp, 13 TeV
$0.68^{+1.25}_{-1.24}$		[4] SIRUNYAN	19AT	CMS	pp, 13 TeV
$0.7 \pm 1.0 {}^{+0.2}_{-0.1}$		[5] SIRUNYAN	19E	CMS	pp, 13 TeV, 35.9 fb^{-1}

1.0 $\pm$1.0 $\pm$0.1		[5] SIRUNYAN	19E	CMS	pp, 7, 8, 13 TeV	OCCUR=2
$-$0.1 $\pm$1.4		[6] AABOUD	17Y	ATLS	pp, 7, 8, 13 TeV	
$-$0.1 $\pm$1.5		[6] AABOUD	17Y	ATLS	pp, 13 TeV	OCCUR=2
0.1 $\pm$2.5		[7] AAD	16AN	LHC	pp, 7, 8 TeV	
$-$0.6 $\pm$3.6		[7] AAD	16AN	ATLS	pp, 7, 8 TeV	OCCUR=2
0.9 $^{+3.6}_{-3.5}$		[7] AAD	16AN	CMS	pp, 7, 8 TeV	OCCUR=3
< 7.4	95	[8] KHACHATRY...	15H	CMS	$pp \to HX$, 7, 8 TeV	
< 7.0	95	[9] AAD	14AS	ATLS	$pp \to HX$, 7, 8 TeV	

[1] CMS 22 report combined results (see their Extended Data Table 2) using up to 138 fb^{-1} of data at E_{cm} = 13 TeV, assuming m_H = 125.38 GeV. See their Fig. 2 right. NODE=S126SMU;LINKAGE=K

[2] AAD 21 search for $H \to \mu^+\mu^-$ using 139 fb^{-1} of pp collision data at E_{cm} = 13 TeV. The quoted signal strength corresponds to a significance of 2.0 standard deviations and is given for m_H = 125.09 GeV. The upper limit on the cross section times branching fraction is 2.2 times the SM prediction at 95% CL, which corresponds to the branching fraction upper limit of 4.7 $\times$ 10^{-4} (assuming SM production cross sections). NODE=S126SMU;LINKAGE=I

[3] SIRUNYAN 21 search for $H \to \mu^+\mu^-$ using 137 fb^{-1} of pp collision data at E_{cm} = 13 TeV. The quoted signal strength corresponds to a significance of 3.0 standard deviations and is given for m_H = 125.38 GeV. NODE=S126SMU;LINKAGE=J

[4] SIRUNYAN 19AT perform a combine fit to 35.9 fb^{-1} of data at E_{cm} = 13 TeV. NODE=S126SMU;LINKAGE=H

[5] SIRUNYAN 19E search for $H \to \mu^+\mu^-$ using 35.9 fb^{-1} of pp collisions at E_{cm} = 13 TeV and combine with results of 7 TeV (5.0 fb^{-1}) and 8 TeV (19.7 fb^{-1}). The upper limit at 95% CL on the signal strength is 2.9, which corresponds to the SM Higgs boson branching fraction to a muon pair of 6.4 $\times$ 10^{-4}. NODE=S126SMU;LINKAGE=F

[6] AABOUD 17Y use 36.1 fb^{-1} of pp collisions at E_{cm} = 13 TeV, 20.3 fb^{-1} at 8 TeV and 4.5 fb^{-1} at 7 TeV. The quoted signal strength is given for m_H = 125 GeV. NODE=S126SMU;LINKAGE=E

[7] AAD 16AN: In the fit, relative production cross sections are fixed to those in the Standard Model. The quoted signal strength is given for m_H = 125.09 GeV. NODE=S126SMU;LINKAGE=D

[8] KHACHATRYAN 15H use 5.0 fb^{-1} of pp collisions at E_{cm} = 7 TeV and 19.7 fb^{-1} at 8 TeV. The quoted signal strength is given for m_H = 125 GeV. NODE=S126SMU;LINKAGE=B

[9] AAD 14AS search for $H \to \mu^+\mu^-$ in 4.5 fb^{-1} of pp collisions at E_{cm} = 7 TeV and 20.3 fb^{-1} at E_{cm} = 8 TeV. The quoted signal strength is given for m_H = 125.5 GeV. NODE=S126SMU;LINKAGE=A

$\tau^+\tau^-$ Final State

NODE=S126STT
NODE=S126STT

VALUE	DOCUMENT ID		TECN	COMMENT	
0.91$\pm$0.09 OUR AVERAGE					
0.85$\pm$0.10	[1] CMS	22	CMS	pp, 13 TeV	
1.09 $^{+0.18}_{-0.17}$ $^{+0.26}_{-0.22}$ $^{+0.16}_{-0.11}$	[2] AABOUD	19AQ	ATLS	pp, 13 TeV	
1.11 $^{+0.24}_{-0.22}$	[3,4] AAD	16AN	LHC	pp, 7, 8 TeV	
1.68 $^{+2.28}_{-1.68}$	[5] AALTONEN	13M	TEVA	$p\overline{p} \to HX$, 1.96 TeV	
• • • We do not use the following data for averages, fits, limits, etc. • • •					
0.82 $^{+0.11}_{-0.10}$	[6,7] TUMASYAN	23Y	CMS	pp, 13 TeV	
0.67 $^{+0.20}_{-0.18}$	[6,8] TUMASYAN	23Y	CMS	pp, 13 TeV	OCCUR=2
0.81 $^{+0.17}_{-0.16}$	[6,9] TUMASYAN	23Y	CMS	pp, 13 TeV	OCCUR=3
1.79 $^{+0.47}_{-0.42}$	[6,10] TUMASYAN	23Y	CMS	pp, 13 TeV	OCCUR=4
	[11] AAD	22Q	ATLS	pp, 13 TeV	
	[12] TUMASYAN	22AJ	CMS	pp, 13 TeV	
2.5 $^{+1.4}_{-1.3}$	[13] SIRUNYAN	19AF	CMS	$pp \to HW/HZ$, $H \to \tau\tau$, 13 TeV	
1.24 $^{+0.29}_{-0.27}$	[14] SIRUNYAN	19AF	CMS	pp, 13 TeV	OCCUR=2
1.02 $^{+0.26}_{-0.24}$	[15] SIRUNYAN	19AT	CMS	pp, 13 TeV	
1.09 $^{+0.27}_{-0.26}$	[16] SIRUNYAN	18Y	CMS	pp, 13 TeV	
0.98$\pm$0.18	[17] SIRUNYAN	18Y	CMS	pp, 7, 8, 13 TeV	OCCUR=2
2.3 $\pm$1.6	[18] AAD	16AC	ATLS	$pp \to HW/ZX$, 8 TeV	
1.41 $^{+0.40}_{-0.36}$	[4] AAD	16AN	ATLS	pp, 7, 8 TeV	OCCUR=2

$0.88^{+0.30}_{-0.28}$	4 AAD	16AN	CMS	pp, 7, 8 TeV		OCCUR=3
$1.44^{+0.30}_{-0.29}{}^{+0.29}_{-0.23}$	19 AAD	16K	ATLS	pp, 7, 8 TeV		
$1.43^{+0.27}_{-0.26}{}^{+0.32}_{-0.25}\pm0.09$	20 AAD	15AH	ATLS	$pp \to HX$, 7, 8 TeV		
0.78 ± 0.27	21 CHATRCHYAN	14K	CMS	$pp \to HX$, 7, 8 TeV		
$0.00^{+8.44}_{-0.00}$	22 AALTONEN	13L	CDF	$p\overline{p} \to HX$, 1.96 TeV		
$3.96^{+4.11}_{-3.38}$	23 ABAZOV	13L	D0	$p\overline{p} \to HX$, 1.96 TeV		
$0.4\ {}^{+1.6}_{-2.0}$	24 AAD	12AI	ATLS	$pp \to HX$, 7 TeV		
$0.09^{+0.76}_{-0.74}$	25 CHATRCHYAN	12N	CMS	$pp \to HX$, 7, 8 TeV		

[1] CMS 22 report combined results (see their Extended Data Table 2) using up to 138 fb^{-1} of data at E_{cm} = 13 TeV, assuming m_H = 125.38 GeV. See their Fig. 2 right. NODE=S126STT;LINKAGE=N

[2] AABOUD 19AQ use 36.1 fb^{-1} of data. The first, second and third quoted errors are statistical, experimental systematic and theory systematic uncertainties, respectively. The quoted signal strength is given for m_H = 125 GeV and corresponds to 4.4 standard deviations. Combining with 7 TeV and 8 TeV results (AAD 15AH), the observed significance is 6.4 standard deviations. The cross sections in the $H \to \tau\tau$ decay channel (m_H = 125 GeV) are measured to $3.77^{+0.60}_{-0.59}$ (stat) $^{+0.87}_{-0.74}$ (syst) pb for the inclusive, $0.28 \pm 0.09^{+0.11}_{-0.09}$ pb for VBF, and $3.1 \pm 1.0^{+1.6}_{-1.3}$ pb for gluon-fusion production. See their Table XI for the cross sections in the framework of simplified template cross sections. NODE=S126STT;LINKAGE=K

[3] AAD 16AN perform fits to the ATLAS and CMS data at E_{cm} = 7 and 8 TeV. The signal strengths for individual production processes are 1.0 ± 0.6 for gluon fusion, 1.3 ± 0.4 for vector boson fusion, -1.4 ± 1.4 for WH production, $2.2^{+2.2}_{-1.8}$ for ZH production, and $-1.9^{+3.7}_{-3.3}$ for $t\overline{t}H$ production. NODE=S126STT;LINKAGE=G

[4] AAD 16AN: In the fit, relative production cross sections are fixed to those in the Standard Model. The quoted signal strength is given for m_H = 125.09 GeV. NODE=S126STT;LINKAGE=H

[5] AALTONEN 13M combine all Tevatron data from the CDF and D0 Collaborations with up to 10.0 fb^{-1} and 9.7 fb^{-1}, respectively, of $p\overline{p}$ collisions at E_{cm} = 1.96 TeV. The quoted signal strength is given for m_H = 125 GeV. NODE=S126STT;LINKAGE=AT

[6] TUMASYAN 23Y measure Higgs production with $pp \to H \to \tau\tau$ at E_{cm} = 13 TeV with 138 fb^{-1} data. The quoted results are given for m_H = 125.38 GeV. NODE=S126STT;LINKAGE=P

[7] The inclusive $\sigma{\cdot}B$ is 2800^{+356}_{-335} fb (see their Figs. 10 and 14). See their Fig. 15 for the 68 % and 95 % CL contours in the $\kappa_V - \kappa_F$ plane. NODE=S126STT;LINKAGE=Q

[8] The quoted result is for the stage-0 simplified template cross section (STXS) and the $\sigma_{ggF} \cdot B$ is 2030^{+598}_{-555} fb (see their Figs. 10 and 14). Measured cross sections and ratios to the SM predictions in the reduced stage-1.2 STXS (see their Fig. 1) are shown in their Table 9 and Figs. 12 and 14. NODE=S126STT;LINKAGE=R

[9] The quoted result is for the stage-0 STXS and the $\sigma_{VBF} \cdot B$ is $267^{+53.9}_{-52.6}$ fb (see their Figs. 10 and 14). Measured cross sections and ratios to the SM predictions in the reduced stage-1.2 STXS (see their Fig. 2) are shown in their Table 9 and Figs. 12, 14. NODE=S126STT;LINKAGE=S

[10] The quoted result is for the stage-0 STXS and the $\sigma_{VH} \cdot B$ is $79.0^{+20.5}_{-18.6}$ fb (see their Figs. 10 and 14). Measured cross sections and ratios to the SM predictions in the reduced stage-1.2 STXS (see their Fig. 3) are shown in their Table 9 and Figs. 12, 14. NODE=S126STT;LINKAGE=T

[11] AAD 22Q measure cross sections of $pp \to H \to \tau\tau$ at E_{cm} = 13 TeV with 139 fb^{-1} data. The quoted results are given for m_H = 125.09 GeV and $|y(H)|$ <2.5 is required. The inclusive fiducial $\sigma \cdot B$ is $2.94 \pm 0.21^{+0.37}_{-0.32}$ pb. The fiducial $\sigma \cdot B$ for the four dominant production modes are $2.65 \pm 0.41^{+0.91}_{-0.67}$ pb for ggF, $0.197 \pm 0.028^{+0.032}_{-0.026}$ pb for VBF, $0.115 \pm 0.058^{+0.042}_{-0.040}$ pb for VH, $0.033 \pm 0.031^{+0.022}_{-0.017}$ pb for $t\overline{t}H$. The cross sections using simplified template cross section framework (STXS) are given in their Fig. 14(a) and Table 15. The STXS bins (a reduced stage 1.2) are defined in their Fig. 1. NODE=S126STT;LINKAGE=M

[12] TUMASYAN 22AJ measure cross sections with $pp \to H \to \tau\tau$ at E_{cm} = 13 TeV with 138 fb^{-1} data. The fiducial inclusive $\sigma{\cdot}B$ is 426 ± 102 fb while 408 ± 27 fb is expected in the Standard Mode for m_H = 125.38 GeV. Three differential cross sections are given; see their Fig. 1. NODE=S126STT;LINKAGE=U

[13] SIRUNYAN 19AF use 35.9 fb^{-1} of data. The quoted signal strength is given for m_H = 125 GeV and corresponds to 2.3 standard deviations. NODE=S126STT;LINKAGE=I

[14] SIRUNYAN 19AF use 35.9 fb^{-1} of data. HW/Z channels are added with a few updates on gluon fusion and vector boson fusion with respect to SIRUNYAN 18Y. The quoted signal strength is given for m_H = 125 GeV and corresponds to 5.5 standard deviations. The signal strengths for the individual production modes are: $1.12^{+0.53}_{-0.50}$ for gluon fusion, $1.13^{+0.45}_{-0.42}$ for vector boson fusion, $3.39^{+1.68}_{-1.54}$ for WH and $1.23^{+1.62}_{-1.35}$ for ZH. See their Fig. 7 for other couplings (κ_V, κ_f). NODE=S126STT;LINKAGE=J

[15] SIRUNYAN 19AT perform a combine fit to 35.9 fb^{-1} of data at E_{cm} = 13 TeV. This combination is based on SIRUNYAN 18Y. NODE=S126STT;LINKAGE=L

[16] SIRUNYAN 18Y use 35.9 fb^{-1} of pp collisions at E_{cm} = 13 TeV. The quoted signal strength is given for m_H = 125.09 GeV and corresponds to 4.9 standard deviations. NODE=S126STT;LINKAGE=D

[17] SIRUNYAN 18Y combine the result of 35.9 fb^{-1} at E_{cm} = 13 TeV with the results obtained from data of 4.9 fb^{-1} at E_{cm} = 7 TeV and 19.7 fb^{-1} at E_{cm} = 8 TeV (KHACHATRYAN 15AM). The quoted signal strength is given for m_H = 125.09 GeV and corresponds to 5.9 standard deviations. NODE=S126STT;LINKAGE=E

[18] AAD 16AC measure the signal strength with $pp \to HW/ZX$ processes using 20.3 fb^{-1} of E_{cm} = 8 TeV. The quoted signal strength is given for m_H = 125 GeV. NODE=S126STT;LINKAGE=F

[19] AAD 16K use up to 4.7 fb^{-1} of pp collisions at E_{cm} = 7 TeV and up to 20.3 fb^{-1} at E_{cm} = 8 TeV. The quoted signal strength is given for m_H = 125.36 GeV. NODE=S126STT;LINKAGE=C

[20] AAD 15AH use 4.5 fb^{-1} of pp collisions at E_{cm} = 7 TeV and 20.3 fb^{-1} at E_{cm} = 8 TeV. The third uncertainty in the measurement is theory systematics. The signal strength for the gluon fusion mode is $2.0 \pm 0.8^{+1.2}_{-0.8} \pm 0.3$ and that for vector boson fusion and W/ZH production modes is $1.24^{+0.49}_{-0.45}{}^{+0.31}_{-0.29} \pm 0.08$. The quoted signal strength is given for m_H = 125.36 GeV. NODE=S126STT;LINKAGE=B

[21] CHATRCHYAN 14K use 4.9 fb^{-1} of pp collisions at E_{cm} = 7 TeV and 19.7 fb^{-1} at E_{cm} = 8 TeV. The quoted signal strength is given for m_H = 125 GeV. See also CHATRCHYAN 14AJ. NODE=S126STT;LINKAGE=A

[22] AALTONEN 13L combine all CDF results with 9.45–10.0 fb^{-1} of $p\overline{p}$ collisions at E_{cm} = 1.96 TeV. The quoted signal strength is given for m_H = 125 GeV. NODE=S126STT;LINKAGE=LL

[23] ABAZOV 13L combine all D0 results with up to 9.7 fb^{-1} of $p\overline{p}$ collisions at E_{cm} = 1.96 TeV. The quoted signal strength is given for m_H = 125 GeV. NODE=S126STT;LINKAGE=AB

[24] AAD 12AI obtain results based on 4.7 fb^{-1} of pp collisions at E_{cm} = 7 TeV. The quoted signal strengths are given in their Fig. 10 for m_H = 126 GeV. See also Fig. 13 of AAD 12DA. NODE=S126STT;LINKAGE=AA

[25] CHATRCHYAN 12N obtain results based on 4.9 fb^{-1} of pp collisions at E_{cm}=7 TeV and 5.1 fb^{-1} at E_{cm}=8 TeV. The quoted signal strength is given for m_H=125.5 GeV. See also CHATRCHYAN 13Y . NODE=S126STT;LINKAGE=CA

$Z\gamma$ Final State

NODE=S126SZG
NODE=S126SZG

VALUE	CL%	DOCUMENT ID		TECN	COMMENT
2.2 ±0.7		[1] AAD	24D	LHC	pp, 13 TeV
• • • We do not use the following data for averages, fits, limits, etc. • • •					
2.4 ±0.9		[2] TUMASYAN	23F	CMS	pp, 13 TeV
$2.59^{+1.07}_{-0.96}$		[3] CMS	22	CMS	pp, 13 TeV
< 3.6	95	[4] AAD	20AG	ATLS	pp, 13 TeV
< 7.4	95	[5] SIRUNYAN	18DQ	CMS	pp, 13 TeV
< 6.6	95	[6] AABOUD	17AW	ATLS	pp, 13 TeV
<11	95	[7] AAD	14J	ATLS	pp, 7, 8 TeV
< 9.5	95	[8] CHATRCHYAN	13BK	CMS	pp, 7, 8 TeV

[1] AAD 24D report combined results of ATLAS (AAD 20AG) and CMS (TUMASYAN 23F). The reported signal strength corresponds to a significance of 3.4 σ. NODE=S126SZG;LINKAGE=G

[2] TUMASYAN 23F search for $H \to Z\gamma$, $Z \to ee$, $\mu\mu$ in 138 fb^{-1} of pp collisions at E_{cm} = 13 TeV, assuming m_H = 125.38 GeV. $\sigma(pp \to H)\cdot$B$(H \to Z\gamma)$ is measured to be 0.21 ± 0.08 pb. The ratio of branching fractions B$(H \to Z\gamma)$/B$(H \to \gamma\gamma)$ is measured to be $1.5^{+0.7}_{-0.6}$. NODE=S126SZG;LINKAGE=F

[3] CMS 22 report combined results (see their Extended Data Table 2) using up to 138 fb^{-1} of data at E_{cm} = 13 TeV, assuming m_H = 125.38 GeV. See their Fig. 2 right. NODE=S126SZG;LINKAGE=E

[4] AAD 20AG search for $H \to Z\gamma$, $Z \to ee$, $\mu\mu$ in 139 fb^{-1} of pp collisions at E_{cm} = 13 TeV. The signal strength is $2.0 \pm 0.9^{+0.4}_{-0.3}$ at m_H = 125.09 GeV, which corresponds to a significance of 2.2 σ. The upper limit of $\sigma(pp \to H)\cdot$B$(H \to Z\gamma)$ is 305 fb at 95% CL. NODE=S126SZG;LINKAGE=D

[5] SIRUNYAN 18DQ search for $H \to Z\gamma$, $Z \to ee$, $\mu\mu$ in 35.9 fb^{-1} of pp collisions at E_{cm} = 13 TeV. The quoted signal strength (see their Figs. 6 and 7) is given for m_H = 125 GeV. NODE=S126SZG;LINKAGE=C

[6] AABOUD 17AW search for $H \to Z\gamma$, $Z \to ee$, $\mu\mu$ in 36.1 fb^{-1} of pp collisions at E_{cm} = 13 TeV. The quoted signal strength is given for m_H = 125.09 GeV. The upper limit on the branching ratio of $H \to Z\gamma$ is 1.0% at 95% CL assuming the SM Higgs boson production. NODE=S126SZG;LINKAGE=B

[7] AAD 14J search for $H \to Z\gamma \to \ell\ell\gamma$ in 4.5 fb^{-1} of pp collisions at E_{cm} = 7 TeV and 20.3 fb^{-1} at E_{cm} = 8 TeV. The quoted signal strength is given for m_H = 125.5 GeV. NODE=S126SZG;LINKAGE=A

[8] CHATRCHYAN 13BK search for $H \to Z\gamma \to \ell\ell\gamma$ in 5.0 fb^{-1} of pp collisions at E_{cm} = 7 TeV and 19.6 fb^{-1} at E_{cm} = 8 TeV. A limit on cross section times branching ratio which corresponds to (4–25) times the expected Standard Model cross section is given in the range m_H = 120–160 GeV at 95% CL. The quoted limit is given for m_H = 125 GeV, where 10 is expected for no signal. NODE=S126SZG;LINKAGE=TH

$\gamma^*\gamma$ Final State

NODE=S126A01
NODE=S126A01

VALUE	CL%	DOCUMENT ID		TECN	COMMENT
$1.5\pm0.5^{+0.2}_{-0.1}$		[1] AAD	21I	ATLS	pp, 13 TeV, $H\to\ \ell\ell\gamma$, 139 fb^{-1}
• • • We do not use the following data for averages, fits, limits, etc. • • •					
<4.0	95	[2] SIRUNYAN	18DQ	CMS	$pp\to\ HX$, 13 TeV, $H\to\ \gamma^*\gamma$
<6.7	95	[3] KHACHATRY...	16B	CMS	pp, 8 TeV, $ee\gamma$, $\mu\mu\gamma$

[1] AAD 21I search for $H\to\ \ell\ell\gamma$ ($\ell = e,\ \mu$) in 139 fb^{-1} of pp collisions at $E_{\rm cm}$ = 13 TeV. The mass of dilepton $m_{\ell\ell}$ is smaller than 30 GeV. This region is dominated by the decay through γ^*. The quoted signal strength corresponds to a significance of 3.2 standard deviations and is given for m_H = 125.09 GeV. The cross section times the branching ratio of $H\to\ \ell\ell\gamma$ for $m_{\ell\ell} < 30$ GeV is measured to be $8.7\pm2.7^{+0.7}_{-0.6}$ fb. NODE=S126A01;LINKAGE=C

[2] SIRUNYAN 18DQ search for $H\to\ \gamma^*\gamma$, $\gamma^*\to\ \mu\mu$ in 35.9 fb^{-1} of pp collisions at $E_{\rm cm}$ = 13 TeV. The mass of γ^* is smaller than 50 GeV except in J/ψ and Υ mass regions. The quoted signal strength (see their Figs. 6 and 7) is given for m_H = 125 GeV. NODE=S126A01;LINKAGE=A

[3] KHACHATRYAN 16B search for $H\to\ \gamma^*\gamma\to\ e^+e^-\gamma$ and $\mu^+\mu^-\gamma$ (with m(e^+e^-) $<$ 3.5 GeV and m($\mu^+\mu^-$) $<$ 20 GeV) in 19.7 fb^{-1} of pp collisions at $E_{\rm cm}$ = 8 TeV. See their Fig. 6 for limits on individual channels. NODE=S126A01;LINKAGE=B

Higgs couplings

NODE=S126250

Fermion coupling (κ_F)

NODE=S126KFC
NODE=S126KFC

VALUE	DOCUMENT ID		TECN	COMMENT
0.94 ±0.05 OUR AVERAGE				
[0.95 ± 0.05 OUR 2023 AVERAGE]				
$0.86\ ^{+0.14}_{-0.11}$	[1] TUMASYAN	23W	CMS	pp, 13 TeV, $H\to\ WW^*$
$0.95\ \pm0.05$	[2] ATLAS	22	ATLS	pp, 13 TeV
• • • We do not use the following data for averages, fits, limits, etc. • • •				
$1.00\ ^{+0.16}_{-0.13}$	[3] AAD	23Y	ATLS	pp, 13 TeV, $H\to\ \gamma\gamma$
0.906	[4] CMS	22	CMS	pp, 13 TeV

NEW

[1] TUMASYAN 23W measure Higgs production rates with $H\to\ WW^*$ at $E_{\rm cm}$ = 13 TeV with 138 fb^{-1} data, assuming m_H = 125.38 GeV. See their Fig. 25 for the 68% and 95% CL contours in the $\kappa_V-\kappa_f$ plane. NODE=S126KFC;LINKAGE=C

[2] ATLAS 22 report combined results (see their Extended Data Table 1) using up to 139 fb^{-1} of data at $E_{\rm cm}$ = 13 TeV, assuming m_H = 125.09 GeV, $\kappa_V\ \geq\ 0$, and $\kappa_F\ \geq$ 0 ($B_{inv} = B_{undetected} = 0$). See their Fig. 4. NODE=S126KFC;LINKAGE=A

[3] AAD 23Y measure Higgs production rates with $H\to\ \gamma\gamma$ at $E_{\rm cm}$ = 13 TeV with 139 fb^{-1} data, assuming m_H = 125.09 GeV. See their Fig. 23 for the 68% and 95% CL contours in the $\kappa_V-\kappa_F$ plane, where $\kappa_F\ > 0$ is assumed. NODE=S126KFC;LINKAGE=D

[4] CMS 22 report combined results (see their Extended Data Table 2) using up to 138 fb^{-1} of data at $E_{\rm cm}$ = 13 TeV, assuming m_H = 125.38 GeV. No uncertainty is given while their Fig. 3 left shows 68% and 95% CL contours. NODE=S126KFC;LINKAGE=B

Gauge boson coupling (κ_V)

NODE=S126KVC
NODE=S126KVC

VALUE	DOCUMENT ID		TECN	COMMENT
1.023±0.026 OUR AVERAGE				
[1.035 ± 0.031 OUR 2023 AVERAGE]				
$0.99\ \pm0.05$	[1] TUMASYAN	23W	CMS	pp, 13 TeV, $H\to\ WW^*$
1.035 ± 0.031	[2] ATLAS	22	ATLS	pp, 13 TeV
• • • We do not use the following data for averages, fits, limits, etc. • • •				
$1.02\ ^{+0.06}_{-0.05}$	[3] AAD	23Y	ATLS	pp, 13 TeV, $H\to\ \gamma\gamma$
1.014	[4] CMS	22	CMS	pp, 13 TeV

NEW

[1] TUMASYAN 23W measure Higgs production rates with $H\to\ WW^*$ at $E_{\rm cm}$ = 13 TeV with 138 fb^{-1} data, assuming m_H = 125.38 GeV. See their Fig. 25 for the 68% and 95% CL contours in the $\kappa_V-\kappa_f$ plane. NODE=S126KVC;LINKAGE=C

[2] ATLAS 22 report combined results (see their Extended Data Table 1) using up to 139 fb^{-1} of data at $E_{\rm cm}$ = 13 TeV, assuming m_H = 125.09 GeV, $\kappa_V\ \geq\ 0$, and $\kappa_F\ \geq$ 0 ($B_{inv} = B_{undetected} = 0$). See their Fig. 4. NODE=S126KVC;LINKAGE=A

[3] AAD 23Y measure Higgs production rates with $H\to\ \gamma\gamma$ at $E_{\rm cm}$ = 13 TeV with 139 fb^{-1} data, assuming m_H = 125.09 GeV. See their Fig. 23 for the 68% and 95% CL contours in the $\kappa_V-\kappa_F$ plane, where $\kappa_F\ > 0$ is assumed. NODE=S126KVC;LINKAGE=D

[4] CMS 22 report combined results (see their Extended Data Table 2) using up to 138 fb^{-1} of data at $E_{\rm cm}$ = 13 TeV, assuming m_H = 125.38 GeV. See their Fig. 3 left. NODE=S126KVC;LINKAGE=B

W boson coupling (κ_W)

NODE=S126KWC
NODE=S126KWC

VALUE	DOCUMENT ID		TECN	COMMENT	
• • • We do not use the following data for averages, fits, limits, etc. • • •					
1.02 ± 0.05	[1,2] ATLAS	22	ATLS	pp, 13 TeV	
1.05 ± 0.06	[1,3] ATLAS	22	ATLS	pp, 13 TeV	OCCUR=2
$1.00^{+0.00}_{-0.02}$	[1,4] ATLAS	22	ATLS	pp, 13 TeV	OCCUR=3
1.06 ± 0.07	[5,6] CMS	22	CMS	pp, 13 TeV	
1.02 ± 0.08	[5,7] CMS	22	CMS	pp, 13 TeV	OCCUR=2

[1] ATLAS 22 report combined results (see their Extended Data Table 1) using up to 139 fb^{-1} of data at $E_{\rm cm}$ = 13 TeV, assuming m_H = 125.09 GeV. NODE=S126KWC;LINKAGE=A

[2] All modifiers(κ) > 0, and $\kappa_c = \kappa_t$ ($B_{inv} = B_{undetected} = 0$) are assumed. Only SM particles assume to contribute to the loop-induced processes.See their Fig. 5, which shows both $\kappa_c = \kappa_t$ andκ_c floating. NODE=S126KWC;LINKAGE=F

[3] $B_{inv} = B_{undetected} = 0$ is assumed. Coupling strength modifiers including effective photon, $Z\gamma$ and gluon are measured. See their Fig. 6. NODE=S126KWC;LINKAGE=B

[4] B_{inv} floating, $B_{undetected} \geq 0$, and $\kappa_V \leq 1$ are assumed. Coupling strength modifiers including effective photon, $Z\gamma$ and gluon are measured. See their Fig. 6. NODE=S126KWC;LINKAGE=E

[5] CMS 22 report combined results (see their Extended Data Table 2) using up to 138 fb^{-1} of data at $E_{\rm cm}$ = 13 TeV, assuming m_H = 125.38 GeV. NODE=S126KWC;LINKAGE=C

[6] Only SM particles assume to contribute to the loop-induced processes. See their Fig. 3 right. NODE=S126KWC;LINKAGE=G

[7] Coupling strength modifiers including effective photon, $Z\gamma$ and gluon are measured. See their Fig. 4 left. NODE=S126KWC;LINKAGE=D

Z boson coupling (κ_Z)

NODE=S126KZC
NODE=S126KZC

VALUE	DOCUMENT ID		TECN	COMMENT	
• • • We do not use the following data for averages, fits, limits, etc. • • •					
$0.99^{+0.06}_{-0.05}$	[1,2] ATLAS	22	ATLS	pp, 13 TeV	
0.99 ± 0.06	[1,3] ATLAS	22	ATLS	pp, 13 TeV	OCCUR=2
$0.98^{+0.02}_{-0.05}$	[1,4] ATLAS	22	ATLS	pp, 13 TeV	OCCUR=3
1.04 ± 0.07	[5,6] CMS	22	CMS	pp, 13 TeV	
1.04 ± 0.07	[5,7] CMS	22	CMS	pp, 13 TeV	OCCUR=2

[1] ATLAS 22 report combined results (see their Extended Data Table 1) using up to 139 fb^{-1} of data at $E_{\rm cm}$ = 13 TeV, assuming m_H = 125.09 GeV. NODE=S126KZC;LINKAGE=A

[2] All modifiers(κ) > 0, and $\kappa_c = \kappa_t$ ($B_{inv} = B_{undetected} = 0$) are assumed. Only SM particles assume to contribute to the loop-induced processes.See their Fig. 5, which shows both $\kappa_c = \kappa_t$ andκ_c floating. NODE=S126KZC;LINKAGE=F

[3] $B_{inv} = B_{undetected} = 0$ is assumed. Coupling strength modifiers including effective photon, $Z\gamma$ and gluon are measured. See their Fig. 6. NODE=S126KZC;LINKAGE=B

[4] B_{inv} floating, $B_{undetected} \geq 0$, and $\kappa_V \leq 1$ are assumed. Coupling strength modifiers including effective photon, $Z\gamma$ and gluon are measured. See their Fig. 6. NODE=S126KZC;LINKAGE=E

[5] CMS 22 report combined results (see their Extended Data Table 2) using up to 138 fb^{-1} of data at $E_{\rm cm}$ = 13 TeV, assuming m_H = 125.38 GeV. NODE=S126KZC;LINKAGE=C

[6] Only SM particles assume to contribute to the loop-induced processes. See their Fig. 3 right. NODE=S126KZC;LINKAGE=G

[7] Coupling strength modifiers including effective photon, $Z\gamma$ and gluon are measured. See their Fig. 4 left. NODE=S126KZC;LINKAGE=D

top Yukawa coupling (κ_t)

NODE=S126YTC
NODE=S126YTC

VALUE	CL%	DOCUMENT ID		TECN	COMMENT	
• • • We do not use the following data for averages, fits, limits, etc. • • •						
<1.8	95	[1] AAD	23BC	ATLS	pp, 13 TeV	
0.87–1.20	95	[2] AAD	23Y	ATLS	pp, 13 TeV	
0.65–1.25	95	[3] AAD	23Y	ATLS	pp, 13 TeV	OCCUR=2
-1.09– $-$ 0.74 or 0.77–1.3	95	[4] TUMASYAN	23P	CMS	pp, 13 TeV	
0.86–1.26		[4,5] TUMASYAN	23P	CMS	pp, 13 TeV	OCCUR=2
0.95 ± 0.07		[6,7] ATLAS	22	ATLS	pp, 13 TeV	
0.94 ± 0.11		[6,8] ATLAS	22	ATLS	pp, 13 TeV	OCCUR=2
0.94 ± 0.11		[6,9] ATLAS	22	ATLS	pp, 13 TeV	OCCUR=3
$0.95^{+0.07}_{-0.08}$		[10,11] CMS	22	CMS	pp, 13 TeV	
$1.01^{+0.11}_{-0.10}$		[10,12] CMS	22	CMS	pp, 13 TeV	OCCUR=2
-0.9– $-$ 0.7 or 0.7–1.1	95	[13] SIRUNYAN	21R	CMS	pp, 13 TeV	
<1.7	95	[14] SIRUNYAN	20C	CMS	pp, 13 TeV	
<1.67	95	[15] SIRUNYAN	19BY	CMS	pp, 13 TeV	
<2.1	95	[16] SIRUNYAN	18BU	CMS	pp, 13 TeV	

[1] AAD 23BC measure the production of four top quarks with same-sign and multilepton final states with 140 fb^{-1} pp collision data at E_{cm} = 13 TeV. The results constraint the ratio of the top quark Yukawa coupling y_t to its Standard Model value, yielding $|y_t/y_t^{SM}|$ < 1.8 at 95% CL. See their Fig. 8 as a function of κ_t and CP-mixing angle. NODE=S126YTC;LINKAGE=Q

[2] AAD 23Y constrain κ_t from Higgs production rates with $H \to \gamma\gamma$ with 139 fb^{-1} pp collision data at E_{cm} = 13 TeV. The quoted result is obtained assuming the SM loop structure in $gg \to H$ and $H \to \gamma\gamma$. See their Fig. 14. NODE=S126YTC;LINKAGE=O

[3] AAD 23Y constrain κ_t from Higgs production rates with $H \to \gamma\gamma$ with 139 fb^{-1} pp collision data at E_{cm} = 13 TeV. The quoted result is obtained assuming effective couplings κ_{gluon} and κ_γ for $gg \to H$ and $H \to \gamma\gamma$, respectively. See their Fig. 14. NODE=S126YTC;LINKAGE=P

[4] TUMASYAN 23P constrain κ_t from $t\bar{t}H$ and tH decaying $H \to WW^*$ and $H \to \tau\tau$ (multilepton decay mode) with 138 fb^{-1} pp collision data at E_{cm} = 13 TeV. The κ_t is obtained by fixing $\tilde{\kappa}_t = 0$ and other couplings (κ_V etc.) to the SM values. See their Fig. 9 for 2-dim contours and Table 6. NODE=S126YTC;LINKAGE=M

[5] The quoted result is obtained by combining with other $t\bar{t}H$ decaying $H \to \gamma\gamma$ (SIRUNYAN 20AS) and $H \to 4\ell$ (SIRUNYAN 21AE) and $\tilde{\kappa}_t = 0$. See their Fig. 12 for 2-dim contours and Table 7. NODE=S126YTC;LINKAGE=N

[6] ATLAS 22 report combined results (see their Extended Data Table 1) using up to 139 fb^{-1} of data at E_{cm} = 13 TeV, assuming m_H = 125.09 GeV. NODE=S126YTC;LINKAGE=E

[7] All modifiers(κ) > 0, and $\kappa_c = \kappa_t$ ($B_{inv} = B_{undetected} = 0$) are assumed. Only SM particles assume to contribute to the loop-induced processes.See their Fig. 5, which shows both $\kappa_c = \kappa_t$ andκ_c floating. NODE=S126YTC;LINKAGE=J

[8] $B_{inv} = B_{undetected} = 0$ is assumed. Coupling strength modifiers including effective photon, $Z\gamma$ and gluon are measured. See their Fig. 6. NODE=S126YTC;LINKAGE=F

[9] B_{inv} floating, $B_{undetected} \geq 0$, and $\kappa_V \leq 1$ are assumed. Coupling strength modifiers including effective photon, $Z\gamma$ and gluon are measured. See their Fig. 6. NODE=S126YTC;LINKAGE=I

[10] CMS 22 report combined results (see their Extended Data Table 2) using up to 138 fb^{-1} of data at E_{cm} = 13 TeV, assuming m_H = 125.38 GeV. NODE=S126YTC;LINKAGE=G

[11] Only SM particles assume to contribute to the loop-induced processes. See their Fig. 3 right. NODE=S126YTC;LINKAGE=K

[12] Coupling strength modifiers including effective photon, $Z\gamma$ and gluon are measured. See their Fig. 4 left. NODE=S126YTC;LINKAGE=H

[13] SIRUNYAN 21R constrain the ratio of the top quark Yukawa coupling y_t to its Standard Model value from $t\bar{t}H$ and tH production rates using 137 fb^{-1} pp collision data at E_{cm} = 13 TeV. Assuming a SM Higgs couplings to τ's, the joint interval $-0.9 < \kappa_t(=y_t/y_t^{SM}) < -0.7$ and $0.7 < \kappa_t < 1.1$ is obtained at 95% CL (see their Fig. 17). NODE=S126YTC;LINKAGE=D

[14] SIRUNYAN 20C search for the production of four top quarks with same-sign and multilepton final states with 137 fb^{-1} pp collision data at E_{cm} = 13 TeV. The results constraint the ratio of the top quark Yukawa coupling y_t to its Standard Model value by comparing to the central value of a theoretical prediction (see their Refs. [1-2]), yielding $|y_t/y_t^{SM}|$ < 1.7 at 95% CL. See their Fig. 5. NODE=S126YTC;LINKAGE=A

[15] SIRUNYAN 19BY measure the top quark Yukawa coupling from $t\bar{t}$ kinematic distributions, the invariant mass of the top quark pair and the rapidity difference between t and $\bar{t}$, in the ℓ+jets final state with 35.8 fb^{-1} pp collision data at E_{cm} = 13 TeV. The results constraint the ratio of the top quark Yukawa coupling to its the Standard Model to be $1.07^{+0.34}_{-0.43}$ with an upper limit of 1.67 at 95% CL (see their Table III). NODE=S126YTC;LINKAGE=B

[16] SIRUNYAN 18BU search for the production of four top quarks with same-sign and multilepton final states with 35.9 fb^{-1} pp collision data at E_{cm} = 13 TeV. The results constraint the ratio of the top quark Yukawa coupling y_t to its the Standard Model by comparing to the central value of a theoretical prediction (see their Ref. [16]), yielding $|y_t/y_t^{SM}|$ < 2.1 at 95% CL. NODE=S126YTC;LINKAGE=C

bottom Yukawa coupling (κ_b)

NODE=S126KBC
NODE=S126KBC

VALUE	CL%	DOCUMENT ID		TECN	COMMENT	
• • • We do not use the following data for averages, fits, limits, etc. • • •						
-1.09 to -0.86 OR 0.81 to 1.09	95	[1] AAD	23C	ATLS	pp, 13 TeV, $\gamma\gamma$, $ZZ^* \to 4\ell$ cross sections	
		[2] AAD	23CD	ATLS	pp, 13 TeV, $H \to \Upsilon$(nS)γ	
−1.1 to 1.1	95	[3] HAYRAPETY...	23	CMS	pp, 13 TeV, $ZZ^* \to 4\ell$ cross sections	
0.90±0.11		[4,5] ATLAS	22	ATLS	pp, 13 TeV	
0.89±0.11		[4,6] ATLAS	22	ATLS	pp, 13 TeV	OCCUR=2
$0.82^{+0.09}_{-0.08}$		[4,7] ATLAS	22	ATLS	pp, 13 TeV	OCCUR=3
$1.02^{+0.15}_{-0.17}$		[8,9] CMS	22	CMS	pp, 13 TeV	
$0.99^{+0.17}_{-0.16}$		[8,10] CMS	22	CMS	pp, 13 TeV	OCCUR=2

[1] AAD 23C combine results of $H \to \gamma\gamma$ and $H \to ZZ^* \to 4\ell$ ($\ell = e, \mu$) using 139 fb^{-1} at E_{cm} = 13 TeV. The Higgs boson transverse momentum (p_T^H) distribution constrains κ_b and κ_c, assuming other couplings fixed to the SM values. The κ_b is obtained using the p_T^H shape and normalisation. Other cases are given in their Tables 6 and 7. NODE=S126KBC;LINKAGE=I

[2] AAD 23CD search for $H \to \Upsilon(nS)\gamma$, $\Upsilon(nS) \to \mu^+\mu^-$ (n=1,2,3) with 138 fb^{-1} of pp collision data at E_{cm} = 13 TeV. They interpret the $H \to \Upsilon(nS)\gamma$ search to constraint the bottom Yukawa coupling by comparing to $H \to \gamma\gamma$. An observed 95% CL interval of (-37, 40) is obtained for κ_b/κ_γ. NODE=S126KBC;LINKAGE=J

[3] HAYRAPETYAN 23 measure the cross sections for $pp \to H \to ZZ^* \to 4\ell$ ($\ell = e, \mu$) using 138 fb^{-1} at E_{cm} = 13 TeV. The κ_b is obtained from the p_T differential cross section of the ggF production employing the dependence of the branching fraction on κ_b and κ_c. NODE=S126KBC;LINKAGE=H

[4] ATLAS 22 report combined results (see their Extended Data Table 1) using up to 139fb^{-1} of data at E_{cm} = 13 TeV, assuming m_H = 125.09 GeV. NODE=S126KBC;LINKAGE=A

[5] All modifiers (κ) > 0, and $\kappa_c = \kappa_t$ ($B_{inv} = B_{undetected} = 0$) are assumed. Only SM particles assume to contribute to the loop-induced processes. See their Fig. 5, which shows both $\kappa_c = \kappa_t$ and κ_c floating. NODE=S126KBC;LINKAGE=G

[6] $B_{inv} = B_{undetected} = 0$ is assumed. Coupling strength modifiers including effective photon, $Z\gamma$ and gluon are measured. See their Fig. 6. NODE=S126KBC;LINKAGE=B

[7] B_{inv} floating, $B_{undetected} \geq 0$, and $\kappa_V \leq 1$ are assumed. Coupling strength modifiers including effective photon, $Z\gamma$ and gluon are measured. See their Fig. 6. NODE=S126KBC;LINKAGE=E

[8] CMS 22 report combined results (see their Extended Data Table 2) using up to 138 fb^{-1} of data at E_{cm} = 13 TeV, assuming m_H = 125.38 GeV. NODE=S126KBC;LINKAGE=C

[9] Only SM particles assume to contribute to the loop-induced processes. See their Fig. 3 right. NODE=S126KBC;LINKAGE=F

[10] Coupling strength modifiers including effective photon, $Z\gamma$ and gluon are measured. See their Fig. 4 left. NODE=S126KBC;LINKAGE=D

charm Yukawa coupling (κ_c)

NODE=S126KCC
NODE=S126KCC

VALUE	CL%	DOCUMENT ID		TECN	COMMENT
• • • We do not use the following data for averages, fits, limits, etc. • • •					
$\lvert\kappa_c\rvert < 2.27$	95	[1] AAD	23C	ATLS	pp, 13 TeV, $\gamma\gamma$, $ZZ^* \to 4\ell$ cross sections
		[2] AAD	23CD	ATLS	pp, 13 TeV, $H \to J/\psi\gamma$
−5.3 to 5.2	95	[3] HAYRAPETY...	23	CMS	pp, 13 TeV, $ZZ^* \to 4\ell$ cross sections
$1.1 < \lvert\kappa_c\rvert < 5.5$	95	[4] TUMASYAN	23AH	CMS	$pp \to WH/ZH$, 13 TeV
$0.03^{+3.02}_{-0.03}$		[5] ATLAS	22	ATLS	pp, 13 TeV

[1] AAD 23C combine results of $H \to \gamma\gamma$ and $H \to ZZ^* \to 4\ell$ ($\ell = e, \mu$) using 139 fb^{-1} at E_{cm} = 13 TeV. The Higgs boson transverse momentum (p_T^H) distribution constrains κ_b and κ_c, assuming other couplings fixed to the SM values. The κ_c is obtained using the p_T^H shape and normalisation. Other cases are given in their Tables 6 and 7. See their Table 8 for results combined with VH, $H \to b\bar{b}$ and $c\bar{c}$. NODE=S126KCC;LINKAGE=D

[2] AAD 23CD search for $H \to J/\psi\gamma$, $J/\psi \to \mu^+\mu^-$ with 138 fb^{-1} of pp collision data at E_{cm} = 13 TeV. They interpret the $H \to J/\psi\gamma$ search to constraint the charm Yukawa coupling by comparing to $H \to \gamma\gamma$. An observed 95% CL interval of (-133, 175) is obtained for κ_c/κ_γ. NODE=S126KCC;LINKAGE=E

[3] HAYRAPETYAN 23 measure the cross sections for $pp \to H \to ZZ^* \to 4\ell$ ($\ell = e, \mu$) using 138 fb^{-1} at E_{cm} = 13 TeV. The κ_c is obtained from the p_T differential cross section of the ggF production employing the dependence of the branching fraction of κ_b and κ_c. NODE=S126KCC;LINKAGE=C

[4] TUMASYAN 23AH search for VH, $H \to c\bar{c}$ ($V = W, Z$) using 138 fb^{-1} of pp collision data at E_{cm} = 13 TeV. The quoted values are obtained from the measured signal strength in the κ-framework, where only the Higgs decay width for $H \to c\bar{c}$ is changed while assuming all the other decay widths and the production cross section to be SM ones. The quoted values are given for m_H = 125.38 GeV. NODE=S126KCC;LINKAGE=B

[5] ATLAS 22 report combined results (see their Extended Data Table 1) using up to 139 fb^{-1} of data at E_{cm} = 13 TeV, assuming m_H = 125.09 GeV, and all modifiers (κ) > 0 ($B_{inv} = B_{undetected} = 0$). Only SM particles assume to contribute to the loop-induced processes. See their Fig. 5, which shows both $\kappa_c = \kappa_t$ and κ_c floating. NODE=S126KCC;LINKAGE=A

tau Yukawa coupling (κ_τ)

NODE=S126KTA
NODE=S126KTA

VALUE	DOCUMENT ID		TECN	COMMENT	
• • • We do not use the following data for averages, fits, limits, etc. • • •					
0.94±0.07	[1,2] ATLAS	22	ATLS	pp, 13 TeV	
0.93±0.07	[1,3] ATLAS	22	ATLS	pp, 13 TeV	OCCUR=2
$0.91^{+0.07}_{-0.06}$	[1,4] ATLAS	22	ATLS	pp, 13 TeV	OCCUR=3
0.93±0.08	[5,6] CMS	22	CMS	pp, 13 TeV	
0.92±0.08	[5,7] CMS	22	CMS	pp, 13 TeV	OCCUR=2

[1] ATLAS 22 report combined results (see their Extended Data Table 1) using up to 139 fb^{-1} of data at E_{cm} = 13 TeV, assuming m_H = 125.09 GeV. NODE=S126KTA;LINKAGE=A

[2] All modifiers(κ) > 0, and $\kappa_c = \kappa_t$ (B_{inv} =$B_{undetected}$ = 0) are assumed. Only SM particles assume to contribute to the loop-induced processes.See their Fig. 5, which shows both $\kappa_c = \kappa_t$ andκ_c floating. NODE=S126KTA;LINKAGE=F

[3] $B_{inv} = B_{undetected} = 0$ is assumed. Coupling strength modifiers including effective photon, $Z\gamma$ and gluon are measured. See their Fig. 6. NODE=S126KTA;LINKAGE=B

[4] B_{inv} floating, $B_{undetected} \geq 0$, and $\kappa_V \leq 1$ are assumed. Coupling strength modifiers including effective photon, $Z\gamma$ and gluon are measured. See their Fig. 6. NODE=S126KTA;LINKAGE=E

[5] CMS 22 report combined results (see their Extended Data Table 2) using up to 138 fb^{-1} of data at E_{cm} = 13 TeV, assuming m_H = 125.38 GeV. NODE=S126KTA;LINKAGE=C

[6] Only SM particles assume to contribute to the loop-induced processes. See their Fig. 3 right. NODE=S126KTA;LINKAGE=G

[7] Coupling strength modifiers including effective photon, $Z\gamma$ and gluon are measured. See their Fig. 4 left. NODE=S126KTA;LINKAGE=D

muon Yukawa couping (κ_μ)

NODE=S126KMU
NODE=S126KMU

VALUE	DOCUMENT ID		TECN	COMMENT	
• • • We do not use the following data for averages, fits, limits, etc. • • •					
$1.07^{+0.25}_{-0.31}$	[1,2] ATLAS	22	ATLS	pp, 13 TeV	
$1.06^{+0.25}_{-0.30}$	[1,3] ATLAS	22	ATLS	pp, 13 TeV	OCCUR=2
$1.04^{+0.23}_{-0.30}$	[1,4] ATLAS	22	ATLS	pp, 13 TeV	OCCUR=3
1.12 ± 0.20	[5,6] CMS	22	CMS	pp, 13 TeV	
$1.12^{+0.21}_{-0.22}$	[5,7] CMS	22	CMS	pp, 13 TeV	OCCUR=2

[1] ATLAS 22 report combined results (see their Extended Data Table 1) using up to 139 fb^{-1} of data at E_{cm} = 13 TeV, assuming m_H = 125.09 GeV. NODE=S126KMU;LINKAGE=A

[2] All modifiers(κ) > 0, and $\kappa_c = \kappa_t$ (B_{inv} =$B_{undetected}$ = 0) are assumed. Only SM particles assume to contribute to the loop-induced processes.See their Fig. 5, which shows both $\kappa_c = \kappa_t$ andκ_c floating. NODE=S126KMU;LINKAGE=F

[3] $B_{inv} = B_{undetected} = 0$ is assumed. Coupling strength modifiers including effective photon, $Z\gamma$ and gluon are measured. See their Fig. 6. NODE=S126KMU;LINKAGE=B

[4] B_{inv} floating, $B_{undetected} \geq 0$, and $\kappa_V \leq 1$ are assumed. Coupling strength modifiers including effective photon, $Z\gamma$ and gluon are measured. See their Fig. 6. NODE=S126KMU;LINKAGE=E

[5] CMS 22 report combined results (see their Extended Data Table 2) using up to 138 fb^{-1} of data at E_{cm} = 13 TeV, assuming m_H = 125.38 GeV. NODE=S126KMU;LINKAGE=C

[6] Only SM particles assume to contribute to the loop-induced processes. See their Fig. 3 right. NODE=S126KMU;LINKAGE=G

[7] Coupling strength modifiers including effective photon, $Z\gamma$ and gluon are measured. See their Fig. 4 left. NODE=S126KMU;LINKAGE=D

photon effective coupling (κ_γ)

NODE=S126KGC
NODE=S126KGC

VALUE	DOCUMENT ID		TECN	COMMENT	
• • • We do not use the following data for averages, fits, limits, etc. • • •					
$1.02^{+0.08}_{-0.07}$	[1] AAD	23Y	ATLS	pp, 13 TeV	
1.01 ± 0.06	[2,3] ATLAS	22	ATLS	pp, 13 TeV	
0.98 ± 0.05	[2,4] ATLAS	22	ATLS	pp, 13 TeV	OCCUR=2
1.10 ± 0.08	[5] CMS	22	CMS	pp, 13 TeV	

[1] AAD 23Y constrain κ_γ from Higgs production rates with $H \to \gamma\gamma$ with 139 fb^{-1} pp collision data at E_{cm} = 13 TeV. The quoted result is obtained assuming effective couplings κ_{gluon} and κ_γ for $gg \to H$ and $H \to \gamma\gamma$, respectively and other couplings fixed to the SM values. See their Fig. 15. NODE=S126KGC;LINKAGE=E

[2] ATLAS 22 report combined results (see their Extended Data Table 1) using up to 139 fb^{-1} of data at E_{cm} = 13 TeV, assuming m_H = 125.09 GeV. Coupling strength modifiers including effective photon, $Z\gamma$ and gluon are measured. See their Fig. 6. NODE=S126KGC;LINKAGE=A

[3] $B_{inv} = B_{undetected} = 0$ is assumed. NODE=S126KGC;LINKAGE=D

[4] B_{inv} floating, $B_{undetected} \geq 0$, and $\kappa_V \leq 1$ are assumed. NODE=S126KGC;LINKAGE=C

[5] CMS 22 report combined results (see their Extended Data Table 2) using up to 138 fb^{-1} of data at E_{cm} = 13 TeV, assuming m_H = 125.38 GeV. Coupling strength modifiers including effective photon, $Z\gamma$ and gluon are measured. See their Fig. 4 left. NODE=S126KGC;LINKAGE=B

gluon effective coupling (κ_{gluon})

NODE=S126KGL
NODE=S126KGL

VALUE	DOCUMENT ID	TECN	COMMENT
• • • We do not use the following data for averages, fits, limits, etc. • • •			
$1.01^{+0.11}_{-0.09}$	[1] AAD 23Y	ATLS	pp, 13 TeV
0.95 ± 0.07	[2,3] ATLAS 22	ATLS	pp, 13 TeV
$0.94^{+0.07}_{-0.06}$	[2,4] ATLAS 22	ATLS	pp, 13 TeV
0.92 ± 0.08	[5] CMS 22	CMS	pp, 13 TeV

OCCUR=2

[1] AAD 23Y constrain κ_{gluon} from Higgs production rates with $H \to \gamma\gamma$ with 139 fb^{-1} pp collision data at $E_{\rm cm}$ = 13 TeV. The quoted result is obtained assuming effective couplings κ_{gluon} and κ_γ for $gg \to H$ and $H \to \gamma\gamma$, respectively and other couplings fixed to the SM values. See their Fig. 15. NODE=S126KGL;LINKAGE=D

[2] ATLAS 22 report combined results (see their Extended Data Table 1) using up to 139fb^{-1} of data at $E_{\rm cm}$ = 13 TeV, assuming m_H = 125.09 GeV. Coupling strength modifiers including effective photon, $Z\gamma$ andgluon are measured. See their Fig. 6. NODE=S126KGL;LINKAGE=A

[3] $B_{inv} = B_{undetected} = 0$ is assumed. NODE=S126KGL;LINKAGE=E

[4] B_{inv} floating, $B_{undetected} \ge 0$, and $\kappa_V \le 1$ are assumed. NODE=S126KGL;LINKAGE=C

[5] CMS 22 report combined results (see their Extended Data Table 2) using up to 138 fb^{-1} of data at $E_{\rm cm}$ = 13 TeV, assuming m_H = 125.38 GeV. Coupling strength modifiers including effective photon, $Z\gamma$ and gluon are measured. See their Fig. 4 left. NODE=S126KGL;LINKAGE=B

$Z\gamma$ effective coupling ($\kappa_{Z\gamma}$)

NODE=S126KZG
NODE=S126KZG

VALUE	DOCUMENT ID	TECN	COMMENT
• • • We do not use the following data for averages, fits, limits, etc. • • •			
$1.38^{+0.31}_{-0.37}$	[1,2] ATLAS 22	ATLS	pp, 13 TeV
$1.35^{+0.29}_{-0.36}$	[1,3] ATLAS 22	ATLS	pp, 13 TeV
$1.65^{+0.34}_{-0.37}$	[4] CMS 22	CMS	pp, 13 TeV

OCCUR=2

[1] ATLAS 22 report combined results (see their Extended Data Table 1) using up to 139 fb^{-1} of data at $E_{\rm cm}$ = 13 TeV, assuming m_H = 125.09 GeV. Coupling strength modifiers including effective photon, $Z\gamma$ and gluon are measured. See their Fig. 6. NODE=S126KZG;LINKAGE=A

[2] $B_{inv} = B_{undetected} = 0$ is assumed. NODE=S126KZG;LINKAGE=D

[3] B_{inv} floating, $B_{undetected} \ge 0$, and $\kappa_V \le 1$ are assumed. NODE=S126KZG;LINKAGE=C

[4] CMS 22 report combined results (see their Extended Data Table 2) using up to 138 fb^{-1} of data at $E_{\rm cm}$ = 13 TeV, assuming m_H = 125.38 GeV. Coupling strength modifiers including effective photon, $Z\gamma$ and gluon are measured. See their Fig. 4 left. NODE=S126KZG;LINKAGE=B

OTHER H PRODUCTION PROPERTIES

NODE=S126240

$t\bar{t}H$ Production

NODE=S126STH

Signal strength relative to the Standard Model cross section.

NODE=S126STH
NODE=S126STH

VALUE	DOCUMENT ID	TECN	COMMENT
1.10±0.18 OUR AVERAGE			
$0.92\pm0.19^{+0.17}_{-0.13}$	[1] SIRUNYAN 21R	CMS	pp, 13 TeV, $H \to \tau\tau$, WW^*, ZZ^*
1.2 ± 0.3	[2] AABOUD 18AC	ATLS	pp, 13 TeV, $H \to b\bar{b}\,\tau\tau$, $\gamma\gamma$, WW^*, ZZ^*
$1.9^{+0.8}_{-0.7}$	[3] AAD 16AN	ATLS	pp, 7, 8 TeV
• • • We do not use the following data for averages, fits, limits, etc. • • •			
$-0.27^{+0.86}_{-0.83}$	[4] TUMASYAN 23AI	ATLS	pp, 13 TeV, boosted $H \to b\bar{b}$
$0.35^{+0.36}_{-0.34}$	[5] AAD 22M	ATLS	pp, 13 TeV, $H \to b\bar{b}$
$1.43^{+0.33}_{-0.31}{}^{+0.21}_{-0.15}$	[6] AAD 20Z	ATLS	pp, 13 TeV, $H \to \gamma\gamma$
$1.38^{+0.36}_{-0.29}$	[7] SIRUNYAN 20AS	CMS	pp, 13 TeV, $H \to \gamma\gamma$
$0.72\pm0.24\pm0.38$	[8] SIRUNYAN 19R	CMS	pp, 13 TeV, $H \to b\bar{b}$
$1.6^{+0.5}_{-0.4}$	[9] AABOUD 18AC	ATLS	pp, 13 TeV, $H \to \tau\tau$, WW^*, ZZ^*
	[10] AABOUD 18BK	ATLS	pp, 13 TeV, $H \to b\bar{b}\,\tau\tau$, $\gamma\gamma$, WW^*, ZZ^*
$0.84^{+0.64}_{-0.61}$	[11] AABOUD 18T	ATLS	pp, 13 TeV, $H \to b\bar{b}$
0.9 ± 1.5	[12] SIRUNYAN 18BD	CMS	pp, 13 TeV, $H \to b\bar{b}$
$1.23^{+0.45}_{-0.43}$	[13] SIRUNYAN 18BQ	CMS	pp, 13 TeV, $H \to \tau\tau$, WW^*, ZZ^*

OCCUR=2
OCCUR=2

$1.26^{+0.31}_{-0.26}$	[14] SIRUNYAN	18L	CMS	pp, 7, 8, 13 TeV, $H \to b\overline{b}$, $\tau\tau$, $\gamma\gamma$, WW^*, ZZ^*	
1.7 ± 0.8	[15] AAD	16AL	ATLS	pp, 7, 8 TeV, $H \to b\overline{b}$, $\tau\tau$, $\gamma\gamma$, WW^*, and ZZ^*	
$2.3\ ^{+0.7}_{-0.6}$	[3,16] AAD	16AN	LHC	pp, 7, 8 TeV	
$2.9\ ^{+1.0}_{-0.9}$	[3] AAD	16AN	CMS	pp, 7, 8 TeV	OCCUR=3
$1.81^{+0.52}_{-0.50}{}^{+0.58}_{-0.55}{}^{+0.31}_{-0.12}$	[17] AAD	16K	ATLS	pp, 7, 8 TeV	
$1.4\ ^{+2.1}_{-1.4}\ ^{+0.6}_{-0.3}$	[18] AAD	15	ATLS	pp, 7, 8 TeV	
1.5 ± 1.1	[19] AAD	15BC	ATLS	pp, 8 TeV	
$2.1\ ^{+1.4}_{-1.2}$	[20] AAD	15T	ATLS	pp, 8 TeV	
$1.2\ ^{+1.6}_{-1.5}$	[21] KHACHATRY...	15AN	CMS	pp, 8 TeV	
$2.8\ ^{+1.0}_{-0.9}$	[22] KHACHATRY...	14H	CMS	pp, 7, 8 TeV	
$9.49^{+6.60}_{-6.28}$	[23] AALTONEN	13L	CDF	$p\overline{p}$, 1.96 TeV	OCCUR=2
< 5.8 at 95% CL	[24] CHATRCHYAN	13X	CMS	pp, 7, 8 TeV, $H \to b\overline{b}$	

[1] SIRUNYAN 21R search for $t\overline{t}H$ in final states with electrons, muons and hadronically decaying τ leptons ($H \to WW^*$, ZZ^*, $\tau\tau$) with 137 fb^{-1} of pp collision data at $E_{cm} = 13$ TeV. The quoted signal strength corresponds to a significance of 4.7 standard deviations and is given for $m_H = 125$ GeV. NODE=S126STH;LINKAGE=W

[2] AABOUD 18AC combine results of $t\overline{t}H$, $H \to \tau\tau$, $WW^*(\to \ell\nu\ell\nu, \ell\nu q\overline{q})$, $ZZ^*(\to \ell\ell\nu\nu, \ell\ell q\overline{q})$ with results of $t\overline{t}H$, $H \to b\overline{b}$ (AABOUD 18T), $\gamma\gamma$ (AABOUD 18BO), $ZZ^*(\to 4\ell)$ (AABOUD 18AJ) in 36.1 fb^{-1} of pp collisions at $E_{cm} = 13$ TeV. The quoted signal strength is given for $m_H = 125$ GeV. See their Table 14. NODE=S126STH;LINKAGE=N

[3] AAD 16AN: In the fit, relative branching ratios are fixed to those in the Standard Model. The quoted signal strength is given for $m_H = 125.09$ GeV. NODE=S126STH;LINKAGE=K

[4] TUMASYAN 23AI measure boosted $H \to b\overline{b}$ ($p_T > 200$ GeV) in $t\overline{t}H$ production using 138 fb^{-1} of data at $E_{cm} = 13$ TeV. The differential cross section for the Higgs p_T is shown in their Fig. 8 and Table V. Limits on eight Wilson coefficients at 68% and 95% CL are shown in their Fig. 10 and Table VI. NODE=S126STH;LINKAGE=Z

[5] AAD 22M measure $H \to b\overline{b}$ in $t\overline{t}H$ production using 139 fb^{-1} of data at $E_{cm} = 13$ TeV. See their Fig. 14. The signal strengths and 95% CL cross section upper limits with simplified template cross section bins are given in their Figs. 18 and 19, respectively. NODE=S126STH;LINKAGE=Y

[6] AAD 20Z measure $\sigma_{t\overline{t}H} \cdot$ B($H \to \gamma\gamma$) to be $1.64^{+0.38}_{-0.36}{}^{+0.17}_{-0.14}$ fb in 139 fb^{-1} of data at $E_{cm} = 13$ TeV. NODE=S126STH;LINKAGE=V

[7] SIRUNYAN 20AS measure $\sigma_{t\overline{t}H} \cdot$ B($H \to \gamma\gamma$) to be $1.56^{+0.34}_{-0.32}$ fb in 137 fb^{-1} of data at $E_{cm} = 13$ TeV. NODE=S126STH;LINKAGE=U

[8] SIRUNYAN 19R search for $t\overline{t}H$ production with H decaying to $b\overline{b}$ in 35.9 fb^{-1} of data at $E_{cm} = 13$ TeV. The quoted signal strength is given for $m_H = 125$ GeV. NODE=S126STH;LINKAGE=S

[9] AABOUD 18AC search for $t\overline{t}H$ production with H decaying to $\tau\tau$, $WW^*(\to \ell\nu\ell\nu, \ell\nu q\overline{q})$, $ZZ^*(\to \ell\ell\nu\nu, \ell\ell q\overline{q})$ in 36.1 fb^{-1} of pp collisions at $E_{cm} = 13$ TeV. The quoted signal strength is given for $m_H = 125$ GeV. See their Table 13 and Fig. 13. NODE=S126STH;LINKAGE=M

[10] AABOUD 18BK use 79.8 fb^{-1} data for $t\overline{t}H$ production with $H \to \gamma\gamma$ and $ZZ^* \to 4\ell$ ($\ell = e$, μ) and 36.1 fb^{-1} for other decay channels at $E_{cm} = 13$ TeV. A significance of 5.8 standard deviations is observed for $m_H = 125.09$ GeV and its signal strength without the uncertainty of the $t\overline{t}H$ cross section is $1.32^{+0.28}_{-0.26}$. Combining with results of 7 and 8 TeV (AAD 16K), the significance is 6.3 standard deviations. Assuming Standard Model branching fractions, the total $t\overline{t}H$ production cross section at 13 TeV is measured to be $670 \pm 90^{+110}_{-100}$ fb. NODE=S126STH;LINKAGE=O

[11] AABOUD 18T search for $t\overline{t}H$ production with H decaying to $b\overline{b}$ in 36.1 fb^{-1} of pp collisions at $E_{cm} = 13$ TeV. The quoted signal strength is given for $m_H = 125$ GeV. NODE=S126STH;LINKAGE=H

[12] SIRUNYAN 18BD search for $t\overline{t}H$, $H \to b\overline{b}$ in the all-jet final state with 35.9 fb^{-1} pp collision data at $E_{cm} = 13$ TeV. The quoted signal strength is given for $m_H = 125$ GeV. NODE=S126STH;LINKAGE=Q

[13] SIRUNYAN 18BQ search for $t\overline{t}H$ in final states with electrons, muons and hadronically decaying τ leptons ($H \to WW^*$, ZZ^*, $\tau\tau$) with 35.9 fb^{-1} of pp collision data at $E_{cm} = 13$ TeV. The quoted signal strength corresponds to a significance of 3.2 standard deviations and is given for $m_H = 125$ GeV. NODE=S126STH;LINKAGE=P

[14] SIRUNYAN 18L use up to 5.1, 19.7 and 35.9 fb^{-1} of pp collisions at $E_{cm} = 7$, 8, and 13 TeV, respectively. The quoted signal strength corresponds to a significance of 5.2 standard deviations and is given for $m_H = 125.09$ GeV. H decay channels of WW^*, ZZ^*, $\gamma\gamma$, $\tau\tau$, and $b\overline{b}$ are used. See their Table 1 and Fig. 2 for results on individual channels. NODE=S126STH;LINKAGE=G

[15] AAD 16AL search for $t\overline{t}H$ production with H decaying to $\gamma\gamma$ in 4.5 fb^{-1} of pp collisions at $E_{cm} = 7$ TeV and $b\overline{b}$, $\tau\tau$, $\gamma\gamma$, WW^*, and ZZ^* in 20.3 fb^{-1} at $E_{cm} = 8$ TeV. NODE=S126STH;LINKAGE=I

The quoted signal strength is given for m_H = 125 GeV. This paper combines the results of previous papers, and the new result of this paper only is: $\mu = 1.6 \pm 2.6$.

[16] AAD 16AN perform fits to the ATLAS and CMS data at E_{cm} = 7 and 8 TeV. NODE=S126STH;LINKAGE=J

[17] AAD 16K use up to 4.7 fb^{-1} of pp collisions at E_{cm} = 7 TeV and up to 20.3 fb^{-1} at E_{cm} = 8 TeV. The third uncertainty in the measurement is theory systematics. The quoted signal strength is given for m_H = 125.36 GeV. NODE=S126STH;LINKAGE=F

[18] AAD 15 search for $t\bar{t}H$ production with H decaying to $\gamma\gamma$ in 4.5 fb^{-1} of pp collisions at E_{cm} = 7 TeV and 20.3 fb^{-1} at E_{cm} = 8 TeV. The quoted result on the signal strength is equivalent to an upper limit of 6.7 at 95% CL and is given for m_H = 125.4 GeV. NODE=S126STH;LINKAGE=B

[19] AAD 15BC search for $t\bar{t}H$ production with H decaying to $b\bar{b}$ in 20.3 fb^{-1} of pp collisions at E_{cm} = 8 TeV. The corresponding upper limit is 3.4 at 95% CL. The quoted signal strength is given for m_H = 125 GeV. NODE=S126STH;LINKAGE=C

[20] AAD 15T search for $t\bar{t}H$ production with H resulting in multilepton final states (mainly from WW^*, $\tau\tau$, ZZ^*) in 20.3 fb^{-1} of pp collisions at E_{cm} = 8 TeV. The quoted result on the signal strength is given for m_H = 125 GeV and corresponds to an upper limit of 4.7 at 95% CL. The data sample is independent from AAD 15 and AAD 15BC. NODE=S126STH;LINKAGE=D

[21] KHACHATRYAN 15AN search for $t\bar{t}H$ production with H decaying to $b\bar{b}$ in 19.5 fb^{-1} of pp collisions at E_{cm} = 8 TeV. The quoted result on the signal strength is equivalent to an upper limit of 4.2 at 95% CL and is given for m_H = 125 GeV. NODE=S126STH;LINKAGE=E

[22] KHACHATRYAN 14H search for $t\bar{t}H$ production with H decaying to $b\bar{b}$, $\tau\tau$, $\gamma\gamma$, WW^*, and ZZ^*, in 5.1 fb^{-1} of pp collisions at E_{cm} = 7 TeV and 19.7 fb^{-1} at E_{cm} = 8 TeV. The quoted signal strength is given for m_H = 125.6 GeV. NODE=S126STH;LINKAGE=A

[23] AALTONEN 13L combine all CDF results with 9.45–10.0 fb^{-1} of $p\bar{p}$ collisions at E_{cm} = 1.96 TeV. The quoted signal strength is given for m_H = 125 GeV. NODE=S126STH;LINKAGE=LL

[24] CHATRCHYAN 13X search for $t\bar{t}H$ production followed by $H \to b\bar{b}$, one top decaying to $\ell\nu$ and the other to either $\ell\nu$ or $q\bar{q}$ in 5.0 fb^{-1} and 5.1 fb^{-1} of pp collisions at E_{cm} = 7 and 8 TeV. A limit on cross section times branching ratio which corresponds to (4.0–8.6) times the expected Standard Model cross section is given for m_H = 110–140 GeV at 95% CL. The quoted limit is given for m_H = 125 GeV, where 5.2 is expected for no signal. NODE=S126STH;LINKAGE=TY

HH Production Cross Section in pp Collisions

NODE=S126SHH

The HH production cross section relative to the SM prediction. NODE=S126SHH

NODE=S126SHH

< 2.4 (CL = 95%) [<12.7 OUR 2019 BEST LIMIT]

VALUE	CL%	DOCUMENT ID		TECN	COMMENT
< 2.4	95	[1] AAD	23AT	ATLS	13 TeV, $b\bar{b}b\bar{b}$, $b\bar{b}\tau\tau$, $b\bar{b}\gamma\gamma$
• • • We do not use the following data for averages, fits, limits, etc. • • •					
<183	95	[2] AAD	23AD	ATLS	13 TeV, VHH, $HH \to b\bar{b}b\bar{b}$
< 5.4	95	[3] AAD	23BK	ATLS	13 TeV, $b\bar{b}b\bar{b}$
< 4.7	95	[4] AAD	23Z	ATLS	13 TeV, $b\bar{b}\tau\tau$
< 9.9	95	[5] TUMASYAN	23AE	CMS	13 TeV, $b\bar{b}b\bar{b}$
< 3.3	95	[6,7] TUMASYAN	23D	CMS	13 TeV, $b\bar{b}\tau\tau$
<124	95	[6,8] TUMASYAN	23D	CMS	13 TeV, $b\bar{b}\tau\tau$ OCCUR=2
< 32.4	95	[9] TUMASYAN	23I	CMS	13 TeV, $b\bar{b}ZZ^*$ ($ZZ^* \to 4\ell$)
< 21.3	95	[10] TUMASYAN	23O	CMS	13 TeV, WW^*WW^*, $WW^*\tau\tau$, $\tau\tau\tau\tau$
< 4.2	95	[11] AAD	22Y	ATLS	13 TeV, $\gamma\gamma b\bar{b}$
< 3.4	95	[12] CMS	22	CMS	13 TeV, $b\bar{b}ZZ^*$, $b\bar{b}\gamma\gamma$, $b\bar{b}\tau\tau$, $b\bar{b}b\bar{b}$, multilepton
< 3.9	95	[13] TUMASYAN	22AN	CMS	13 TeV, $b\bar{b}b\bar{b}$
< 7.7	95	[14] SIRUNYAN	21K	CMS	13 TeV, $\gamma\gamma b\bar{b}$
< 6.9	95	[15] AAD	20C	ATLS	13 TeV, $b\bar{b}\gamma\gamma$, $b\bar{b}\tau\tau$, $b\bar{b}b\bar{b}$, $b\bar{b}WW^*$, $WW^*\gamma\gamma$, WW^*WW^*
< 40	95	[16] AAD	20E	ATLS	13 TeV, $HH \to b\bar{b}\ell\nu\ell\nu$
<840	95	[17] AAD	20X	ATLS	13 TeV, VBF, $b\bar{b}b\bar{b}$
< 12.9	95	[18] AABOUD	19A	ATLS	13 TeV, $b\bar{b}b\bar{b}$
<300	95	[19] AABOUD	19O	ATLS	13 TeV, $b\bar{b}WW^*$
<160	95	[20] AABOUD	19T	ATLS	13 TeV, WW^*WW^*
< 24	95	[21] SIRUNYAN	19	CMS	13 TeV, $\gamma\gamma b\bar{b}$
< 75	95	[22] SIRUNYAN	19AB	CMS	13 TeV, $b\bar{b}b\bar{b}$
< 22.2	95	[23] SIRUNYAN	19BE	CMS	13 TeV, $b\bar{b}\gamma\gamma$ $b\bar{b}\tau\tau$, $b\bar{b}b\bar{b}$, $b\bar{b}WW^*$, $b\bar{b}ZZ^*$
<179	95	[24] SIRUNYAN	19H	CMS	13 TeV, $b\bar{b}b\bar{b}$
<230	95	[25] AABOUD	18BU	ATLS	13 TeV, $\gamma\gamma WW^*$
< 12.7	95	[26] AABOUD	18CQ	ATLS	13 TeV, $b\bar{b}\tau\tau$
< 22	95	[27] AABOUD	18CW	ATLS	13 TeV, $\gamma\gamma b\bar{b}$
< 30	95	[28] SIRUNYAN	18A	CMS	13 TeV, $b\bar{b}\tau\tau$

$<$ 79	95	[29] SIRUNYAN	18F	CMS	13 TeV, $b\overline{b}\ell\nu\ell\nu$
$<$ 43	95	[30] SIRUNYAN	17CN	CMS	8 TeV, $b\overline{b}\tau\tau$, $\gamma\gamma b\overline{b}$, $b\overline{b}b\overline{b}$
$<$108	95	[31] AABOUD	16I	ATLS	13 TeV, $b\overline{b}b\overline{b}$
$<$ 74	95	[32] KHACHATRY...	16BQ	CMS	8 TeV, $\gamma\gamma b\overline{b}$
$<$ 70	95	[33] AAD	15CE	ATLS	8 TeV, $b\overline{b}b\overline{b}$, $b\overline{b}\tau\tau$, $\gamma\gamma b\overline{b}$, $\gamma\gamma WW$

[1] AAD 23AT combine results from 126–139 fb^{-1} of data at E_{cm} = 13 TeV for $pp \to HH \to b\overline{b}b\overline{b}$ (AAD 23BK), $b\overline{b}\tau\tau$ (AAD 23Z), and $b\overline{b}\gamma\gamma$ (AAD 22Y). NODE=S126SHH;LINKAGE=GA

[2] AAD 23AD search for non-resonant HH production in association with a vector boson using $HH \to b\overline{b}b\overline{b}$ with data of 139 fb^{-1} at E_{cm} = 13 TeV. The vector boson decays leptonically ($W \to \ell\nu$, $Z \to \ell\ell, \nu\nu$, $\ell = e, \mu$). NODE=S126SHH;LINKAGE=Z

[3] AAD 23BK search for non-resonant HH production using $HH \to b\overline{b}b\overline{b}$ with data of 126 fb^{-1} at E_{cm} = 13 TeV. NODE=S126SHH;LINKAGE=FA

[4] AAD 23Z search for non-resonant HH production using $HH \to b\overline{b}\tau\tau$ with data of 139 fb^{-1} at E_{cm} = 13 TeV. The upper limit on the $pp \to HH$ production cross section at 95% CL is measured to be 140 fb, which corresponds to 4.7 times the SM prediction (see their Table 6). NODE=S126SHH;LINKAGE=X

[5] TUMASYAN 23AE search for HH production using $HH \to b\overline{b}b\overline{b}$, where both $b\overline{b}$ pairs are highly boosted, with data of 138 fb^{-1} at E_{cm} = 13 TeV. NODE=S126SHH;LINKAGE=AA

[6] TUMASYAN 23D search for non-resonant HH production using $HH \to b\overline{b}\tau\tau$ with data of 138 fb^{-1} at E_{cm} = 13 TeV. NODE=S126SHH;LINKAGE=BA

[7] The upper limit on the $pp \to HH$ production cross section (gluon fusion and VBF) at 95% CL is measured to be 102 fb, which corresponds to 3.3 times the SM prediction (see their Table 2). NODE=S126SHH;LINKAGE=DA

[8] The upper limit on the VBF $pp \to HH$ production cross section at 95% CL is measured to be 212 fb, which corresponds to 124 times the SM prediction (see their Table 3). NODE=S126SHH;LINKAGE=CA

[9] TUMASYAN 23I search for non-resonant HH production using $HH \to b\overline{b}ZZ^*$ ($ZZ^* \to 4\ell$, $\ell = e, \mu$) with data of 138 fb^{-1} at E_{cm} = 13 TeV. NODE=S126SHH;LINKAGE=Y

[10] TUMASYAN 23O search for non-resonant HH production using $HH \to WW^*WW^*$, $WW^*\tau\tau$, and $\tau\tau\tau\tau$ (multilepton) with data of 138 fb^{-1} at E_{cm} = 13 TeV. See their Fig. 9 for different final states and these combination. NODE=S126SHH;LINKAGE=EA

[11] AAD 22Y search for non-resonant HH production using $HH \to \gamma\gamma b\overline{b}$ with data of 139 fb^{-1} at E_{cm} = 13 TeV. The upper limit on the $pp \to HH$ production cross section at 95% CL is measured to be 130 fb, which corresponds to 4.2 times the SM prediction. NODE=S126SHH;LINKAGE=V

[12] CMS 22 report combined results (see their Extended Data Table 2) using 138 fb^{-1} of data at E_{cm} = 13 TeV. See their Fig. 5 (left) for different final states and these combination. NODE=S126SHH;LINKAGE=U

[13] TUMASYAN 22AN search for non-resonant HH production using $HH \to b\overline{b}b\overline{b}$ with data of 138 fb^{-1} at E_{cm} = 13 TeV. The upper limit on the $pp \to HH$ production cross section at 95% CL is measured to be 120 fb, which corresponds to 3.9 times the SM prediction. NODE=S126SHH;LINKAGE=W

[14] SIRUNYAN 21K search for non-resonant HH production using $HH \to \gamma\gamma b\overline{b}$ with data of 137 fb^{-1} at E_{cm} = 13 TeV. The upper limit on the $pp \to HH \to \gamma\gamma b\overline{b}$ production cross section at 95% CL is measured to be 0.67 fb, which corresponds to about 7.7 times the SM prediction. NODE=S126SHH;LINKAGE=T

[15] AAD 20C combine results of up to 36.1 fb^{-1} data at E_{cm} = 13 TeV for $pp \to HH \to b\overline{b}\gamma\gamma$, $b\overline{b}\tau\tau$, $b\overline{b}b\overline{b}$, $b\overline{b}WW^*$, $WW^*\gamma\gamma$, WW^*WW^* (AABOUD 18CW, AABOUD 18CQ, AABOUD 19A, AABOUD 19O, AABOUD 18BU, and AABOUD 19T). NODE=S126SHH;LINKAGE=Q

[16] AAD 20E search non-resonant for HH production using $HH \to b\overline{b}\ell\nu\ell\nu$, where one of the Higgs bosons decays to $b\overline{b}$ and the other decays to either WW^*, ZZ^*, or $\tau\tau$, with data of 139 fb^{-1} at E_{cm} = 13 TeV. The upper limit on the $pp \to HH$ production cross section at 95% CL is measured to be 1.2 pb, which corresponds to about 40 times the SM prediction. NODE=S126SHH;LINKAGE=R

[17] AAD 20X search for $HH \to b\overline{b}b\overline{b}$ process via VBF with data of 126 fb^{-1} at E_{cm} = 13 TeV. The upper limit on the SM non-resonant HH production cross section is 1460 fb at 95% CL, which corresponds to 840 times the SM prediction. NODE=S126SHH;LINKAGE=S

[18] AABOUD 19A search for HH production using $HH \to b\overline{b}b\overline{b}$ with data of 36.1 fb^{-1} at E_{cm} = 13 TeV. The upper limit on the $pp \to HH \to b\overline{b}b\overline{b}$ production cross section at 95% is measured to be 147 fb, which corresponds to about 12.9 times the SM prediction. NODE=S126SHH;LINKAGE=J

[19] AABOUD 19O search for HH production using $HH \to b\overline{b}WW^*$ with data of 36.1 fb^{-1} at E_{cm} = 13 TeV. The upper limit on the $pp \to HH$ production cross section at 95% CL is calculated to be 10 pb from the observed upper limit on the $pp \to HH \to b\overline{b}WW^*$ production cross section of 2.5 pb assuming the SM branching fractions. The former corresponds to about 300 times the SM prediction. NODE=S126SHH;LINKAGE=N

[20] AABOUD 19T search for HH production using $HH \to WW^*WW^*$ with data of 36.1 fb^{-1} at E_{cm} = 13 TeV. The upper limit on the $pp \to HH$ production cross section at 95% is measured to be 5.3 pb, which corresponds to about 160 times the SM prediction. NODE=S126SHH;LINKAGE=O

[21] SIRUNYAN 19 search for HH production using $HH \to \gamma\gamma b\overline{b}$ with data of 35.9 fb^{-1} at E_{cm} = 13 TeV. The upper limit on the $pp \to HH \to \gamma\gamma b\overline{b}$ production cross NODE=S126SHH;LINKAGE=H

section at 95% CL is measured to be 2.0 fb, which corresponds to about 24 times the SM prediction.

[22] SIRUNYAN 19AB search for HH production using $HH \to b\overline{b}b\overline{b}$, where 4 heavy flavor jets from two Higgs bosons are resolved, with data of 35.9 fb^{-1} at $E_{\rm cm}$ = 13 TeV. The upper limit on the $pp \to HH \to b\overline{b}b\overline{b}$ production cross section at 95% is measured to be 847 fb, which corresponds to about 75 times the SM prediction. NODE=S126SHH;LINKAGE=M

[23] SIRUNYAN 19BE combine results of 13 TeV 35.9 fb^{-1} data: SIRUNYAN 19, SIRUNYAN 18A, SIRUNYAN 19AB, SIRUNYAN 19H, and SIRUNYAN 18F. NODE=S126SHH;LINKAGE=P

[24] SIRUNYAN 19H search for HH production using $HH \to b\overline{b}b\overline{b}$, where one of $b\overline{b}$ pairs is highly boosted and the other one is resolved, with data of 35.9 fb^{-1} at $E_{\rm cm}$ = 13 TeV. The upper limit on the $pp \to HH \to b\overline{b}b\overline{b}$ production cross section at 95% is measured to be 1980 fb, which corresponds to about 179 times the SM prediction. NODE=S126SHH;LINKAGE=L

[25] AABOUD 18BU search for HH production using $\gamma\gamma WW^*$ with the final state of $\gamma\gamma\ell\nu jj$ using data of 36.1 fb^{-1} at $E_{\rm cm}$ = 13 TeV. The upper limit on the $pp \to HH$ production cross section at 95% CL is measured to be 7.7 pb, which corresponds to about 230 times the SM prediction. The upper limit on the $pp \to HH \to \gamma\gamma WW^*$ at 95% CL is measured to be 7.5 fb (see thier Table 6). NODE=S126SHH;LINKAGE=G

[26] AABOUD 18CQ search for HH production using $HH \to b\overline{b}\tau\tau$ with data of 36.1 fb^{-1} at $E_{\rm cm}$ = 13 TeV. The upper limit on the $pp \to HH \to b\overline{b}\tau\tau$ production cross section at 95% is measured to be 30.9 fb, which corresponds to about 12.7 times the SM prediction. NODE=S126SHH;LINKAGE=K

[27] AABOUD 18CW search for HH production using $HH \to \gamma\gamma b\overline{b}$ with data of 36.1 fb^{-1} at $E_{\rm cm}$ = 13 TeV. The upper limit on the $pp \to HH$ production cross section at 95% is measured to be 0.73 pb, which corresponds to about 22 times the SM prediction. NODE=S126SHH;LINKAGE=I

[28] SIRUNYAN 18A search for HH production using $HH \to b\overline{b}\tau\tau$ with data of 35.9 fb^{-1} at $E_{\rm cm}$ = 13 TeV. The upper limit on the $gg \to HH \to b\overline{b}\tau\tau$ production cross section is measured to be 75.4 fb, which corresponds to about 30 times the SM prediction. NODE=S126SHH;LINKAGE=B

[29] SIRUNYAN 18F search non-resonant for HH production using $HH \to b\overline{b}\ell\nu\ell\nu$, where $\ell\nu\ell\nu$ is either $WW \to \ell\nu\ell\nu$ or $ZZ \to \ell\ell\nu\nu$ (ℓ is e, μ or a leptonically decaying τ), with data of 35.9 fb^{-1} at $E_{\rm cm}$ = 13 TeV. The upper limit on the $HH \to b\overline{b}\ell\nu\ell\nu$ production cross section at 95% CL is measured to be 72 fb, which corresponds to about 79 times the SM prediction. NODE=S126SHH;LINKAGE=F

[30] SIRUNYAN 17CN search for HH production using $HH \to b\overline{b}\tau\tau$ with data of 18.3 fb^{-1} at $E_{\rm cm}$ = 8 TeV. Results are then combined with the published results of the $HH \to \gamma\gamma b\overline{b}$ and $HH \to b\overline{b}b\overline{b}$, which use data of up to 19.7 fb^{-1} at $E_{\rm cm}$ = 8 TeV. The upper limit on the $gg \to HH$ production cross section is measured to be 0.59 pb from $b\overline{b}\tau\tau$, which corresponds to about 59 times the SM prediction (gluon fusion). The combined upper limit is 0.43 pb, which is about 43 times the SM prediction. The quoted values are given for m_H = 125 GeV. NODE=S126SHH;LINKAGE=E

[31] AABOUD 16I search for HH production using $HH \to b\overline{b}b\overline{b}$ with data of 3.2 fb^{-1} at $E_{\rm cm}$ = 13 TeV. The upper limit on the $pp \to HH \to b\overline{b}b\overline{b}$ production cross section is measured to be 1.22 pb. This result corresponds to about 108 times the SM prediction (gluon fusion), which is $11.3^{+0.9}_{-1.0}$ fb (NNLO+NNLL) including top quark mass effects. The quoted values are given for m_H = 125 GeV . NODE=S126SHH;LINKAGE=D

[32] KHACHATRYAN 16BQ search for HH production using $HH \to \gamma\gamma b\overline{b}$ with data of 19.7 fb^{-1} at $E_{\rm cm}$ = 8 TeV. The upper limit on the $gg \to HH \to \gamma\gamma b\overline{b}$ production is measured to be 1.85 fb, which corresponds to about 74 times the SM prediction and is translated into 0.71 pb for $gg \to HH$ production cross section. NODE=S126SHH;LINKAGE=A

[33] AAD 15CE search for HH production using $HH \to b\overline{b}\tau\tau$ and $HH \to \gamma\gamma WW$ with data of 20.3 fb^{-1} at $E_{\rm cm}$ = 8 TeV. These results are then combined with the published results of the $HH \to \gamma\gamma b\overline{b}$ and $HH \to b\overline{b}b\overline{b}$, which use data of up to 20.3 fb^{-1} at $E_{\rm cm}$ = 8 TeV. The upper limits on the $gg \to HH$ production cross section are measured to be 1.6 pb, 11.4 pb, 2.2 pb and 0.62 pb from $b\overline{b}\tau\tau$, $\gamma\gamma WW$, $\gamma\gamma b\overline{b}$ and $b\overline{b}b\overline{b}$, respectively. The combined upper limit is 0.69 pb, which corresponds to about 70 times the SM prediction. The quoted results are given for m_H = 125.4 GeV. See their Table 4. NODE=S126SHH;LINKAGE=C

Higgs trilinear self coupling modifier κ_λ

NODE=S126KLA

Signal strength relative to the SM prediction, $\kappa_\lambda = \lambda_{HHH} / \lambda^{SM}_{HHH}$.

NODE=S126KLA
NODE=S126KLA

VALUE	CL%	DOCUMENT ID		TECN	COMMENT	
• • • We do not use the following data for averages, fits, limits, etc. • • •						
−34.4 to 33.3	95	[1] AAD	23AD	ATLS	13 TeV, VHH, $HH \to b\overline{b}b\overline{b}$	
− 0.6 to 6.6	95	[2] AAD	23AT	ATLS	13 TeV, $b\overline{b}b\overline{b}$, $b\overline{b}\tau\tau$, $b\overline{b}\gamma\gamma$	
− 0.4 to 6.3	95	[3] AAD	23AT	ATLS	13 TeV, $b\overline{b}b\overline{b}$, $b\overline{b}\tau\tau$, $b\overline{b}\gamma\gamma$	OCCUR=2
− 3.5 to 11.3	95	[4] AAD	23BK	ATLS	13 TeV, $b\overline{b}b\overline{b}$	
− 5.4 to 14.9	95	[5] HAYRAPETY...	23	CMS	13 TeV, $ZZ^* \to 4\ell$ cross sections	
− 9.9 to 16.9	95	[6] TUMASYAN	23AE	CMS	13 TeV, $b\overline{b}b\overline{b}$	
− 1.7 to 8.7	95	[7] TUMASYAN	23D	CMS	13 TeV, $b\overline{b}\tau\tau$	
− 8.8 to 13.4	95	[8] TUMASYAN	23I	CMS	13 TeV, $b\overline{b}ZZ^*$ ($ZZ^* \to 4\ell$)	

− 6.9	to 11.1	95	[9] TUMASYAN	23O	CMS	13 TeV, WW^*WW^*, $WW^*\tau\tau$, $\tau\tau\tau\tau$
− 1.5	to 6.7	95	[10] AAD	22Y	ATLS	13 TeV, $\gamma\gamma b\overline{b}$
− 1.24	to 6.49	95	[11] CMS	22	CMS	13 TeV, $b\overline{b}ZZ^*$, $b\overline{b}\gamma\gamma$, $b\overline{b}\tau\tau$, $b\overline{b}b\overline{b}$, multilepton
− 2.3	to 9.4	95	[12] TUMASYAN	22AN	CMS	13 TeV, $b\overline{b}b\overline{b}$
− 3.3	to 8.5	95	[13] SIRUNYAN	21K	CMS	13 TeV, $\gamma\gamma b\overline{b}$
− 5.0	to 12.0	95	[14] AAD	20C	ATLS	13 TeV, $b\overline{b}\gamma\gamma$, $b\overline{b}\tau\tau$, $b\overline{b}b\overline{b}$, $b\overline{b}WW^*$, $WW^*\gamma\gamma$, WW^*WW^*
−11	to 17	95	[15] SIRUNYAN	19	CMS	13 TeV, $\gamma\gamma b\overline{b}$
−11.8	to 18.8	95	[16] SIRUNYAN	19BE	CMS	13 TeV, $b\overline{b}\gamma\gamma$ $b\overline{b}\tau\tau$, $b\overline{b}b\overline{b}$, $b\overline{b}WW^*$, $b\overline{b}ZZ^*$
− 8.2	to 13.2	95	[17] AABOUD	18CW	ATLS	13 TeV, $\gamma\gamma b\overline{b}$
			[18] SIRUNYAN	18A	CMS	13 TeV, $b\overline{b}\tau\tau$
−17	to 22.5	95	[19] KHACHATRY...	16BQ	CMS	8 TeV, $\gamma\gamma b\overline{b}$

[1] AAD 23AD search for non-resonant HH production in association with a vector boson using $HH \to b\overline{b}b\overline{b}$ with data of 139 fb^{-1} at E_{cm} = 13 TeV. The vector boson decays leptonically ($W \to \ell\nu$, $Z \to \ell\ell$, $\nu\nu$, $\ell = e$, μ). The quoted κ_λ is measured assuming all other Higgs boson couplings are at their SM value. NODE=S126KLA;LINKAGE=F

[2] AAD 23AT combine results from 126–139 fb^{-1} of data at E_{cm} = 13 TeV for $pp \to HH \to b\overline{b}b\overline{b}$ (AAD 23BK), $b\overline{b}\tau\tau$ (AAD 23Z), and $b\overline{b}\gamma\gamma$ (AAD 22Y). The quoted values are obtained from the profile likelihood scan as a function of κ_λ as shown in their Fig. 5(a). All other coupling modifiers are assumed to have their SM values. NODE=S126KLA;LINKAGE=M

[3] AAD 23AT combine results from 126–139 fb^{-1} of data at E_{cm} = 13 TeV for $pp \to HH \to b\overline{b}b\overline{b}$ (AAD 23BK), $b\overline{b}\tau\tau$ (AAD 23Z), and $b\overline{b}\gamma\gamma$ (AAD 22Y) with single-Higgs boson analyses ($\gamma\gamma$, ZZ^*, WW^*, $\tau\tau$, $b\overline{b}$, see their Table 1). The quoted values are obtained from the profile likelihood scan as a function of κ_λ as shown in their Fig. 5(a), assuming that all other Higgs boson couplings are at their SM values. Results with other assumptions are shown in their Table 2. NODE=S126KLA;LINKAGE=N

[4] AAD 23BK search for non-resonant HH production using $HH \to b\overline{b}b\overline{b}$ with data of 126 fb^{-1} at E_{cm} = 13 TeV. The quoted values are obtained from the one-dimensional profile likelihood scan as a function of κ_λ. See their Fig. 12 (a). The $\mu_{ggF+VBF}$ measurement for different values of κ_λ constrains -3.9 < κ_λ < 11.1 at 95% CL as shown in their Fig. 10 (a). $\kappa_{2V}= \kappa_V$=1 is assumed in both cases. NODE=S126KLA;LINKAGE=L

[5] HAYRAPETYAN 23 measure the cross sections for $pp \to H \to ZZ^* \to 4\ell$ ($\ell = e$, μ) using 138 fb^{-1} at E_{cm} = 13 TeV. NODE=S126KLA;LINKAGE=O

[6] TUMASYAN 23AE search for HH production using $HH \to b\overline{b}b\overline{b}$, where both $b\overline{b}$ pairs are highly boosted, with data of 138 fb^{-1} at E_{cm} = 13 TeV. The quoted κ_λ is measured assuming all other Higgs boson couplings are at their SM values. NODE=S126KLA;LINKAGE=G

[7] TUMASYAN 23D search for non-resonant HH production using $HH \to b\overline{b}\tau\tau$ with data of 138 fb^{-1} at E_{cm} = 13 TeV. The quoted values are obtained from the upper limit on the HH production cross section times the $b\overline{b}\tau\tau$ branching fraction for different values of κ_λ. See their Fig. 8 (left). All other coupling modifiers are assumed to be 1. In addition, two-dimensional exclusion regions as a function of the κ_λ and κ_t couplings, with $\kappa_{2V} = \kappa_V = 1$, are shown in their Fig. 9 (left). The one-dimensional likelihood scan as a function of κ_λ is given in their Fig 10 (left), from which a 95% confidence interval of -1.77 < κ_λ < 8.73 is extracted. NODE=S126KLA;LINKAGE=J

[8] TUMASYAN 23AI search for non-resonant HH production using $HH \to b\overline{b}ZZ^*$ ($ZZ^* \to 4\ell$, ℓ=e,μ) with data of 138 fb^{-1} at E_{cm} = 13 TeV. See their Fig. 4. NODE=S126KLA;LINKAGE=E

[9] TUMASYAN 23O search for non-resonant HH production using $HH \to WW^*WW^*$, $WW^*\tau\tau$, and $\tau\tau\tau\tau$ (multilepton) with data of 138 fb^{-1} at E_{cm} = 13 TeV. See their Fig. 10 for different final states and these combination. Limits are set on a variety of new-physics models using an effective field theory approach. See their Figs. 11, 12, and 13. NODE=S126KLA;LINKAGE=K

[10] AAD 22Y search for non-resonant HH production using $HH \to \gamma\gamma b\overline{b}$ with data of 139 fb^{-1} at E_{cm} = 13 TeV. The quoted κ_λ is obtained from their Fig. 12 where the theory uncertainties are not included while a negative log-likelihood scan vs. $\kappa_\lambda$is shown in their Fig. 13 with the theory uncertainties, which provides $\kappa_\lambda = 2.8^{+2.0}_{-2.2}$ for the 1σ confidence interval. NODE=S126KLA;LINKAGE=V

[11] CMS 22 report combined results (see their Extended Data Table 2) using 138 fb^{-1} of data at E_{cm} = 13 TeV. See their Fig. 6 (left). NODE=S126KLA;LINKAGE=U

[12] TUMASYAN 22AN search for non-resonant HH production using $HH \to b\overline{b}b\overline{b}$ with data of 138 fb^{-1} at E_{cm} = 13 TeV. The upper limit on the $pp \to HH$ production cross section at 95% CL is shown as a function of κ_λ in their Fig. 2 (top). NODE=S126KLA;LINKAGE=W

[13] SIRUNYAN 21K search for non-resonant HH production using $HH \to \gamma\gamma b\overline{b}$ with data of 137 fb^{-1} at E_{cm} = 13 TeV. NODE=S126KLA;LINKAGE=T

[14] AAD 20C combine results of up to 36.1 fb^{-1} data at E_{cm} = 13 TeV for $pp \to HH \to b\overline{b}\gamma\gamma$, $b\overline{b}\tau\tau$, $b\overline{b}b\overline{b}$, $b\overline{b}WW^*$, $WW^*\gamma\gamma$, WW^*WW^* (AABOUD 18CW, AABOUD 18CQ, AABOUD 19A, AABOUD 19O, AABOUD 18BU, and AABOUD 19T). NODE=S126KLA;LINKAGE=Q

[15] SIRUNYAN 19 search for HH production using $HH \to \gamma\gamma b\overline{b}$ with data of 35.9 fb^{-1} at E_{cm} = 13 TeV. The quoted κ_λ is measured assuming all other Higgs boson couplings are at their SM value. NODE=S126KLA;LINKAGE=H

[16] SIRUNYAN 19BE combine results of 13 TeV 35.9 fb^{-1} data: SIRUNYAN 19, SIRUNYAN 18A, SIRUNYAN 19AB, SIRUNYAN 19H, and SIRUNYAN 18F. NODE=S126KLA;LINKAGE=P

[17] AABOUD 18CW search for HH production using $HH \to \gamma\gamma b\overline{b}$ with data of 36.1 fb^{-1} at E_{cm} = 13 TeV. The quoted κ_λ is measured assuming all other Higgs boson couplings are at their SM value. NODE=S126KLA;LINKAGE=I

[18] SIRUNYAN 18A search for HH production using $HH \to b\overline{b}\tau\tau$ with data of 35.9 fb^{-1} at E_{cm} = 13 TeV. The upper limit on production cross section times branching fraction at 95% CL is shown as a function of κ_λ/κ_t in their Fig. 6 (top) where $\kappa_t = y_t \,/\, y_t^{SM}$ (top Yukawa coupling y_t). NODE=S126KLA;LINKAGE=C

[19] KHACHATRYAN 16BQ search for HH production using $HH \to \gamma\gamma b\overline{b}$ with data of 19.7 fb^{-1} at E_{cm} = 8 TeV. NODE=S126KLA;LINKAGE=D

Higgs-gauge boson quartic coupling modifier κ_{2V}

NODE=S126K2V

Signal strength relative to the SM prediction, $\kappa_{2V} = \lambda_{VVHH} \,/\, \lambda^{SM}_{VVHH}$, V = W, Z. NODE=S126K2V

NODE=S126K2V

VALUE	CL%	DOCUMENT ID		TECN	COMMENT
• • • We do not use the following data for averages, fits, limits, etc. • • •					
−8.6 to 10.0	95	[1] AAD	23AD	ATLS	13 TeV, VHH, $HH \to b\overline{b}b\overline{b}$
0.1 to 2.0	95	[2] AAD	23AT	ATLS	13 TeV, $b\overline{b}b\overline{b}$, $b\overline{b}\tau\tau$, $b\overline{b}\gamma\gamma$
0.0 to 2.1	95	[3] AAD	23BK	ATLS	13 TeV, $b\overline{b}b\overline{b}$
0.62 to 1.41	95	[4] TUMASYAN	23AE	CMS	13 TeV, $b\overline{b}b\overline{b}$
−0.4 to 2.6	95	[5] TUMASYAN	23D	CMS	13 TeV, $b\overline{b}\tau\tau$
0.67 to 1.38	95	[6] CMS	22	CMS	13 TeV, $b\overline{b}ZZ^*$, $b\overline{b}\gamma\gamma$, $b\overline{b}\tau\tau$, $b\overline{b}b\overline{b}$, multilepton
−0.1 to 2.2	95	[7] TUMASYAN	22AN	CMS	13 TeV, $b\overline{b}b\overline{b}$
−1.3 to 3.5	95	[8] SIRUNYAN	21K	CMS	13 TeV, $\gamma\gamma b\overline{b}$
−0.43 to 2.56	95	[9] AAD	20X	ATLS	13 TeV, VBF, $b\overline{b}b\overline{b}$

[1] AAD 23AD search for non-resonant HH production in association with a vector boson using $HH \to b\overline{b}b\overline{b}$ with data of 139 fb^{-1} at E_{cm} = 13 TeV. The vector boson decays leptonically ($W \to \ell\nu$, $Z \to \ell\ell$, $\nu\nu$, $\ell = e$, μ). The constraints on κ_{2W} and κ_{2Z} are separately measured to be -12.3 < κ_{2W} < 13.5 and -9.9 < κ_{2Z} < 11.3 (95% CL). The quoted κ_{2V} ($V = W$, Z) is measured assuming all other Higgs boson couplings are at their SM value. NODE=S126K2V;LINKAGE=H

[2] AAD 23AT combine results from 126–139 fb^{-1} of data at E_{cm} = 13 TeV for $pp \to HH \to b\overline{b}b\overline{b}$ (AAD 23BK), $b\overline{b}\tau\tau$ (AAD 23Z), and $b\overline{b}\gamma\gamma$ (AAD 22Y). The quoted values are obtained from the 95% CL VBF HH cross-section upper limit as a function of κ_{2V} as shown in their Fig. 4(b). All other coupling modifiers are assumed to have their SM values. NODE=S126K2V;LINKAGE=L

[3] AAD 23BK search for non-resonant HH production using $HH \to b\overline{b}b\overline{b}$ with data of 126 fb^{-1} at E_{cm} = 13 TeV. The quoted values are obtained from the one-dimensional profile likelihood scan as a function of κ_{2V}. See their Fig. 12 (b). The μ_{VBF} measurement for different values of κ_{2V} constrains -0.03 < κ_{2V} < 2.11 at 95% CL as shown in their Fig. 10 (b). $\kappa_\lambda = \kappa_V = 1$ is assumed in both cases. NODE=S126K2V;LINKAGE=K

[4] TUMASYAN 23AE search for HH production using $HH \to b\overline{b}b\overline{b}$, where both $b\overline{b}$ pairs are highly boosted, with data of 138 fb^{-1} at E_{cm} = 13 TeV. The $\kappa_{2V} = 0$ is excluded at 6.3 σ assuming all other Higgs boson couplings are at their SM values. NODE=S126K2V;LINKAGE=I

[5] TUMASYAN 23D search for non-resonant HH production using $HH \to b\overline{b}\tau\tau$ with data of 138 fb^{-1} at E_{cm} = 13 TeV. The quoted values are obtained from the upper limits on the HH production cross section times the $b\overline{b}\tau\tau$ branching fraction for different values of κ_{2V}. See their Fig. 8 (right). All other coupling modifiers are assumed to be 1. In addition, two-dimensional exclusion regions as a function of the κ_{2V} and κ_V couplings, with $\kappa_\lambda = \kappa_t = 1$, are shown in their Fig. 9 (right). The one-dimensional likelihood scan as a function of κ_{2V} is given in their Fig. 10 (right), from which a 95% confidence interval of -0.34 < κ_{2V} < 2.49 is extracted. NODE=S126K2V;LINKAGE=J

[6] CMS 22 report combined results (see their Extended Data Table 2) using 138 fb^{-1} of data at E_{cm} = 13 TeV. See their Fig. 6 (right). NODE=S126K2V;LINKAGE=G

[7] TUMASYAN 22AN search for non-resonant HH production using $HH \to b\overline{b}b\overline{b}$ with data of 138 fb^{-1} at E_{cm} = 13 TeV. The upper limit on the $pp \to HH$ production cross section at 95% CL is shown as a function of κ_{2V} in their Fig. 2 (bottom). NODE=S126K2V;LINKAGE=A

[8] SIRUNYAN 21K search for non-resonant HH production using $HH \to \gamma\gamma b\overline{b}$ with data of 137 fb^{-1} at E_{cm} = 13 TeV. NODE=S126K2V;LINKAGE=E

[9] AAD 20X search for $HH \to b\overline{b}b\overline{b}$ process via VBF with data of 126 fb^{-1} at E_{cm} = 13 TeV. NODE=S126K2V;LINKAGE=F

tH production

NODE=S126PTH
NODE=S126PTH

VALUE	DOCUMENT ID		TECN	COMMENT
5.7±2.7±3.0	[1] SIRUNYAN	21R	CMS	pp, 13 TeV
• • • We do not use the following data for averages, fits, limits, etc. • • •				
	[2] AAD	20Z	ATLS	pp, 13 TeV
	[3] SIRUNYAN	19BK	CMS	pp, 13 TeV
	[4] KHACHATRY...	16AU	CMS	pp, 8 TeV

[1] SIRUNYAN 21R search for tH in final states with electrons, muons and hadronically decaying τ leptons ($H \to WW^*$, ZZ^*, $\tau\tau$) with 137 fb^{-1} of pp collision data at E_{cm} = 13 TeV. The quoted signal strength corresponds to a significance of 1.4 standard deviations and is given for m_H = 125 GeV. NODE=S126PTH;LINKAGE=D

[2] AAD 20Z search for the tH associated production using $H \to \gamma\gamma$ in 139 fb^{-1} of data at E_{cm} = 13 TeV. An upper limit on its rate is set to be 12 times the Standard Model at 95% CL (m_H = 125.09 GeV). NODE=S126PTH;LINKAGE=C

[3] SIRUNYAN 19BK search for the tH associated production using multilepton signatures ($H \to WW^*$, $H \to \tau\tau$, $H \to ZZ^*$) and signatures with a single lepton and a $b\overline{b}$ pair ($H \to b\overline{b}$) using 35.9 fb^{-1} at E_{cm} = 13 TeV. Results are combined with $H \to \gamma\gamma$ (SIRUNYAN 18DS). The observed 95% CL upper limit on the tH production cross section times $H \to WW^* + \tau\tau + ZZ^* + b\overline{b} + \gamma\gamma$ branching fraction is 1.94 pb (assuming SM $t\overline{t}H$ production cross section). See their Table X and Fig. 14. The values outside the ranges of [−0.9, −0.5] and [1.0, 2.1] times the standard model top quark Yukawa coupling are excluded at 95% CL. NODE=S126PTH;LINKAGE=B

[4] KHACHATRYAN 16AU search for the tH associated production in 19.7 fb^{-1} at E_{cm} = 8 TeV. The 95% CL upper limits on the tH associated production cross section is measured to be 600–1000 fb depending on the assumed $\gamma\gamma$ branching ratios of the Higgs boson. The $\gamma\gamma$ branching ratio is varied to be by a factor of 0.5–3.0 of the Standard Model Higgs boson (m_H = 125 GeV). The results of the signal strengths for a negative Higgs-boson trilinear coupling are given. The results are given for m_H = 125 GeV. NODE=S126PTH;LINKAGE=A

H Production Cross Section in pp Collisions at $\sqrt{s}$ = 13 TeV

NODE=S126A02

Assumes m_H = 125 GeV

NODE=S126A02
NODE=S126A02

VALUE (pb)	DOCUMENT ID		TECN	COMMENT
56.8± 3.4 OUR AVERAGE NEW				
[56.9 ± 3.4 pb OUR 2023 AVERAGE]				
$55.5^{+4.0}_{-3.8}$	[1] AAD	23C	ATLS	pp, 13 TeV, $\gamma\gamma$, $ZZ^* \to 4\ell$ ($\ell = e, \mu$)
61.1± 6.0±3.7	[2] SIRUNYAN	19BA	CMS	pp, 13 TeV, $\gamma\gamma$, $ZZ^* \to 4\ell$ ($\ell = e, \mu$)
• • • We do not use the following data for averages, fits, limits, etc. • • •				
58 ± 4 ±4	[3] AAD	22N	ATLS	pp, 13 TeV, $\gamma\gamma$
53.5± 4.9±2.1	[4] AAD	20BA	ATLS	pp, 13 TeV, $ZZ^* \to 4\ell$ ($\ell = e, \mu$)
$57.0^{+6.0}_{-5.9}{}^{+4.0}_{-3.3}$	[5] AABOUD	18CG	ATLS	pp, 13 TeV, $\gamma\gamma$, $ZZ^* \to 4\ell$ ($\ell = e, \mu$)
$47.9^{+9.1}_{-8.6}$	[5] AABOUD	18CG	ATLS	pp, 13 TeV, $\gamma\gamma$ OCCUR=2
68^{+11}_{-10}	[5] AABOUD	18CG	ATLS	pp, 13 TeV, $ZZ^* \to 4\ell$ ($\ell = e, \mu$) OCCUR=3
69^{+10}_{-9} ±5	[6] AABOUD	17CO	ATLS	pp, 13 TeV, $ZZ^* \to 4\ell$

[1] AAD 23C combine AAD 22N and AAD 20BA, where both use 139 fb^{-1} of pp collisions at E_{cm} = 13 TeV. The Higgs production cross sections at E_{cm} = 7 and 8 TeV are obtained to be 34^{+11}_{-10} pb and $33.3^{+5.8}_{-5.4}$ pb, respectively. The quoted value is given for m_H = 125.09 GeV. The differential cross sections are given in their Figs. 3 and 4. NODE=S126A02;LINKAGE=F

[2] SIRUNYAN 19BA use 35.9 fb^{-1} of pp collisions at E_{cm} = 13 TeV. NODE=S126A02;LINKAGE=C

[3] AAD 22N use 139 fb^{-1} of pp collisions at E_{cm} = 13 TeV. The quoted value is given for m_H = 125.09 GeV. NODE=S126A02;LINKAGE=E

[4] AAD 20BA use 139 fb^{-1} of pp collisions at E_{cm} = 13 TeV with $H \to ZZ^* \to 4\ell$ where $\ell = e, \mu$. The quoted value is given for m_H = 125 GeV and assumes the Standard Model branching ratio. NODE=S126A02;LINKAGE=D

[5] AABOUD 18CG use 36.1 fb^{-1} of pp collisions at E_{cm} = 13 TeV. NODE=S126A02;LINKAGE=A

[6] AABOUD 17CO use 36.1 fb^{-1} of pp collisions at E_{cm} = 13 TeV with $H \to ZZ^* \to 4\ell$ where $\ell = e, \mu$ for m_H = 125 GeV. Differential cross sections for the Higgs boson transverse momentum, Higgs boson rapidity, and other related quantities are measured as shown in their Figs. 8 and 9. NODE=S126A02;LINKAGE=B

H REFERENCES

NODE=S126

AAD	24D	PRL 132 021803	G. Aad *et al.*	(ATLAS and CMS Collabs.)	REFID=62627
AABOUD	23A	JHEP 2312 158 (errat.)	M. Aaboud *et al.*	(ATLAS Collab.)	REFID=62575
AAD	23A	PL B842 137963	G. Aad *et al.*	(ATLAS Collab.)	REFID=62107
AAD	23AD	EPJ C83 519	G. Aad *et al.*	(ATLAS Collab.)	REFID=62169
AAD	23AF	EPJ C83 503	G. Aad *et al.*	(ATLAS Collab.)	REFID=62171
AAD	23AK	EPJ C83 563	G. Aad *et al.*	(ATLAS Collab.)	REFID=62180
AAD	23AN	PRL 131 061802	G. Aad *et al.*	(ATLAS Collab.)	REFID=62321
AAD	23AP	PR D108 032005	G. Aad *et al.*	(ATLAS Collab.)	REFID=62344
AAD	23AT	PL B843 137745	G. Aad *et al.*	(ATLAS Collab.)	REFID=62361
AAD	23AU	PL B843 137880	G. Aad *et al.*	(ATLAS Collab.)	REFID=62363
AAD	23BC	EPJ C83 496	G. Aad *et al.*	(ATLAS Collab.)	REFID=62381
AAD	23BK	PR D108 052003	G. Aad *et al.*	(ATLAS Collab.)	REFID=62408
AAD	23BP	PRL 131 251802	G. Aad *et al.*	(ATLAS Collab.)	REFID=62471
AAD	23BR	PL B846 138223	G. Aad *et al.*	(ATLAS Collab.)	REFID=62477
AAD	23BS	PL B847 138292	G. Aad *et al.*	(ATLAS Collab.)	REFID=62479
AAD	23BU	PL B847 138315	G. Aad *et al.*	(ATLAS Collab.)	REFID=62481
AAD	23BV	PR D108 072003	G. Aad *et al.*	(ATLAS Collab.)	REFID=62488
AAD	23C	JHEP 2305 028	G. Aad *et al.*	(ATLAS Collab.)	REFID=62115
AAD	23CD	EPJ C83 781	G. Aad *et al.*	(ATLAS Collab.)	REFID=62546
AAD	23Q	JHEP 2307 166	G. Aad *et al.*	(ATLAS Collab.)	REFID=62138
AAD	23Y	JHEP 2307 088	G. Aad *et al.*	(ATLAS Collab.)	REFID=62154
AAD	23Z	JHEP 2307 040	G. Aad *et al.*	(ATLAS Collab.)	REFID=62161
HAYRAPETY...	23	JHEP 2308 040	A. Hayrapetyan *et al.*	(CMS Collab.)	REFID=62378
HAYRAPETY...	23C	PR D108 072004	A. Hayrapetyan *et al.*	(CMS Collab.)	REFID=62489
TUMASYAN	23AD	PRL 131 041801	A. Tumasyan *et al.*	(CMS Collab.)	REFID=62238
TUMASYAN	23AE	PRL 131 041803	A. Tumasyan *et al.*	(CMS Collab.)	REFID=62239
TUMASYAN	23AH	PRL 131 061801	A. Tumasyan *et al.*	(CMS Collab.)	REFID=62320
TUMASYAN	23AI	PR D108 032008	A. Tumasyan *et al.*	(CMS Collab.)	REFID=62347
TUMASYAN	23AJ	PR D108 032013	A. Tumasyan *et al.*	(CMS Collab.)	REFID=62351
TUMASYAN	23AU	PL B846 137783	A. Tumasyan *et al.*	(CMS Collab.)	REFID=62475
TUMASYAN	23BA	EPJ C83 933	A. Tumasyan *et al.*	(CMS Collab.)	REFID=62551
TUMASYAN	23C	PL B842 137534	A. Tumasyan *et al.*	(CMS Collab.)	REFID=62104
TUMASYAN	23D	PL B842 137531	A. Tumasyan *et al.*	(CMS Collab.)	REFID=62105
TUMASYAN	23F	JHEP 2305 233	A. Tumasyan *et al.*	(CMS Collab.)	REFID=62112
TUMASYAN	23I	JHEP 2306 130	A. Tumasyan *et al.*	(CMS Collab.)	REFID=62125
TUMASYAN	23O	JHEP 2307 095	A. Tumasyan *et al.*	(CMS Collab.)	REFID=62150
TUMASYAN	23P	JHEP 2307 092	A. Tumasyan *et al.*	(CMS Collab.)	REFID=62151
TUMASYAN	23Q	JHEP 2307 091	A. Tumasyan *et al.*	(CMS Collab.)	REFID=62152
TUMASYAN	23W	EPJ C83 667	A. Tumasyan *et al.*	(CMS Collab.)	REFID=62174
TUMASYAN	23Y	EPJ C83 562	A. Tumasyan *et al.*	(CMS Collab.)	REFID=62181
AAD	22D	PL B829 137066	G. Aad *et al.*	(ATLAS Collab.)	REFID=61705
AAD	22M	JHEP 2206 097	G. Aad *et al.*	(ATLAS Collab.)	REFID=61806
AAD	22N	JHEP 2208 027	G. Aad *et al.*	(ATLAS Collab.)	REFID=61815
AAD	22P	JHEP 2208 104	G. Aad *et al.*	(ATLAS Collab.)	REFID=61818
AAD	22Q	JHEP 2208 175	G. Aad *et al.*	(ATLAS Collab.)	REFID=61819
AAD	22S	EPJ C82 105	G. Aad *et al.*	(ATLAS Collab.)	REFID=61823
AAD	22V	EPJ C82 622	G. Aad *et al.*	(ATLAS Collab.)	REFID=61835
AAD	22W	EPJ C82 717	G. Aad *et al.*	(ATLAS Collab.)	REFID=61837
AAD	22X	PR D105 092003	G. Aad *et al.*	(ATLAS Collab.)	REFID=61869
AAD	22Y	PR D106 052001	G. Aad *et al.*	(ATLAS Collab.)	REFID=61938
ATLAS	22	NAT 607 52	ATLAS Collaboration	(ATLAS Collab.)	REFID=61850;ERROR=1
Also		NAT 612 E24 (errat.)	ATLAS Collaboration	(ATLAS Collab.)	REFID=61997;ERROR=2
CMS	22	NAT 607 60	CMS Collaboration	(CMS Collab.)	REFID=61851;ERROR=3
TUMASYAN	22AJ	PRL 128 081805	A. Tumasyan *et al.*	(CMS Collab.)	REFID=61864
TUMASYAN	22AM	NATP 18 1329	A. Tumasyan *et al.*	(CMS Collab.)	REFID=61979
TUMASYAN	22AN	PRL 129 081802	A. Tumasyan *et al.*	(CMS Collab.)	REFID=61984
TUMASYAN	22G	PR D105 092007	A. Tumasyan *et al.*	(CMS Collab.)	REFID=61742
TUMASYAN	22Y	JHEP 2206 012	A. Tumasyan *et al.*	(CMS Collab.)	REFID=61803
AAD	21	PL B812 135980	G. Aad *et al.*	(ATLAS Collab.)	REFID=60710
AAD	21AB	EPJ C81 178	G. Aad *et al.*	(ATLAS Collab.)	REFID=61324
AAD	21AJ	EPJ C81 537	G. Aad *et al.*	(ATLAS Collab.)	REFID=61338
AAD	21F	PR D103 112006	G. Aad *et al.*	(ATLAS Collab.)	REFID=61247
AAD	21H	PL B816 136204	G. Aad *et al.*	(ATLAS Collab.)	REFID=61268
AAD	21I	PL B819 136412	G. Aad *et al.*	(ATLAS Collab.)	REFID=61272
AAD	21M	JHEP 2103 268	G. Aad *et al.*	(ATLAS Collab.)	REFID=61284
SIRUNYAN	21	PL B812 135992	A.M. Sirunyan *et al.*	(CMS Collab.)	REFID=60712
SIRUNYAN	21A	EPJ C81 13	A.M. Sirunyan *et al.*	(CMS Collab.)	REFID=60775
Also		EPJ C81 333 (errat.)	A.M. Sirunyan *et al.*	(CMS Collab.)	REFID=61322
SIRUNYAN	21AE	PR D104 052004	A.M. Sirunyan *et al.*	(CMS Collab.)	REFID=61514
SIRUNYAN	21B	EPJ C81 3	A.M. Sirunyan *et al.*	(CMS Collab.)	REFID=60776
SIRUNYAN	21C	JHEP 2101 148	A.M. Sirunyan *et al.*	(CMS Collab.)	REFID=61041
SIRUNYAN	21K	JHEP 2103 257	A.M. Sirunyan *et al.*	(CMS Collab.)	REFID=61285
SIRUNYAN	21L	JHEP 2103 011	A.M. Sirunyan *et al.*	(CMS Collab.)	REFID=61292
SIRUNYAN	21O	JHEP 2107 027	A.M. Sirunyan *et al.*	(CMS Collab.)	REFID=61320
SIRUNYAN	21R	EPJ C81 378	A.M. Sirunyan *et al.*	(CMS Collab.)	REFID=61331
SIRUNYAN	21S	EPJ C81 488	A.M. Sirunyan *et al.*	(CMS Collab.)	REFID=61339
SIRUNYAN	21Z	PR D104 032013	A.M. Sirunyan *et al.*	(CMS Collab.)	REFID=61390
TUMASYAN	21D	JHEP 2111 153	A. Tumasyan *et al.*	(CMS Collab.)	REFID=61559
AAD	20	PR D101 012002	G. Aad *et al.*	(ATLAS Collab.)	REFID=60046
AAD	20A	PL B800 135069	G. Aad *et al.*	(ATLAS Collab.)	REFID=60143
AAD	20AE	PRL 125 221802	G. Aad *et al.*	(ATLAS Collab.)	REFID=60697
AAD	20AG	PL B809 135754	G. Aad *et al.*	(ATLAS Collab.)	REFID=60706
AAD	20AQ	EPJ C80 957	G. Aad *et al.*	(ATLAS Collab.)	REFID=60770
Also		EPJ C81 29 (errat.)	G. Aad *et al.*	(ATLAS Collab.)	REFID=61321
Also		EPJ C81 398 (errat.)	G. Aad *et al.*	(ATLAS Collab.)	REFID=61336
AAD	20BA	EPJ C80 942	G. Aad *et al.*	(ATLAS Collab.)	REFID=60917
AAD	20C	PL B800 135103	G. Aad *et al.*	(ATLAS Collab.)	REFID=60147
AAD	20E	PL B801 135145	G. Aad *et al.*	(ATLAS Collab.)	REFID=60193
AAD	20F	PL B801 135148	G. Aad *et al.*	(ATLAS Collab.)	REFID=60194
AAD	20N	PL B805 135426	G. Aad *et al.*	(ATLAS Collab.)	REFID=60399
AAD	20X	JHEP 2007 108	G. Aad *et al.*	(ATLAS Collab.)	REFID=60511
Also		JHEP 2101 145 (errat.)	G. Aad *et al.*	(ATLAS Collab.)	REFID=61275
Also		JHEP 2105 207 (errat.)	G. Aad *et al.*	(ATLAS Collab.)	REFID=61301
AAD	20Z	PRL 125 061802	G. Aad *et al.*	(ATLAS Collab.)	REFID=60576
SIRUNYAN	20AE	JHEP 2003 131	A.M. Sirunyan *et al.*	(CMS Collab.)	REFID=60483
SIRUNYAN	20AH	JHEP 2005 032	A.M. Sirunyan *et al.*	(CMS Collab.)	REFID=60491
SIRUNYAN	20AS	PRL 125 061801	A.M. Sirunyan *et al.*	(CMS Collab.)	REFID=60575
SIRUNYAN	20BK	JHEP 2011 039	A.M. Sirunyan *et al.*	(CMS Collab.)	REFID=60763
SIRUNYAN	20BL	JHEP 2012 085	A.M. Sirunyan *et al.*	(CMS Collab.)	REFID=60766

SIRUNYAN	20C	EPJ C80 75	A.M. Sirunyan *et al.*	(CMS Collab.)	REFID=60222
SIRUNYAN	20L	PL B805 135425	A.M. Sirunyan *et al.*	(CMS Collab.)	REFID=60398
AABOUD	19A	JHEP 1901 030	M. Aaboud *et al.*	(ATLAS Collab.)	REFID=59370
AABOUD	19AI	PL B793 499	M. Aaboud *et al.*	(ATLAS Collab.)	REFID=59755
AABOUD	19AL	PRL 122 231801	M. Aaboud *et al.*	(ATLAS Collab.)	REFID=59792
AABOUD	19AQ	PR D99 072001	M. Aaboud *et al.*	(ATLAS Collab.)	REFID=59853
AABOUD	19F	PL B789 508	M. Aaboud *et al.*	(ATLAS Collab.)	REFID=59431
AABOUD	19N	JHEP 1904 048	M. Aaboud *et al.*	(ATLAS Collab.)	REFID=59669
AABOUD	19O	JHEP 1904 092	M. Aaboud *et al.*	(ATLAS Collab.)	REFID=59672
AABOUD	19T	JHEP 1905 124	M. Aaboud *et al.*	(ATLAS Collab.)	REFID=59684
AABOUD	19U	JHEP 1905 141	M. Aaboud *et al.*	(ATLAS Collab.)	REFID=59685
AAD	19A	PL B798 134949	G. Aad *et al.*	(ATLAS Collab.)	REFID=59981
SIRUNYAN	19	PL B788 7	A.M. Sirunyan *et al.*	(CMS Collab.)	REFID=59412
SIRUNYAN	19AB	JHEP 1904 112	A.M. Sirunyan *et al.*	(CMS Collab.)	REFID=59674
SIRUNYAN	19AF	JHEP 1906 093	A.M. Sirunyan *et al.*	(CMS Collab.)	REFID=59691
SIRUNYAN	19AJ	EPJ C79 94	A.M. Sirunyan *et al.*	(CMS Collab.)	REFID=59703
SIRUNYAN	19AT	EPJ C79 421	A.M. Sirunyan *et al.*	(CMS Collab.)	REFID=59725
SIRUNYAN	19AX	PL B791 96	A.M. Sirunyan *et al.*	(CMS Collab.)	REFID=59745
SIRUNYAN	19BA	PL B792 369	A.M. Sirunyan *et al.*	(CMS Collab.)	REFID=59752
SIRUNYAN	19BE	PRL 122 121803	A.M. Sirunyan *et al.*	(CMS Collab.)	REFID=59768
SIRUNYAN	19BK	PR D99 092005	A.M. Sirunyan *et al.*	(CMS Collab.)	REFID=59875
SIRUNYAN	19BL	PR D99 112003	A.M. Sirunyan *et al.*	(CMS Collab.)	REFID=59886
SIRUNYAN	19BO	PL B793 520	A.M. Sirunyan *et al.*	(CMS Collab.)	REFID=59927
SIRUNYAN	19BR	PL B797 134811	A.M. Sirunyan *et al.*	(CMS Collab.)	REFID=59934
SIRUNYAN	19BY	PR D100 072007	A.M. Sirunyan *et al.*	(CMS Collab.)	REFID=60014
SIRUNYAN	19BZ	PR D100 112002	A.M. Sirunyan *et al.*	(CMS Collab.)	REFID=60038
SIRUNYAN	19CG	JHEP 1910 139	A.M. Sirunyan *et al.*	(CMS Collab.)	REFID=60087
SIRUNYAN	19E	PRL 122 021801	A.M. Sirunyan *et al.*	(CMS Collab.)	REFID=59555
SIRUNYAN	19H	JHEP 1901 040	A.M. Sirunyan *et al.*	(CMS Collab.)	REFID=59630
SIRUNYAN	19L	JHEP 1901 183	A.M. Sirunyan *et al.*	(CMS Collab.)	REFID=59634
SIRUNYAN	19R	JHEP 1903 026	A.M. Sirunyan *et al.*	(CMS Collab.)	REFID=59655
AABOUD	18	PL B776 318	M. Aaboud *et al.*	(ATLAS Collab.)	REFID=58621
AABOUD	18AC	PR D97 072003	M. Aaboud *et al.*	(ATLAS Collab.)	REFID=58991
AABOUD	18AJ	JHEP 1803 095	M. Aaboud *et al.*	(ATLAS Collab.)	REFID=59087
AABOUD	18AU	JHEP 1807 127	M. Aaboud *et al.*	(ATLAS Collab.)	REFID=59128
Also		JHEP 2312 158 (errat.)	M. Aaboud *et al.*	(ATLAS Collab.)	REFID=62575
AABOUD	18BK	PL B784 173	M. Aaboud *et al.*	(ATLAS Collab.)	REFID=59293
AABOUD	18BL	PL B786 134	M. Aaboud *et al.*	(ATLAS Collab.)	REFID=59294
AABOUD	18BM	PL B784 345	M. Aaboud *et al.*	(ATLAS Collab.)	REFID=59295
AABOUD	18BN	PL B786 59	M. Aaboud *et al.*	(ATLAS Collab.)	REFID=59290
AABOUD	18BO	PR D98 052005	M. Aaboud *et al.*	(ATLAS Collab.)	REFID=59291
AABOUD	18BP	PL B786 223	M. Aaboud *et al.*	(ATLAS Collab.)	REFID=59297
AABOUD	18BQ	PR D98 052003	M. Aaboud *et al.*	(ATLAS Collab.)	REFID=59298
AABOUD	18BU	EPJ C78 1007	M. Aaboud *et al.*	(ATLAS Collab.)	REFID=59333
AABOUD	18CA	JHEP 1810 180	M. Aaboud *et al.*	(ATLAS Collab.)	REFID=59356
AABOUD	18CG	PL B786 114	M. Aaboud *et al.*	(ATLAS Collab.)	REFID=59405
AABOUD	18CQ	PRL 121 191801	M. Aaboud *et al.*	(ATLAS Collab.)	REFID=59529
AABOUD	18CW	JHEP 1811 040	M. Aaboud *et al.*	(ATLAS Collab.)	REFID=59567
AABOUD	18M	PRL 120 211802	M. Aaboud *et al.*	(ATLAS Collab.)	REFID=58831
AABOUD	18T	PR D97 072016	M. Aaboud *et al.*	(ATLAS Collab.)	REFID=58927
AAIJ	18AM	EPJ C78 1008	R. Aaij *et al.*	(LHCb Collab.)	REFID=59334
AALTONEN	18C	PR D98 072002	T. Aaltonen *et al.*	(CDF Collab.)	REFID=59454
SIRUNYAN	18A	PL B778 101	A.M. Sirunyan *et al.*	(CMS Collab.)	REFID=58627
SIRUNYAN	18AE	PL B780 501	A.M. Sirunyan *et al.*	(CMS Collab.)	REFID=59010
SIRUNYAN	18BD	JHEP 1806 101	A.M. Sirunyan *et al.*	(CMS Collab.)	REFID=59116
SIRUNYAN	18BH	JHEP 1806 001	A.M. Sirunyan *et al.*	(CMS Collab.)	REFID=59124
SIRUNYAN	18BQ	JHEP 1808 066	A.M. Sirunyan *et al.*	(CMS Collab.)	REFID=59144
SIRUNYAN	18BU	EPJ C78 140	A.M. Sirunyan *et al.*	(CMS Collab.)	REFID=59154
SIRUNYAN	18BV	EPJ C78 291	A.M. Sirunyan *et al.*	(CMS Collab.)	REFID=59173
SIRUNYAN	18DB	PRL 121 121801	A.M. Sirunyan *et al.*	(CMS Collab.)	REFID=59308
SIRUNYAN	18DQ	JHEP 1811 152	A.M. Sirunyan *et al.*	(CMS Collab.)	REFID=59366
SIRUNYAN	18DS	JHEP 1811 185	A.M. Sirunyan *et al.*	(CMS Collab.)	REFID=59368
SIRUNYAN	18E	PRL 120 071802	A.M. Sirunyan *et al.*	(CMS Collab.)	REFID=58729
SIRUNYAN	18F	JHEP 1801 054	A.M. Sirunyan *et al.*	(CMS Collab.)	REFID=58787
SIRUNYAN	18L	PRL 120 231801	A.M. Sirunyan *et al.*	(CMS Collab.)	REFID=58837
SIRUNYAN	18S	PR D97 092005	A.M. Sirunyan *et al.*	(CMS Collab.)	REFID=58938
SIRUNYAN	18Y	PL B779 283	A.M. Sirunyan *et al.*	(CMS Collab.)	REFID=59001
AABOUD	17AW	JHEP 1710 112	M. Aaboud *et al.*	(ATLAS Collab.)	REFID=58335
AABOUD	17BA	JHEP 1712 024	M. Aaboud *et al.*	(ATLAS Collab.)	REFID=58352
AABOUD	17BD	EPJ C77 765	M. Aaboud *et al.*	(ATLAS Collab.)	REFID=58360
AABOUD	17CO	JHEP 1710 132	M. Aaboud *et al.*	(ATLAS Collab.)	REFID=59637
AABOUD	17Y	PRL 119 051802	M. Aaboud *et al.*	(ATLAS Collab.)	REFID=57947
AAD	17	EPJ C77 70	G. Aad *et al.*	(ATLAS Collab.)	REFID=57780
KHACHATRY...	17F	JHEP 1702 135	V. Khachatryan *et al.*	(CMS Collab.)	REFID=57781
SIRUNYAN	17AM	PL B775 1	A.M. Sirunyan *et al.*	(CMS Collab.)	REFID=58295
SIRUNYAN	17AV	JHEP 1711 047	A.M. Sirunyan *et al.*	(CMS Collab.)	REFID=58345
SIRUNYAN	17CN	PR D96 072004	A.M. Sirunyan *et al.*	(CMS Collab.)	REFID=58658
AABOUD	16I	PR D94 052002	M. Aaboud *et al.*	(ATLAS Collab.)	REFID=57426
AABOUD	16K	PRL 117 111802	M. Aaboud *et al.*	(ATLAS Collab.)	REFID=57462
AABOUD	16X	JHEP 1611 112	M. Aaboud *et al.*	(ATLAS Collab.)	REFID=57661
AAD	16	PL B753 69	G. Aad *et al.*	(ATLAS Collab.)	REFID=57004
AAD	16AC	PR D93 092005	G. Aad *et al.*	(ATLAS Collab.)	REFID=57281
AAD	16AF	JHEP 1601 172	G. Aad *et al.*	(ATLAS Collab.)	REFID=57316
AAD	16AL	JHEP 1605 160	G. Aad *et al.*	(ATLAS Collab.)	REFID=57334
AAD	16AN	JHEP 1608 045	G. Aad *et al.*	(ATLAS and CMS Collabs.)	REFID=57343
AAD	16AO	JHEP 1608 104	G. Aad *et al.*	(ATLAS Collab.)	REFID=57346
AAD	16BL	EPJ C76 658	G. Aad *et al.*	(ATLAS Collab.)	REFID=57683
AAD	16K	EPJ C76 6	G. Aad *et al.*	(ATLAS Collab.)	REFID=57029
KHACHATRY...	16AB	PL B759 672	V. Khachatryan *et al.*	(CMS Collab.)	REFID=57240
KHACHATRY...	16AR	JHEP 1604 005	V. Khachatryan *et al.*	(CMS Collab.)	REFID=57325
KHACHATRY...	16AU	JHEP 1606 177	V. Khachatryan *et al.*	(CMS Collab.)	REFID=57339
KHACHATRY...	16B	PL B753 341	V. Khachatryan *et al.*	(CMS Collab.)	REFID=57005
KHACHATRY...	16BA	JHEP 1609 051	V. Khachatryan *et al.*	(CMS Collab.)	REFID=57356
KHACHATRY...	16BQ	PR D94 052012	V. Khachatryan *et al.*	(CMS Collab.)	REFID=57433

KHACHATRY...	16CD	PL B763 472	V. Khachatryan *et al.*	(CMS Collab.)	REFID=57698
KHACHATRY...	16G	EPJ C76 13	V. Khachatryan *et al.*	(CMS Collab.)	REFID=57026
AAD	15	PL B740 222	G. Aad *et al.*	(ATLAS Collab.)	REFID=56266
AAD	15AA	PR D92 012006	G. Aad *et al.*	(ATLAS Collab.)	REFID=56593
AAD	15AH	JHEP 1504 117	G. Aad *et al.*	(ATLAS Collab.)	REFID=56619
AAD	15AQ	JHEP 1508 137	G. Aad *et al.*	(ATLAS Collab.)	REFID=56647
AAD	15AX	EPJ C75 231	G. Aad *et al.*	(ATLAS Collab.)	REFID=56665
AAD	15B	PRL 114 191803	G. Aad *et al.*	(ATLAS and CMS Collabs.)	REFID=56434
AAD	15BC	EPJ C75 349	G. Aad *et al.*	(ATLAS Collab.)	REFID=56670
AAD	15BD	EPJ C75 337	G. Aad *et al.*	(ATLAS Collab.)	REFID=56671
AAD	15BE	EPJ C75 335	G. Aad *et al.*	(ATLAS Collab.)	REFID=56672
AAD	15CE	PR D92 092004	G. Aad *et al.*	(ATLAS Collab.)	REFID=56909
AAD	15CI	EPJ C75 476	G. Aad *et al.*	(ATLAS Collab.)	REFID=56936
Also		EPJ C76 152 (errat.)	G. Aad *et al.*	(ATLAS Collab.)	REFID=57367
AAD	15CX	JHEP 1511 206	G. Aad *et al.*	(ATLAS Collab.)	REFID=59980
AAD	15F	PR D91 012006	G. Aad *et al.*	(ATLAS Collab.)	REFID=56421
AAD	15G	JHEP 1501 069	G. Aad *et al.*	(ATLAS Collab.)	REFID=56424
AAD	15I	PRL 114 121801	G. Aad *et al.*	(ATLAS Collab.)	REFID=56444
AAD	15P	PRL 115 091801	G. Aad *et al.*	(ATLAS Collab.)	REFID=56492
AAD	15T	PL B749 519	G. Aad *et al.*	(ATLAS Collab.)	REFID=56546
AALTONEN	15	PRL 114 151802	T. Aaltonen *et al.*	(CDF and D0 Collabs.)	REFID=56464
AALTONEN	15B	PRL 114 141802	T. Aaltonen *et al.*	(CDF Collab.)	REFID=56465
KHACHATRY...	15AM	EPJ C75 212	V. Khachatryan *et al.*	(CMS Collab.)	REFID=56657
KHACHATRY...	15AN	EPJ C75 251	V. Khachatryan *et al.*	(CMS Collab.)	REFID=56658
KHACHATRY...	15BA	PR D92 072010	V. Khachatryan *et al.*	(CMS Collab.)	REFID=56895
KHACHATRY...	15H	PL B744 184	V. Khachatryan *et al.*	(CMS Collab.)	REFID=56505
KHACHATRY...	15Q	PL B749 337	V. Khachatryan *et al.*	(CMS Collab.)	REFID=56530
KHACHATRY...	15Y	PR D92 012004	V. Khachatryan *et al.*	(CMS Collab.)	REFID=56538
KHACHATRY...	15Z	PR D92 032008	V. Khachatryan *et al.*	(CMS Collab.)	REFID=56539
AAD	14AR	PL B738 234	G. Aad *et al.*	(ATLAS Collab.)	REFID=56125
AAD	14AS	PL B738 68	G. Aad *et al.*	(ATLAS Collab.)	REFID=56127
AAD	14BC	PR D90 112015	G. Aad *et al.*	(ATLAS Collab.)	REFID=56286
AAD	14BJ	JHEP 1409 112	G. Aad *et al.*	(ATLAS Collab.)	REFID=57146
AAD	14J	PL B732 8	G. Aad *et al.*	(ATLAS Collab.)	REFID=55769
AAD	14O	PRL 112 201802	G. Aad *et al.*	(ATLAS Collab.)	REFID=55849
AAD	14W	PR D90 052004	G. Aad *et al.*	(ATLAS Collab.)	REFID=55885
ABAZOV	14F	PRL 113 161802	V.M. Abazov *et al.*	(D0 Collab.)	REFID=56106
CHATRCHYAN	14AA	PR D89 092007	S. Chatrchyan *et al.*	(CMS Collab.)	REFID=56033
CHATRCHYAN	14AI	PR D89 012003	S. Chatrchyan *et al.*	(CMS Collab.)	REFID=56422
CHATRCHYAN	14AJ	NATP 10 557	S. Chatrchyan *et al.*	(CMS Collab.)	REFID=56423
CHATRCHYAN	14B	EPJ C74 2980	S. Chatrchyan *et al.*	(CMS Collab.)	REFID=55703
CHATRCHYAN	14G	JHEP 1401 096	S. Chatrchyan *et al.*	(CMS Collab.)	REFID=55713
CHATRCHYAN	14K	JHEP 1405 104	S. Chatrchyan *et al.*	(CMS Collab.)	REFID=55733
KHACHATRY...	14D	PL B736 64	V. Khachatryan *et al.*	(CMS Collab.)	REFID=55758
KHACHATRY...	14H	JHEP 1409 087	V. Khachartryan *et al.*	(CMS Collab.)	REFID=56014
KHACHATRY...	14P	EPJ C74 3076	V. Khachatryan *et al.*	(CMS Collab.)	REFID=56183
AAD	13AJ	PL B726 120	G. Aad *et al.*	(ATLAS Collab.)	REFID=55095
AAD	13AK	PL B726 88	G. Aad *et al.*	(ATLAS Collab.)	REFID=55096
Also		PL B734 406 (errat.)	G. Aad *et al.*	(ATLAS Collab.)	REFID=57144
AALTONEN	13L	PR D88 052013	T. Aaltonen *et al.*	(CDF Collab.)	REFID=55191
AALTONEN	13M	PR D88 052014	T. Aaltonen *et al.*	(CDF and D0 Collabs.)	REFID=55192
ABAZOV	13L	PR D88 052011	V.M. Abazov *et al.*	(D0 Collab.)	REFID=55189
CHATRCHYAN	13BK	PL B726 587	S. Chatrchyan *et al.*	(CMS Collab.)	REFID=55436
CHATRCHYAN	13J	PRL 110 081803	S. Chatrchyan *et al.*	(CMS Collab.)	REFID=54942
CHATRCHYAN	13X	JHEP 1305 145	S. Chatrchyan *et al.*	(CMS Collab.)	REFID=55031
CHATRCHYAN	13Y	JHEP 1306 081	S. Chatrchyan *et al.*	(CMS Collab.)	REFID=55035
HEINEMEYER	13A	arXiv:1307.1347	S. Heinemeyer *et al.*	(LHC Higgs CS Working Group)	REFID=57159
AAD	12AI	PL B716 1	G. Aad *et al.*	(ATLAS Collab.)	REFID=54198
AAD	12DA	SCI 338 1576	G. Aad *et al.*	(ATLAS Collab.)	REFID=54986
AALTONEN	12Q	PRL 109 111803	T. Aaltonen *et al.*	(CDF Collab.)	REFID=54246
AALTONEN	12R	PRL 109 111804	T. Aaltonen *et al.*	(CDF Collab.)	REFID=54247
AALTONEN	12S	PRL 109 111805	T. Aaltonen *et al.*	(CDF Collab.)	REFID=54248
AALTONEN	12T	PRL 109 071804	T. Aaltonen *et al.*	(CDF and D0 Collabs.)	REFID=54249
ABAZOV	12K	PL B716 285	V.M. Abazov *et al.*	(D0 Collab.)	REFID=54187
ABAZOV	12O	PRL 109 121803	V.M. Abazov *et al.*	(D0 Collab.)	REFID=54211
ABAZOV	12P	PRL 109 121804	V.M. Abazov *et al.*	(D0 Collab.)	REFID=54212
CHATRCHYAN	12BY	SCI 338 1569	S. Chatrchyan *et al.*	(CMS Collab.)	REFID=54987
CHATRCHYAN	12N	PL B716 30	S. Chatrchyan *et al.*	(CMS Collab.)	REFID=54181
DITTMAIER	12	arXiv:1201.3084	S. Dittmaier *et al.*	(LHC Higgs CS Working Group)	REFID=57158
DITTMAIER	11	arXiv:1101.0593	S. Dittmaier *et al.*	(LHC Higgs CS Working Group)	REFID=57157